

AFTT/GNE/ENP/93M-2

AD-A262 491



DTIC
ELECTE
APR 5 1993
S C D

MITIGATION OF SHOCK WAVES IN
A CYLINDRICAL TUNNEL BY FOAM

THESIS

Grant W. Fondaw, Captain, USA

AFTT/GNE/ENP/93M-2

Approved for public release; distribution unlimited

98 4 02 051

93-06392



1508

Reproduced From
Best Available Copy

2000/026172

MITIGATION OF SHOCK WAVES IN
A CYLINDRICAL TUNNEL BY FOAM

THESIS

Presented to the Faculty of the School of Engineering

of the Air Force Institute of Technology

Air University

In Partial Fulfillment of the

Requirements for the Degree of

Master of Science in Nuclear Engineering

Grant W. Fondaw, B.S.E.E.

Captain, USA

DTIC QUALITY INSPECTED 4

March 1993

Approved for public release; distribution unlimited

Accession For	
NTIS CRA&I	<input checked="checked" type="checkbox"/>
DTIC TAB	<input type="checkbox"/>
Unannounced	<input type="checkbox"/>
Justification	
By	
Distribution /	
Availability Codes	
Dist	Avail and/or Special
A-1	

Preface

The purpose of this study was to explore the shock mitigating effects of foam. I chose this area because I wanted to do numerical modeling. However, I found little work done in this area. I had trouble finding a realistic model for the foam and accepted tradeoffs there. The major limitation was computing power. To do real justice to this problem, I needed a larger limit on the number of cells allowed along with a faster computer and larger storage. Despite the limits of my model, the results showed true promise. My study answered a few questions, but it found many more. I feel that this area has many other avenues to explore.

Throughout my research, I have had much help from others. I owe a large debt to my faculty advisor, Dr. Kirk A. Mathews, for his time and patience while keeping me on track. Further, I would like to thank LTC Mark Byers of the Defense Nuclear Agency for sponsoring my thesis and serving on my committee. Dr. Gene Hertel of Sandia National Laboratory provided invaluable assistance throughout my project, from installing CTH to troubleshooting my input files. I owe Dr. Hertel much gratitude.

More than anyone else, I thank my wife Paula, whose love and encouragement keeps me going each day.

Grant W. Fondaw

Table of Contents

	Page
Preface	ii
List of Figures	v
List of Tables	vi
List of Terms	vii
Abstract	viii
I. Introduction	1
Background	1
Problem and Scope	3
Assumptions	4
Resources and Constraints	5
General Approach	7
Sequence of Presentation	8
II. Problem Analysis	10
Problem	10
Alternative	11
III. Theoretical Development	13
Eulerian Conservation Equations	13
Lagrangian Conservation Equations	14
Equations of State	16
Sound Speed in Foam	20
Foam Response	21
CTH Code System	23
IV. Test Cases and Results	24

	Page
Model Validation	25
Initial Foam Test Case	26
Second Foam Test Case	28
Third Foam Test Case	30
Final Foam Test Case	35
V. Conclusions	42
VI. Recommendations	45
Appendix A: Sample Input File For Modeling Tunnel With Foam	48
Appendix B: Pressure History Plots of Final Foam Test Case	55
Bibliography	104
Vita	105

List of Figures

Figure		Page
1	Diagram of Tunnel Model	6
2	Sample History Plot of Pressure	8
3	Graph of Peak Overpressures from Table 8	34
4	Material Flow as Shock Propagates Down a Foam-Lined Tunnel	36
5	Contour Plot of Peak Pressures vs. Distance in Tunnel With No Foam	37
6	Contour Plot of Peak Pressures vs. Distance in Tunnel With 10 Cm Foam	38
7	Contour Plot of Peak Pressures vs. Distance in Tunnel With 20 Cm Foam	39
8	Contour Plot of Peak Pressures vs. Distance in Tunnel With 30 Cm Foam	40

List of Tables

Table		Page
1	Values of γ for Common Gases	18
2	Comparison of Proof and Normal Test Case	26
3	Overpressures Observed in Initial Foam Test Case	27
4	Overpressures Observed in Initial Foam Test Case	28
5	Overpressures Observed in Second Foam Test Case	29
6	Overpressures Observed in Third Foam Test Case	31
7	Overpressures Observed Between 25 and 50 Meters	32
8	Overpressures Observed Over Tunnel Length	33
9	Overpressures Observed in Final Foam Test Case	41
10	Tentative Criteria for Direct Blast Effects in Man	43

List of Terms

- area plot** A plot of one or more factors at an instant in time versus position. The factors can be material properties, interfaces or tracer locations. The material properties are taken from each computational cell and do not rely on values at tracers.
- CTH** A strong-shock large-deformation multi-dimensional hydrodynamics code from Sandia National Laboratories.
- Eulerian tracer** A tracer that is stationary in the lab frame of reference. The material will flow past this tracer.
- history plot** A plot of one material property, such as pressure, at a tracer versus time.
- Lagrangian tracer** A tracer that travels with the material. This tracer is stationary in the material frame of reference.
- problem** One trial based on a single input deck. A series of problems comprise a test case.
- run** Another term for problem.
- run time** The length of time required for the problem to execute on the computer.
- tracers** A user designated data-collection point. CTH collects data on material properties, such as pressure, temperature, density, position and velocity, at each tracer at time intervals specified by the user.
- tracer plot** An area plot with material interfaces and tracer positions only.

Abstract

This study investigated the effectiveness of foam in mitigating shock waves in tunnels. I modeled a polyurethane foam liner of varying density, crush strength and thickness inside a tunnel and simulated an explosion in the tunnel and then computed and compared graphically the effect of varying each foam parameter.

Using the CTH code system, an Eulerian-Lagrangian hydrodynamics code from Sandia National Laboratories, I developed models for each test. The tunnel measured one meter inside diameter and fifty meters length for the first two series of tests. The final trial calculated the tunnel to a length of one hundred meters. The walls of the tunnel consisted of a perfectly reflecting boundary, and in some cases, a foam liner. About 1.25 kilograms of Composition C-4 explosive placed in the center of the tunnel provided the shock.

Low density foam provided the most shock attenuation, with a twenty-centimeters thick layer of ninety-percent void (0.1265 g/cm^3) foam achieving a seventy percent reduction of the shock pressure at fifty meters. The effects of foam thickness on the shock pressure varied with the distance from the explosion. The thicker foams raised the initial pressure near the explosion due to constriction of the tunnel area. However, the thicker layers reduced the shock faster. Varying the crush strength of the foam from one atmosphere to three atmospheres overpressure did not affect its ability to mitigate shock propagation in the tunnel. The results of this study strongly suggest that foam can mitigate shock waves significantly.

MITIGATION OF SHOCK WAVES IN A CYLINDRICAL TUNNEL BY FOAM

I. Introduction

This study used a production hydrodynamics code to simulate the propagation of an explosively driven blast wave in a tunnel. The model simulated a tunnel with reflecting walls and then simulated the same tunnel with varying amounts and types of foam lining the tunnel walls. The CTH hydrodynamics code system from Sandia National Laboratories performed the calculations and produced history plots of pressure at various points down the tunnel. Comparisons of these plots determined the effectiveness of the particular foam. The sections below discuss the reasons for this study and describe the methodology used to solve this problem.

Background

Despite recent events in the world, there is still no place absolutely safe from terrorism. A main weapon used in the terrorist's war against society is the bomb. The primary purpose of terrorism is to create fear and uncertainty by destroying public or private facilities and killing people. A bomb is an ideal tool to accomplish this goal. Bombs may range in size from an everyday envelope to a semi trailer. They can be hidden in lunch boxes or delivered via the U.S. Postal Service. The imagination of the bomber is the only limit to endless possibilities. Consequently, no facility is absolutely safe from a determined bomber.

Given this risk, there are several ways to protect the facilities themselves. The bomb's blast is the primary mechanism of destruction, so efforts must be directed into a means of reducing the effects of the blast. There are currently several ways to protect facilities or equipment from blast. Venting is the most common method, with containment and shielding used to a lesser extent.

Venting consists of allowing the blast an easy exit to the open atmosphere. Usually, this is more by accident than by design. For example, many building fronts are constructed almost entirely of plate glass windows. When an explosion occurs in one of these buildings, the glass shatters and while this may prevent structural damage, it also creates a missile hazard. Although achieving venting is easy in rooms with an exterior wall, it is more difficult to achieve if there is not an exterior wall, such as in interior rooms or hallways of buildings or entrances to underground facilities.

A bomb basket can contain a small blast. After a suspect device is discovered, it is placed in the bomb basket. Upon detonation of the bomb, the bomb basket will either contain the blast or direct it in a safe direction. Besides the obvious limitation of finding and moving the device, all bomb baskets have a physical limit on the amount of explosives they can contain. An average bomb basket has a rating of five pounds of explosive.

Shielding may consist of deflector walls or blast blankets. Deflector walls consist of solid walls surrounding vital equipment. These walls would deflect the blast around the equipment. This method may require assumptions about where the bomb will be located and may limit access to the equipment for operation and maintenance. Blast

blankets are heavy blankets that may be placed over vital pieces of equipment prior to an explosion. The blast blankets also serve to divert the blast from the equipment. This requires prior warning of the blast.

The most difficult case discussed above is an interior room or hallway and no foreknowledge of the bomb. The use of foam to absorb the blast energy would possibly address both these shortcomings. Foam could absorb blast energy despite the bomb's location and could always be present. If effective, the use of foam could lessen the terrorist threat. More explosive would be required to achieve the same level of destruction, requiring terrorists to use larger bombs. Larger bombs are more difficult to place and easier to detect. The role of foam to absorb the shock from a conventional explosion can easily be expanded to include the protection of underground facilities from nuclear blast. A foam-lined tunnel could significantly reduce the pressure from a nuclear blast observed by an underground facility. Foam also has the advantages of being inexpensive and readily available.

Problem and Scope

The problem investigated was the blast-mitigating effects of foam in an interior hallway or underground tunnel. The model consisted of an infinitely long tunnel with a one meter radius and perfectly reflecting walls. Each problem used various thicknesses and qualities of foam lining inside the tunnel and the program calculated the peak overpressure at various distances along the tunnel following an explosion. Initial analysis used fifty meters of tunnel to narrow the choices of foam. This relatively short tunnel allowed acceptable computer run times while still predicting the important effects

of the foam. Final analysis used one hundred meters of tunnel to find the effectiveness of the foam at greater distances.

The model used various boundary conditions to simulate a tunnel. A symmetry boundary on the outer wall simulated a perfectly reflecting wall. A symmetry boundary used at the left end mirrored the entire tunnel. A semi-infinite boundary on the right end allowed the blast wave to propagate out of the tunnel without reflecting back. A symmetry boundary for the center axis kept the problem two dimensional, while limiting the placement of the explosives.

Approximately 1.25 kilograms of Composition C-4 provided the blast. Composition C-4 is a common military demolition explosive that can be obtained by domestic terrorist groups. It is also similar to SEMTEX, a Soviet bloc plastic explosive. Czechoslovakian SEMTEX has been readily available to terrorists in the past.

The density, crush strength and thickness of the polyurethane-based foam were varied over a range of values. Density was varied from twenty percent to ninety percent void; crush strength was varied from one to four atmospheres overpressure; thickness was varied from five to fifty centimeters.

Assumptions

Program and time constraints required several assumptions. The model of foam used void instead of air. This is assumed to be negligible and is discussed in greater detail in section 4. Also, actual polyurethane foam bounces back to its original shape after the release of pressure. This model's foam did not bounce back, thus simplifying the model. Since the shock wave travels rapidly down the tunnel and foam rebounds

slowly by comparison, the results should not be affected by this short cut. The model did not allow any absorption of the blast's energy by the concrete walls. For the purposes of this research, this was assumed to have negligible effect on the results.

Resources and Constraints

Limited resources were available for this research. The resources consisted of the CTH code, manuals provided with the code, limited technical support from Sandia National Laboratories, several SUN SPARC-2® workstations, limited non-dedicated file storage space, and two network laser printers.

Each of the resources presented constraints. Although most of these constraints had little impact, several had major effects. The CTH code limited the user to a 1000 by 1000 cell mesh. This in turn introduced a trade-off between computational cell size, problem run time and the maximum distance from the explosion one was able to calculate. The smaller the calculation cell size, the better the accuracy and the longer the problem run time; however, the farther away from the explosion, the more transient behavior dies out and the shorter the run time. Using the SUN SPARC-2® workstations led to problem run times expressed in days instead of hours. This determined the setup of the entire model and experiment plan. Finally, the limited non-dedicated file storage space limited the number of problems that could run concurrently. Between the last two constraints, completing a test case could take well over a week.

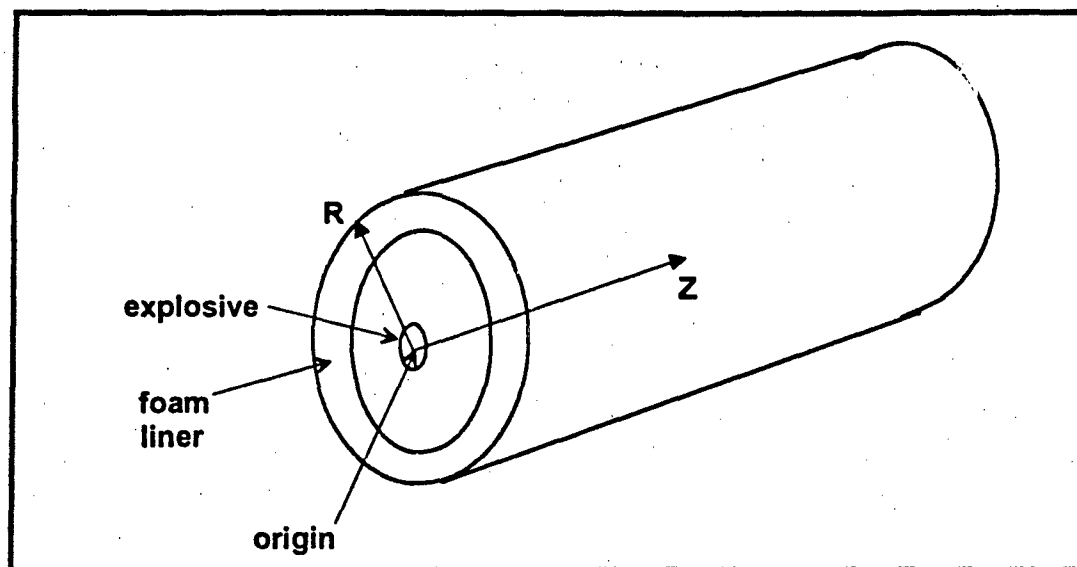


Figure 1. Diagram of Tunnel Model

These constraints were addressed in several ways. To decrease the problem run time, a two-dimensional cylindrical coordinate system was used to model the hallway. Limiting the radius to one meter decreased the number of computational cells and the run time. Placing the explosives in the center of the tunnel and using symmetry cut the run time even further. Limiting peak pressure by using the smallest amount of explosive possible (one cell) cut run time even more. Several experimental runs found that the optimum cell size allowed was five centimeters. This size retained accuracy while allowing the fastest run time. The cell size set the amount of explosive to be 1.25 kilograms. The limit on the number of cells restricted the length of tunnel that could be calculated to fifty meters from the explosion. With these constraints, the initial model consisted of an indefinitely long tunnel with a one meter radius. By using a semi-infinite boundary condition at the end of the tunnel, the shock is allowed to continue down the

tunnel after it has passed the end of the computational mesh. Each computational cell measured five centimeters in the r and z directions and 2π in the θ direction. Thus, each computational cell was a volume, either a cylinder with a radius of five centimeters and a length of five centimeters, or an annulus with a thickness of five centimeters and a length of five centimeters. Hereafter, the size of the cell is referred to by its r and z dimensions, five centimeters square.

General Approach

The experiment plan required a minimum of three test cases. The first test case was a plain tunnel to provide a standard for comparisons. The second test case was the same problem run with a finer computational mesh. This was used to validate the standard. The third test case added foam to the tunnels and varied the foam parameters over several values. From these results, additional test cases were to be chosen to explore any area indicated.

The peak overpressure was obtained from the history plots of pressure (see Figure 2 below). Subtracting one atmosphere from this value gave the overpressure. The overpressures obtained from the graph have an estimated error of less than two percent from the reading of the peak pressure from the graph. This error was minimized by linear interpolation over the entire pressure range on the plot. To determine the effectiveness of the foam, overpressures the same distance from the explosion were compared for each problem and each test case.

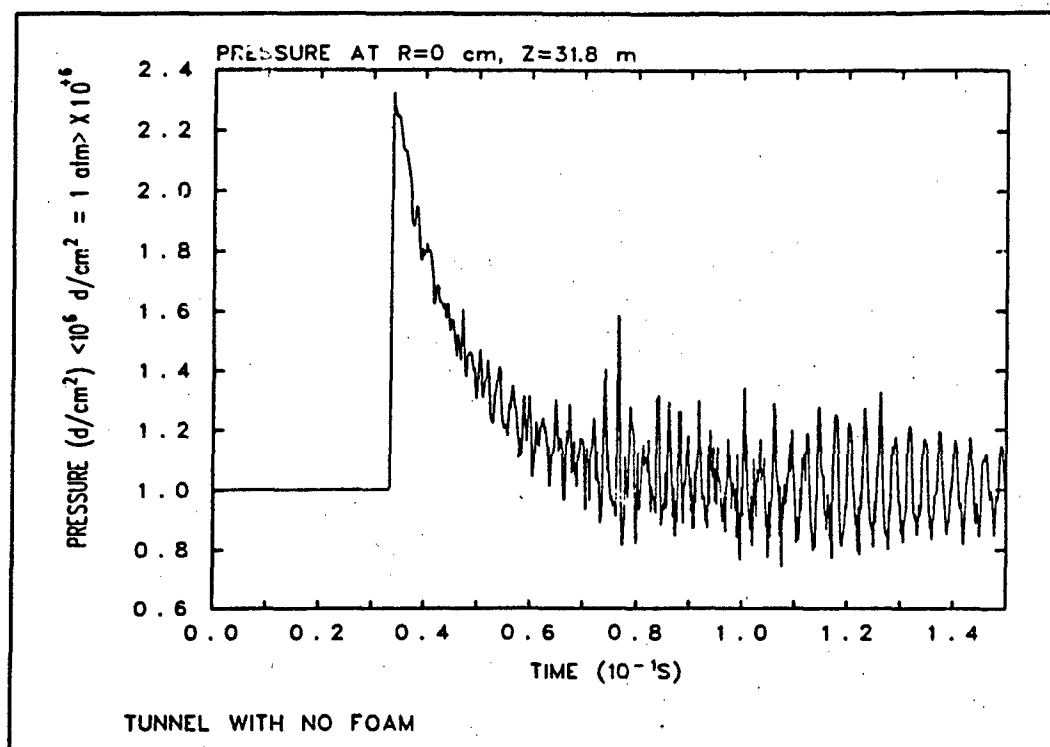


Figure 2. Sample History Plot of Pressure

Sequence of Presentation

Section II covers the problem in detail. It addresses the travel of the shock down the tunnel and the threat of bombs. It also discusses the reasons for considering foam as a possible solution to mitigating blast. Section III gives the Eulerian and Lagrangian methods of calculating shocks. It presents the basic equations and the respective advantages and disadvantages of both methods. This section also discusses different equations of state, the speed of sound in two-phase materials and the boundary conditions at the air-foam interface. Finally, this section presents an overview of the CTH code and how it combines both methods for best results. Section IV discusses the methods used to validate the results and addresses the numerical results obtained. Section V evaluates

these results and presents conclusions. The last section summarizes the conclusions and makes recommendations for further work in this area. The appendices contain the sample input files and various output plots used for the data in this report. Appendix A contains a sample of the input file used to model the tunnel with foam along with a short explanation of the file. From this and the descriptions of the test cases in this report, it is possible to recreate the results. History plots of pressure for the final test case are attached at Appendix B. These figures graphically show the mitigating effects of foam on the shock. The history plots for the other test cases are too numerous to include in this document.

II. Problem Analysis

An explosion deposits a large amount of energy in a small area in a very short time. In a conventional explosion, a major part of this energy appears as heat. This heat causes high pressures and a sudden expansion of the surrounding medium. A shock wave forms and travels outwards from the explosion. If the explosion occurs in a hallway, there are two possibilities. The walls will give way, allowing the blast to vent, or they will hold, reflecting the blast down the hall. This problem studies the latter case and searches for possible ways to mitigate the blast. This section deals with explaining the problem and discussing the reasons for looking at foam as a possible solution.

Problem

This problem examines a hypothetical underground facility. Access to this facility is through a concrete passageway. The concrete walls and the surrounding earth can contain a small explosion. Concrete walls absorb little of the shock energy, reflecting most of the energy back into the hallway. Since there is no venting, the tunnel effectively becomes a shock tube. A shock wave will form and travel in both directions with little divergence. The shock wave may damage any equipment or structures in the tunnel as well as endanger any personnel in the tunnel. Since venting is difficult, another alternative is needed to reduce the overpressure.

Alternative

Foam is a commonly used cushioning material. It is inexpensive and readily available. It can be formed and molded for any application. Its uses range from protecting items during shipments to protecting people's heels during running. Expanding on this role, this problem weighs its usefulness for absorbing the impact of a shock wave.

Three properties of foam, density, crush strength and thickness, were considered likely to affect its ability to absorb the shock's energy. These are the only properties with which this research dealt. The paragraphs below discuss the reasons for considering these properties. This model used polyurethane foam.

The density of the foam is important because the ratio of the two materials, polyurethane and air, and the size of the air bubbles determines the speed of sound in the foam. As shown in the next section, the speed of sound plays an important role in hydrodynamics. If the speed of sound is slower in the foam than the air, the foam will bleed the energy from the sides of the shock wave. This will create a diverging effect and lower the peak overpressure.

The crush strength is the overpressure at which the foam no longer has void space. The foam may absorb more energy when it is stronger, but this advantage may be countered by more reflection. The trials examine crush strengths of one, two and three atmospheres overpressure. This corresponds to about fifteen, twenty-nine and forty-two pounds per square inch overpressure. This range is consistent with the range for polyurethane foams.

The thickness may determine the amount of energy the foam can absorb. Holding other factors constant, a thicker foam can absorb more energy. The tradeoff occurs because the problem is a tunnel. As the thickness of the foam liner increases, the remaining cross-sectional area of the tunnel decreases. A decrease in the open area of the tunnel will result in higher initial pressures. The thickness was varied from five centimeters to forty centimeters. The thicker layers are impractical since they take over half the tunnel area, but they bracket the optimum thickness.

III. Theoretical Development

Understanding how shock waves travel through a medium requires a basic knowledge of fluid dynamics. Fluid dynamics is the study of fluid in motion. Expression of this motion mathematically requires three principles. These are the conservation of mass, momentum and energy. Given a relationship that describes the properties of the fluid, a solution to a specific problem is possible. This relationship is the equation of state. This section covers the Eulerian and Lagrangian forms of the conservation equations, presents simplified equations of state and discusses the role of two-phase flow in this problem. Finally, it describes the techniques that the CTH code employs to benefit from both the Eulerian and Lagrangian methods.

Eulerian Conservation Equations

The general equations for the conservation of mass, momentum and energy in Eulerian coordinates are

$$0 = \frac{\partial \rho}{\partial t} + \nabla \cdot (\rho \vec{u}) \quad (1)$$

$$0 = \frac{\partial (\rho \vec{u})}{\partial t} + \nabla \cdot (\rho \vec{u} \vec{u} + \vec{p}) \quad (2)$$

$$0 = \frac{\partial (\rho E)}{\partial t} + \nabla \cdot (\rho E \vec{u} + \vec{p} \cdot \vec{u}) \quad (3)$$

where ρ is density, t is time and \vec{u} is the velocity vector, \vec{p} is the second order tensor of

pressure and E is the total energy per unit mass (2:Chap 5,31). The variables, ρ , u , p and E , are a function of position and time. For two dimensional cylindrical coordinates, these equations become

$$0 = \frac{\partial \rho}{\partial t} + \frac{\partial(\rho \vec{u})}{\partial r} + \frac{\rho \vec{u}}{r} + \frac{\partial(\rho \vec{u})}{\partial z} \quad (4)$$

$$0 = -\frac{\partial(\rho \vec{u})}{\partial t} + \frac{\partial(\rho \vec{u} \vec{u})}{\partial r} + \frac{\partial \vec{p}}{\partial r} + \frac{\partial(\rho \vec{u} \vec{u})}{\partial z} + \frac{\partial \vec{p}}{\partial z} \quad (5)$$

$$0 = \frac{\partial(\rho E)}{\partial t} + \frac{\partial(\rho E \vec{u})}{\partial r} + \frac{\partial(\vec{p} \vec{u})}{\partial r} + \frac{\rho E \vec{u}}{r} + \frac{\vec{p} \vec{u}}{r} + \frac{\partial(\rho E \vec{u})}{\partial z} + \frac{\partial(\vec{p} \vec{u})}{\partial z} \quad (6)$$

The Eulerian form of the conservation equations has advantages and disadvantages.

They predict material values at fixed points. This is important in that it is common to our frame of reference. However, they are very difficult to solve numerically.

Lagrangian Conservation Equations

Changing from the Eulerian or lab frame of reference to the Lagrangian or particle frame of reference simplifies solving the conservation equations. The method for converting from the Eulerian form of the equations to the Lagrangian form is presented below for the general case. Expand Eqs (1), (2) and (3). Eq (1) becomes Eq (7). Multiply Eq (1) by \vec{u} and subtract from Eq (2). This produces Eq (8). Similarly, multiply Eq (1) by E and subtract from Eq (3) to produce Eq (9). Divide by ρ as necessary. This process breaks the equations into separate, identifiable pieces:

$$0 = \frac{\partial \rho}{\partial t} + (\vec{u} \cdot \nabla) \rho + \rho (\nabla \cdot \vec{u}) \quad (7)$$

$$0 = \frac{\partial \vec{u}}{\partial t} + (\vec{u} \cdot \nabla) \vec{u} + \frac{1}{\rho} (\nabla \cdot \vec{p}) \quad (8)$$

$$0 = \frac{\partial E}{\partial t} + (\vec{u} \cdot \nabla) E + \frac{1}{\rho} \nabla \cdot (\vec{p} \cdot \vec{u}) \quad (9)$$

The first term in each equation is the Eulerian time derivative. The second term is the convective term. These two terms combine to form the Lagrangian time derivative. The Lagrangian time derivative is

$$\frac{df}{dt} = \frac{\partial f}{\partial t} + (\vec{u} \cdot \nabla) f \quad (10)$$

This is the time rate of change as seen by an observer who moves with the particle. This is in contrast with the Eulerian time derivative, where the particle moves with respect to a stationary observer. Applying this relationship in Eq (10) to Eqs (7), (8) and (9), the Lagrangian general conservation equations are (4:4,8) :

$$0 = \frac{d\rho}{dt} + \rho \nabla \cdot \vec{u} \quad (11)$$

$$0 = \frac{d\vec{u}}{dt} + \frac{1}{\rho} \nabla \cdot \vec{p} \quad (12)$$

$$0 = \frac{dE}{dt} + \frac{1}{\rho} \nabla \cdot (\vec{p} \cdot \vec{u}) \quad (13)$$

CTH uses a finite difference analog of these equations. This problem uses a two dimensional cylindrical geometry. The Lagrangian conservation equations for this geometry are:

$$0 = \frac{d\rho}{dt} + \frac{\rho}{r} u_r + \rho \frac{\partial u_r}{\partial r} + \rho \frac{\partial u_z}{\partial z} \quad (14)$$

$$0 = \frac{d\vec{u}}{dt} + \frac{1}{\rho r} \vec{p} + \frac{1}{\rho} \frac{\partial \vec{p}}{\partial r} + \frac{1}{\rho} \frac{\partial \vec{p}}{\partial z} \quad (15)$$

$$0 = \frac{dE}{dt} + \frac{1}{\rho r} \left(\vec{p} u_r \right) + \frac{1}{\rho} \frac{\partial \left(\vec{p} u_r \right)}{\partial r} + \frac{1}{\rho} \frac{\partial \left(\vec{p} u_z \right)}{\partial z} \quad (16)$$

Comparing the Lagrangian two dimensional cylindrical equations (Eqs 14-16) to their Eulerian counterparts (Eqs 4-6) on page 12, notice how the Lagrangian equations are much simpler. Each has one ordinary derivative and only four terms. The Eulerian equations have more terms and each derivative is a partial derivative. CTH uses the Lagrangian form of the conservation equations with an Eulerian mesh. This is discussed in detail later in this section.

Equations of State

The conservation equations present three equations in four unknowns (density, velocity, momentum and energy). To solve a problem requires a relationship describing how the material's pressure varies with density and internal energy, $p=f(\rho, E)$. This

relationship is the equation of state. It introduces a fourth unknown, internal energy per unit mass. But total energy and internal energy are related by

$$E = I + \frac{1}{2} \vec{u} \cdot \vec{u} \quad (17)$$

which completes the system of five equations in five unknowns (4: 7).

There are many equations of state, ranging from the general purpose to the exotic. The general purpose equations of state work well for a wide range of materials and consist of a simple analytical relationship. The more exotic ones address fewer, or even just one, material and consist of elaborate analytical equations or data tables for interpolation. They should, however, provide more accurate answers. Three common equations of state are presented below for purposes of demonstration. A simple equation of state that describes ideal gases is

$$p = (\gamma - 1) \rho I \quad (18)$$

where

$$\gamma = \frac{c_p}{c_v} = \frac{\alpha + 2}{\alpha}$$

and c_p and c_v are the specific heats for the gas at constant pressure and temperature respectively (2:Chap 5,36; 4:3; 6:53-54) and α is the number of degrees of freedom of the gas. For example, monatomic gases have three translational degrees of freedom (they can move in three directions). Diatomic gases have two additional degrees of rotational freedom (7:53-54). Thus a monatomic gas has a $\gamma = 5/3$ and a diatomic gas has a $\gamma = 7/5$.

Table 1 lists some values for γ . The ideal gas equation of state has two main limitations.

It may give poor results if the gas is strongly compressed or if the gas undergoes dissolution or ionization (5:14).

TABLE 1
VALUES OF γ FOR COMMON GASES
(4:3)

GAS	γ	γ_1
air	1.4	0.4
hydrogen	1.4	0.4
helium	1.67	0.67
nitrogen	1.4	0.4
neon	1.67	0.67
carbon dioxide	1.3	0.3

The Gruneisen equation of state, given below, works well for a wide range of gases and metals.

$$p = p_H + \frac{\gamma_1}{V} (I - I_H) \quad (19)$$

where
$$p_H = \frac{s_0^2(V_0 - V)}{[V_0 - \Gamma(V_0 - V)]^2}$$

$$I_H = \frac{1}{2} \left[\frac{s_0(V_0 - V)}{V_0 - \Gamma(V_0 - V)} \right]^2$$

$$\Gamma = \frac{\gamma}{2}$$

$$\gamma_s = \gamma - 1$$

and
$$V = \frac{1}{\rho}$$

The parameters in the equations are γ_s , the Gruneisen ratio; ρ_0 , the density of the material at 0° C and one atmosphere; and s_0 , the speed of sound in the unshocked material.

A simplified form of the Gruneisen equation of state is the "stiffened gas" equation of state. It is useful when the changes in density are relatively small.

$$p = s_0^2(\rho - \rho_0) + \gamma_s \rho I \quad (20)$$

The equations of state presented here are simple cases. The ideal gas equation of state may work fine for gases; however, foam and explosives require much more robust equations of state.

CTH offers a variety of equations of state. The air was modeled using the Sesame equation of state. This is a detailed tabular equation of state that gives pressure and internal energy tabulated on a rectangular grid of discrete densities and temperatures. A special high-order (between quadratic and cubic) interpolation scheme is used to provide continuous derivatives and reasonable behavior near phase changes (5:19). The foam was modeled using the Mie-Gruneisen analytical equation of state. This model accurately represents shocks to pressures of at least 100 GPa (9.9×10^5 atmospheres) (5:13). This is more than two orders of magnitude more than that observed during this research. The Composition C-4 was modeled using the JWL (Jones-Wilkins-Lee) analytical equation of

state. The constants in the JWL formula are determined empirically from detonation experiments and then adjusted to make the calculations fit data from cylinder expansion experiments for explosives (5:14).

Sound Speed in Foam

The speed of sound in foam is not simply a combination or ratio of the speeds of sound of the materials that comprise it. It is dependent upon many properties of the foam and the individual materials. As a shock wave or sound wave strikes foam, some fraction transmits and some reflects. The transmitted wave travels through the foam, encountering the bubbles of air. Each time it encounters a bubble, some reflects, some transmits and some diffuses around the bubble. This process repeats, creating heat. Due to this process, the speed of sound in foam is extremely low. CTH incorporates the sound speed of materials into the equation of state. For this model, the default value of zero was used for the sound speed in foam.

The use of zero as the speed of sound in the foam is justified because of the way it is used in the equation of state. The equation of state defines two regions of behavior for the foam: the first is an elastic region, in which the crushing of the foam is reversible and the second region is a compaction, or inelastic, region, in which the crushing of the foam is irreversible. The speed of sound of the uncrushed foam is used to describe the elastic behavior of the foam and not the inelastic behavior (6:16-17). The foam was chosen to be inelastic because of a lack of data about the speed of sound in foam. Since the foam rebounds slowly in comparison to the propagation of the shock down the

tunnel, the effect of the foam not rebounding is negligible. If the model had used an elastic region for the foam, using a speed of sound of zero may not have been justified.

Foam Response

Understanding the damping effects of foam on acoustical waves is a first step in understanding the mitigating effects of foam on shocks. Let \vec{v} , the velocity of average flow, represent the rate of volume flow through a unit cross-sectional area normal to \vec{v} in either the air or the foam. Looking first at the foam, by defining the relationship between \vec{v} and the velocity potential of the average flow, ψ , to be

$$\vec{v} = -\nabla\psi \quad (21)$$

the equation for ψ becomes

$$\nabla^2\psi + h^2\psi = 0 \quad (22)$$

where h is a complex quantity related to the attenuation and sound speed properties of the foam. Looking at a single frequency of sound wave, the pressure is related to the velocity potential ψ by

$$p = j\omega\rho'\psi \quad (23)$$

ρ' is a second complex quantity related to the acoustic impedance of the material and ω is the frequency of interest. The parameters h and ρ' are determined experimentally.

Together, Eqs (21-23) describe the acoustical disturbance in the foam. The corresponding expressions for the velocity potential of average flow, ϕ , in the air are

$$\vec{v} = -\nabla\phi \quad (24)$$

$$0 = \nabla^2\phi + k^2\phi \quad (25)$$

$$p = j\omega\rho\phi \quad (26)$$

where k is the wavenumber ($2\pi/\lambda$) and ρ is the density of the air. The boundary conditions for a plain tunnel are

$$r = 0, \quad \phi \text{ finite} \quad (27)$$

$$r = b, \quad -\frac{\partial\phi}{\partial r} = 0 \quad (28)$$

where b is the inner radius of the tunnel. Introducing foam, where a represents the radius to the foam surface, changes the boundary conditions to

$$r = 0, \quad \phi \text{ finite} \quad (29)$$

$$r = a, \quad -\frac{\partial\phi}{\partial r} = -\frac{\partial\psi}{\partial r} \text{ and} \quad (30)$$

$$j\omega\rho\phi = j\omega\rho'\psi$$

$$r = b, \quad -\frac{\partial\psi}{\partial r} = 0 \quad (31)$$

These equations apply for a circular pipe lined with a homogenous foam and a single frequency acoustical disturbance (10: 360-364).

By applying a Fourier expansion to the shock front, it is possible to describe the shock as an infinite series of single frequency waves. The same boundary conditions will

apply. In the plain tunnel, the boundary conditions allow a planar shock front to develop. This effect is commonly observed in shock tubes. In the foam-lined tunnel, the boundary conditions at the foam face will force the shock front to become curved instead of planar. As the shock front travels down the tunnel, this curvature causes divergence of the shock, similar to that occurring in open air explosions.

CTH Code System

The CTH code system is a production code from Sandia National Laboratories. It is a multidimensional, multimaterial hydrodynamics code specifically designed for strong shock, large deformation, hydrodynamics calculations. The user sets up a model of the problem using an Eulerian mesh. Then, CTH uses the finite-difference analogs of the Lagrangian equations (1: i) developed earlier in this section. During this step, the cells distort as they follow the material. After each time step, it rezones the problem back to the original Eulerian mesh. It uses an Eulerian differencing scheme during the remesh step (8:1). The purpose of this remesh step is to prevent the computational cells from becoming entangled and to maintain an optimal shape; however it also allows histories of parameters at fixed points. It maintains data at specified intervals for the histories at points and for snapshots over the entire problem. These outputs can then be processed to view graphically. In this way, the CTH code system maximizes performance by using the Lagrangian form of the conservation equations while enabling graphic output in the laboratory frame of reference.

IV. Test Cases and Results

The experiment plan consisted of a series of six test cases, each one building upon the previous. The first test case consisted of a plain tunnel of one meter radius and indefinite length. The calculation mesh extended twenty-five meters down the tunnel and was comprised of five-centimeter square computational cells. This test case provided the standard against which the foam lined tunnels would be judged. The second test case was identical to the first, except that 3.3-centimeter square computational cells were used. The purpose of this test case was to validate the first. If the results between the two are the same, then the calculation mesh of the first test case is sufficiently small. The final four test cases used foam lined tunnels. The initial foam test case varied either the thickness, density or crush strength for three values, while holding the other two constant. Nine problems held the density constant at forty percent void and varied the crush strength and thickness. The crush strength was examined at one, two and three atmospheres overpressure and the thicknesses used were ten, twenty and thirty centimeters. Two additional problems held the crush strength at two atmospheres and the thickness at twenty centimeters while the density was changed to twenty and sixty percent void respectively. From the trends noted in this test case, the second foam test case further explored two of these parameters. This test case consisted of twelve problems. The density was varied in steps of ten from forty to ninety percent void for five and ten centimeters of foam. These results required a third foam test case to evaluate one parameter. The thickness was varied in steps of five from five to forty

centimeters while holding the density constant at ninety percent void. The fourth test case used numerous tracers to track the material flow and confirm previous runs. The model validation and results are presented in the sections below, followed by a summary.

Model Validation

The same problem with a smaller mesh validated the model. Setting the cell size to 3.3 centimeters, the plain-wall tunnel was recalculated. Table 2 presents the results of the proof run and the normal run with five centimeter cells. Although the energy introduced by the explosive is the same in each case, the finer mesh calculates a much higher initial pressure. This is due to the way CTH calculates the material properties at tracer points. For example, to determine the pressure, which is a cell centered value, at a point other than the cell center, CTH uses the values in the surrounding cells to report an averaged pressure. At the center of the explosive, the pressure increase is extremely sharp. The peak of the pressure pulse is not spread out over several cells, but is contained within a fraction of the first cell. The average pressure in a smaller cell would be significantly higher because the peak of the pressure pulse spreads out over more of the cell. However, after the pressure pulse has spread out into a normal shock front and the peak occupies several cells, the difference between the pressures obtained with the five centimeters square mesh and that with the smaller mesh should and does become much less.

At twenty meters from the explosion the results agree to within five percent with the error decreasing, as shown in Table 2. Due to the greater error within twenty meters of the explosion, all conclusions presented will be based on points outside this limit. The

error of the numerical results is unknown due to the limit on the number of cells and the resulting limit on cell size, but subject to the constraint above, it is estimated to be less than 5.0 percent.

TABLE 2
COMPARISON OF PROOF AND NORMAL TEST CASE

Axial Distance (m)	<u>Overpressure (atm)</u>		% Error
	Proof	Normal	
0	2580	155	94
5	10.4	7.6	27
10	3.2	3.0	6.3
15	2.55	2.32	9.0
20	1.85	1.76	4.9
25	1.60	1.48	4.5

*measured on axis of tunnel, radius = 0.

Initial Foam Test Case

The initial foam test case consisted of eleven problems. Nine of these problems held the density constant at forty-percent void. The crush strength values changed between one, two and three atmospheres for each thickness of foam. The thicknesses used were ten, twenty and thirty centimeters. The final two problems set the crush

strength to two atmospheres and the thickness to twenty centimeters. The density values were twenty-percent and sixty-percent void. Tables 3 and 4 display the results of the first test case. The trends noted from Table 3 were: (1) the crush strength has little effect on the overpressure; and (2) the overpressure decreased as the foam thickness decreased. The trend noted from Table 4 was that the overpressure decreased as the foam density decreased. These trends point toward a thin layer of light foam with an arbitrary crush strength.

TABLE 3

**OVERPRESSURES OBSERVED* IN INITIAL FOAM TEST CASE (atm)
(Density 40% Void)**

Crush Strength	<u>Thickness</u>		
	10 cm	20 cm	30 cm
1 atm	1.48	1.54	1.76
2 atm	1.48	1.55	1.76
3 atm	1.48	1.55	1.76

* measured on center axis, 25 meters from explosion

It is interesting to note that the only problem that achieved a reduction in overpressure compared to the plain tunnel was the low density foam. The other foams actually increased the pressure for the first twenty-five meters. This effect is due to the decreased cross sectional area of the tunnel. With twenty centimeters of foam, the cross-

sectional area of the air passage is sixty-four percent of the original tunnel. Yet the densest foam (twenty percent void) shows only a ten percent increase in pressure. From this perspective, it is clear the foam is having an effect on the shock. Determination of the extent of these effects requires additional computations.

TABLE 4
OVERPRESSURES OBSERVED* IN INITIAL FOAM TEST
CASE
(Crush Strength 2 atm; Thickness 20 cm)

<u>Void Space (%)</u>	<u>Overpressure (atm)</u>
20	1.63
40	1.55
60	1.41
*measured on center axis, 25 meters from explosion	

Second Foam Test Case

From the results above, the next test case experimented with a range of lighter and thinner foams. The values of density used were forty, fifty, sixty, seventy, eighty and ninety percent void. Thicknesses used were five and ten centimeters. The five-centimeter calculation mesh imposed a minimum on foam thickness and thinner foam could not be modeled. Crush strength was set at two atmospheres and not changed throughout the rest of the test cases. Table 5 displays the results from this test case.

The trend continued for the density. The overpressure continued to decrease ever more rapidly. This raised concerns that the foam model was inaccurate. The CTH code uses void instead of air, which is found in real foams, and the model employed a simplistic model of foam. This was discussed on page 4. Additionally, the trend of a thinner foam liner being more effective in mitigating the shock reversed. At sixty percent void, both five and ten centimeters of foam resulted in the same overpressure at twenty-five meters distance. For even less dense foams, the thicker layer was the more effective. The pressures for both thicknesses continued to fall as the density shrank.

TABLE 5

OVERPRESSURES OBSERVED* IN SECOND FOAM TEST CASE (atm)

Void (%)	<u>Thickness</u>	
	5 cm	10 cm
40	1.42	1.48
50	1.40	1.45
60	1.38	1.38
70	1.32	1.30
80	1.25	1.18
90	1.10	0.90

* measured on center axis, 25 meters from explosion

Third Foam Test Case

The mixed results above required an addition test case. To check the foam model, I varied the thicknesses over a wider range while keeping density fixed at ninety percent void. As the foam thickens, a minimum should be reached where the constriction of the foam cancels its effects of mitigating the shock. If the overpressure continued to decrease, this would suggest the void in the foam was dominating the calculation and introducing errors. Reaching a minimum overpressure suggests that the foam model is realistic. This would match Morse's conclusion of a stiff, light material absorbing more than a less stiff, heavier material (9:210). Table 6 presents the results of the final runs.

Overpressure at 22.7 meters reaches a minimum with a foam thickness of twenty centimeters. Although a minimum does not occur at fifty meters, the overpressure's rate of descent slows. Table 7 shows a more detailed look at the distance between 22.7 meters and fifty meters. The rate of descent of the overpressure has reversed at 27.3 meters. These results give assurance that the foam model is reasonable and that the trends noted are valid.

TABLE 6

OVERPRESSURES OBSERVED* IN THIRD FOAM TEST CASE (atm)
(90% Void)

Thickness (cm)	<u>Axial Distance</u>	
	22.7 meters	50 meters
0	1.60	0.93
5	1.25	0.65
10	1.08	0.46
15	0.96	0.35
20	0.89	0.29
25	0.98	0.24
30	1.03	0.20
35	1.03	0.18
40	1.01	0.17

* measured on center axis

TABLE 7
OVERPRESSURES OBSERVED* BETWEEN 25 AND 50 METERS (atm)
(90% Void)

Thickness (cm)	<u>Axial Distance (m)</u>				
	27.3	31.8	36.4	40.9	45.5
20	0.79	0.59	0.47	0.40	0.29
25	0.73	0.57	0.44	0.34	0.24
30	0.73	0.56	0.41	0.32	0.20
35	0.73	0.53	0.39	0.31	0.18
40	0.74	0.51	0.36	0.29	0.17

* measured on center axis

Table 8 presents the overpressures from 4.55 to 50.0 meters at the center axis of three tunnels; the plain tunnel and those with ten and twenty centimeters of ninety percent void foam lining. A plot of these values appears in Figure 3.

TABLE 8

OVERPRESSURES* OBSERVED OVER TUNNEL LENGTH (atm)

Axial Distance (m)	Foam Thickness (cm)		
	0	10	20
4.55	4.20	6.50	8.90
9.09	4.25	2.42	2.65
13.64	2.15	1.75	2.72
18.18	2.00	1.28	1.73
22.73	1.60	1.07	0.89
27.27	1.46	0.89	0.79
31.82	1.29	0.80	0.59
36.36	1.24	0.67	0.47
40.91	1.16	0.59	0.40
45.45	1.08	0.51	0.33
50	0.94	0.47	0.22

* measured on center axis

The results from Table 8 present one anomaly. The pressure is not monotonically decreasing. Local peaks occur a short distance from the explosion. The effect is especially noticeable when comparing the original runs with the ones after I had

inadvertently shifted the tracers. There are two possible explanations: (1) the local peak occurs where the reflections of the shock off the walls merge with the leading edge of the shock, forming a mach stem, or (2) the local peak is due to reverberations of the shock traveling radially in the tunnel.

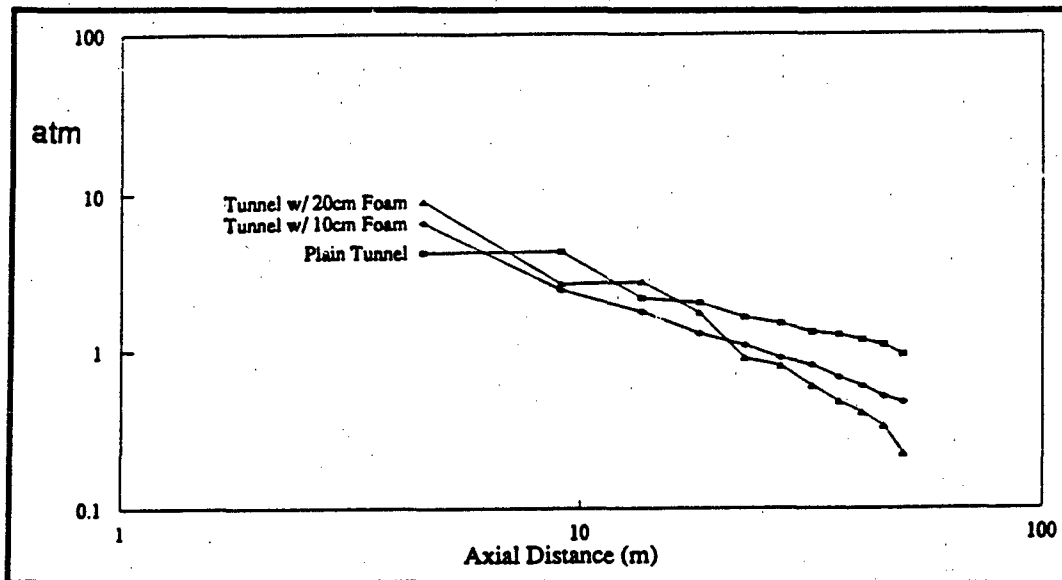


Figure 3. Graph of Peak Overpressures from Table 8

Figure 3 above displays the values from Table 8 on a log-log plot. One would expect a straight line from a fully formed shock, with the slope being the rate of divergence. The tunnel with ten centimeters of foam almost approaches a straight line, while the other two tunnels clearly have oscillations present. It is unwise to assume that no mach stem formed in the tunnel with ten centimeters of foam, and likewise, that the ten-centimeter thick layer of foam completely damped the radial oscillations. To determine which is the case, another test case is required.

Final Foam Test Case

For the fourth foam test case, the previous runs with no foam and ten, twenty and thirty centimeters of foam were rerun, with the addition of numerous tracers. The tracers can be broken into three groups. The first group consisted of fixed (Eulerian) tracers. They were placed along the tunnel axis at radii of zero, thirty and sixty centimeters radius. The next two groups were Lagrangian tracers used to determine material flow. One group was placed along the tunnel axis at radii of thirty and sixty centimeters concurrent with the Eulerian tracers. The last group was placed radially from zero to one meter at distances of zero, fifteen, thirty and forty-five meters down the tunnel.

Figure 4 shows an area snapshot of tracer positions at one point in time. The Eulerian tracers are used in these plots to indicate the original position of the tracers. The Lagrangian tracers indicate material flow. The solid line on the right is the air-foam interface. The remaining lines at the bottom of the plot are the interfaces between air and gases from the explosive and are not of importance for this problem.

Note that the foam does not fully compress. To be fully compressed, the ninety percent void foam would compress to ten percent of its volume, at least. This is reasonable behavior from actual foam, indicating that the foam model is accurate. Actual foam would compress to near its maximum, before rupturing and releasing the air it contained. The foam model compresses by losing void. This has the same effect as actual foam compressing and outside air filling in the empty space left. Thus, the foam model is accurate until pressures are reached where actual foam would rupture. This reinforces the assumption that the void in the foam has negligible effect on the results.

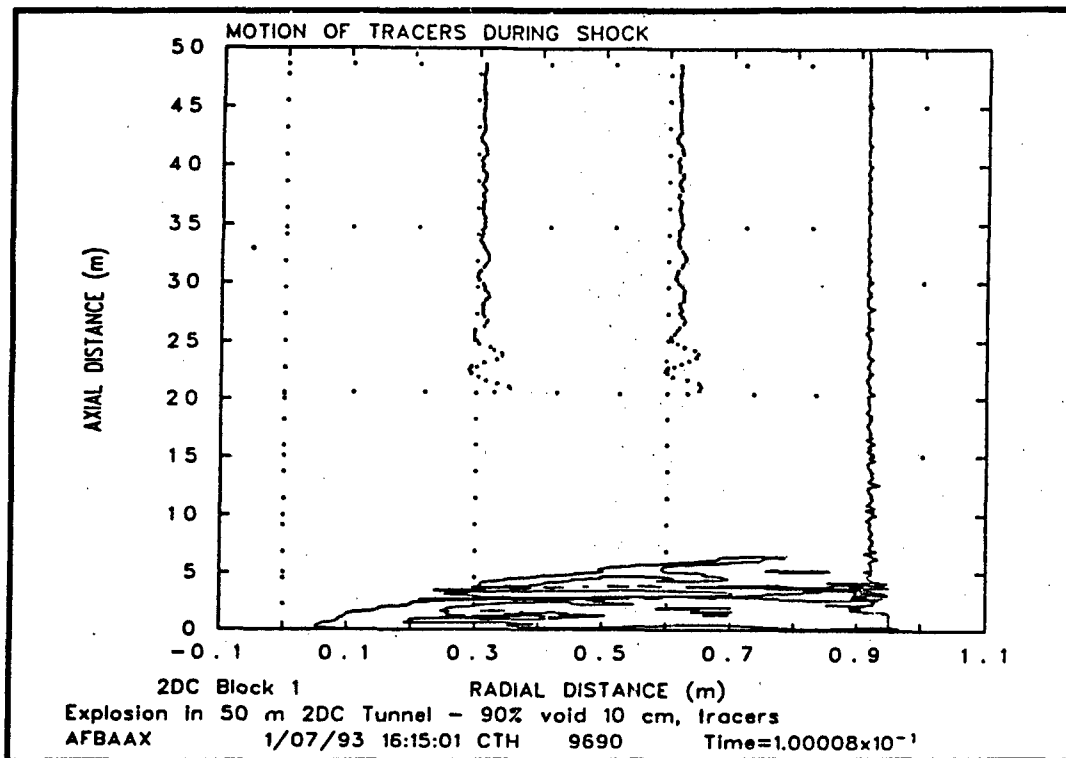


Figure 4. Material Flow as Shock Propagates Down a Foam-Lined Tunnel

In all four problems, the axial Lagrangian tracers indicated that the local peaks were due to reverberations. The tracer pattern is similar to that of a damped sinusoidal wave, indicating that the reverberations die out. Additionally, the tracers move radially outward in the tunnels with foam. This is expected because of the compression of the foam under pressure. Using the peak initial pressures observed at the fixed Eulerian tracers, figures 5 through 8 present contour plots of the peak pressures observed over the tunnel. The plots indicate that the reverberations die out shortly after thirty meters. Each figure uses the same pressure values for contour lines.

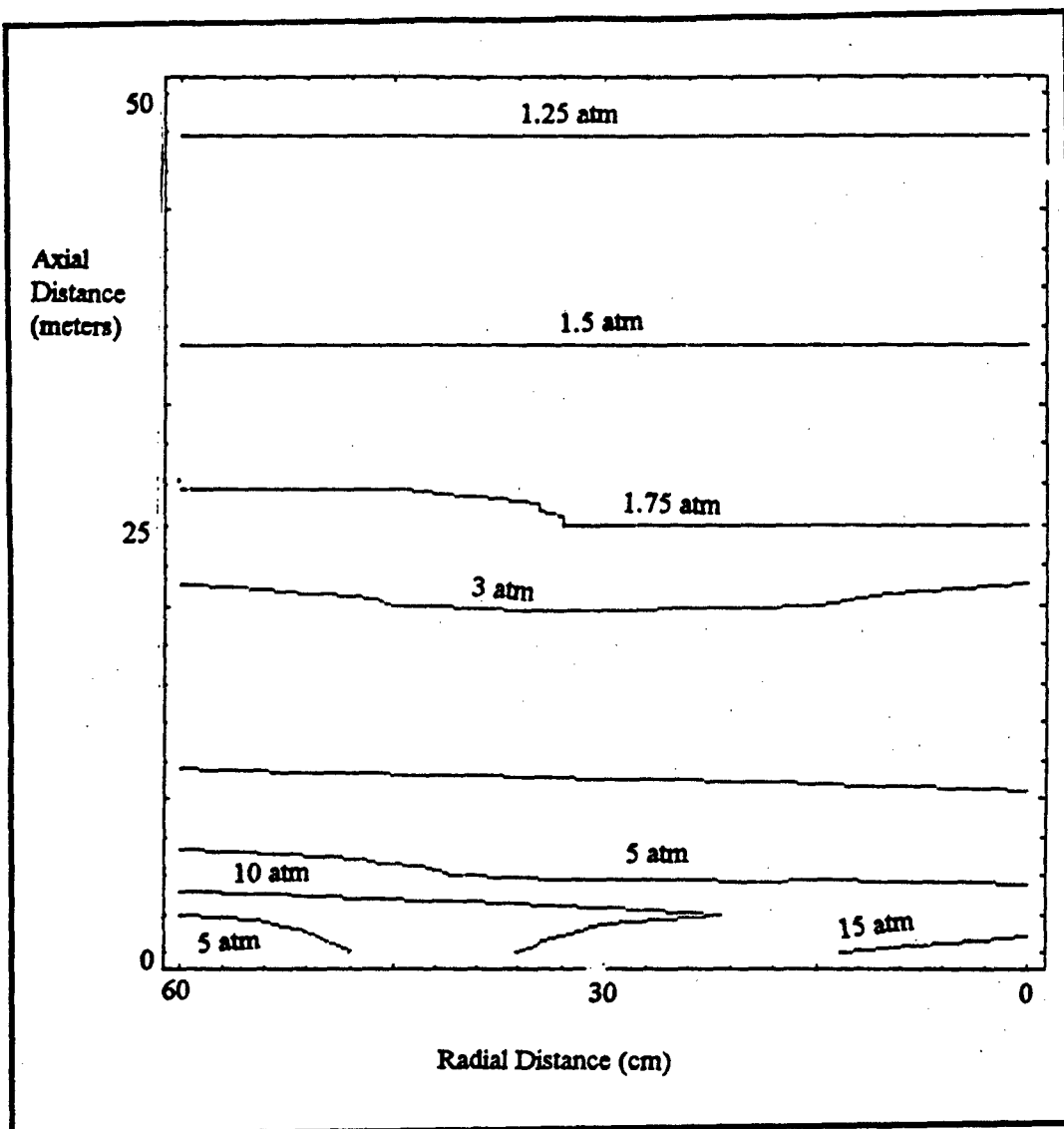


Figure 5. Contour Plot Of Peak Pressures vs. Distance In Tunnel With No Foam

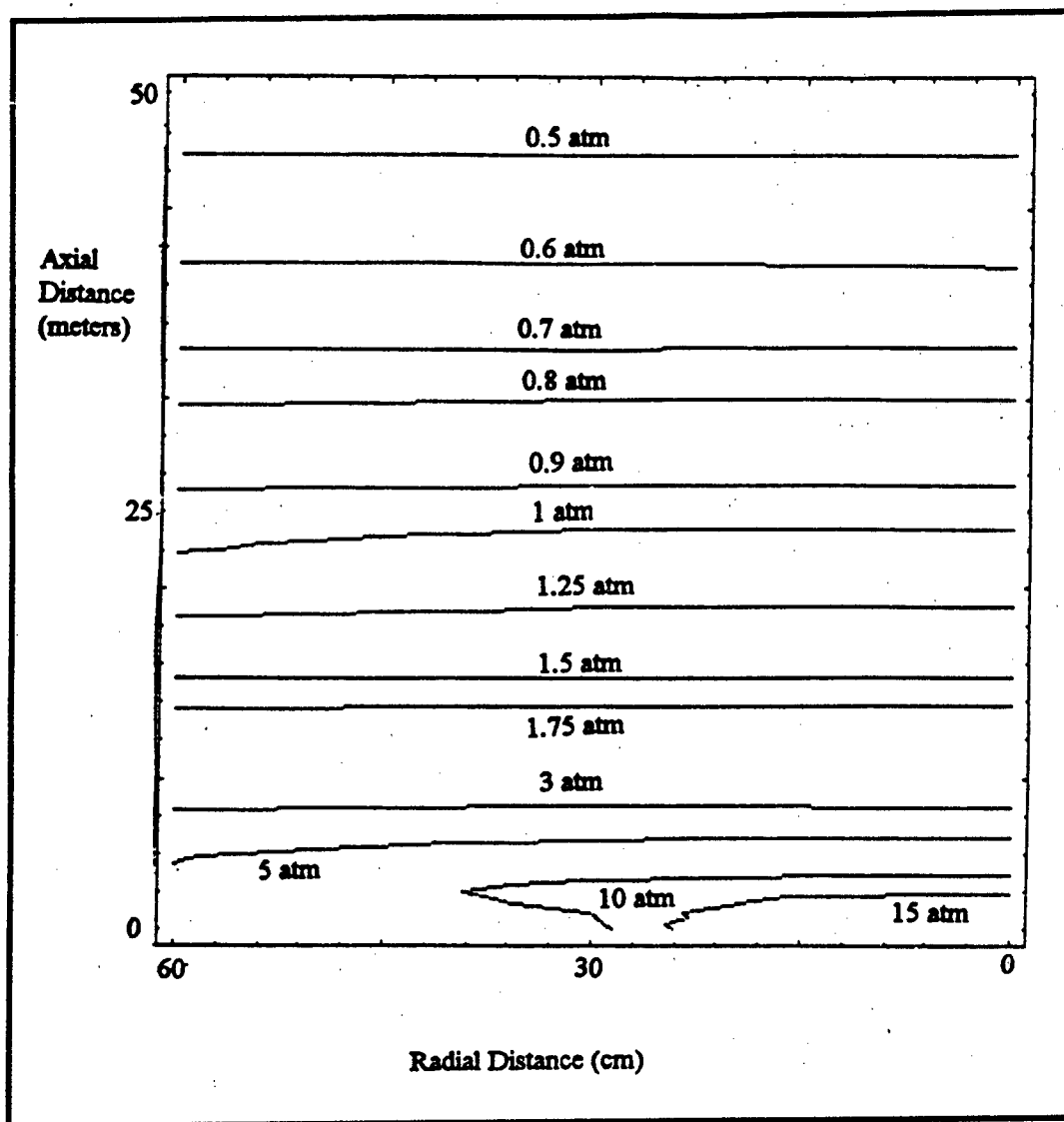


Figure 6. Contour Plot Of Peak Pressures vs. Distance In Tunnel With 10 Cm Foam

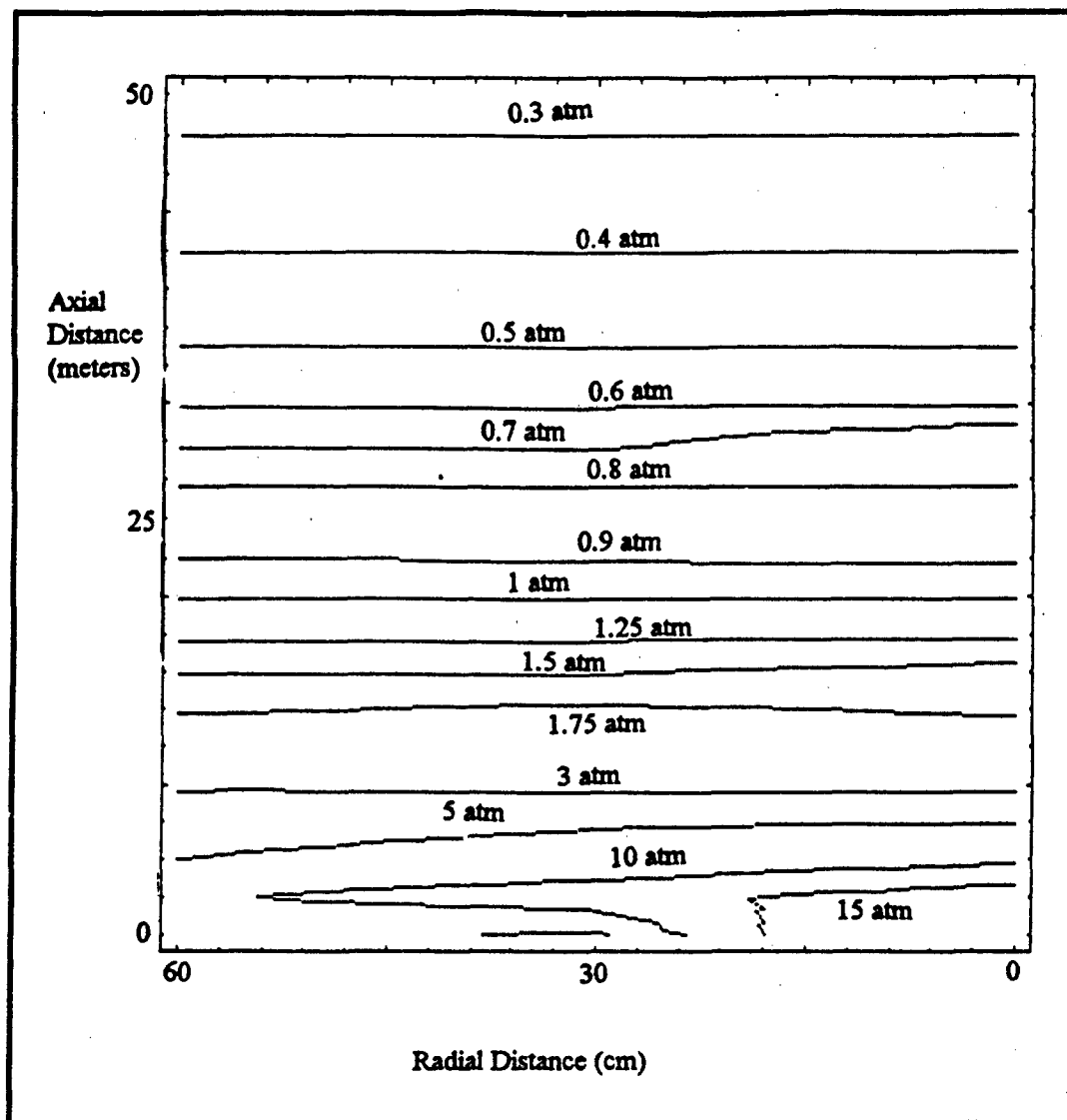


Figure 7. Contour Plot Of Peak Pressures vs. Distance In Tunnel With 20 Cm Foam

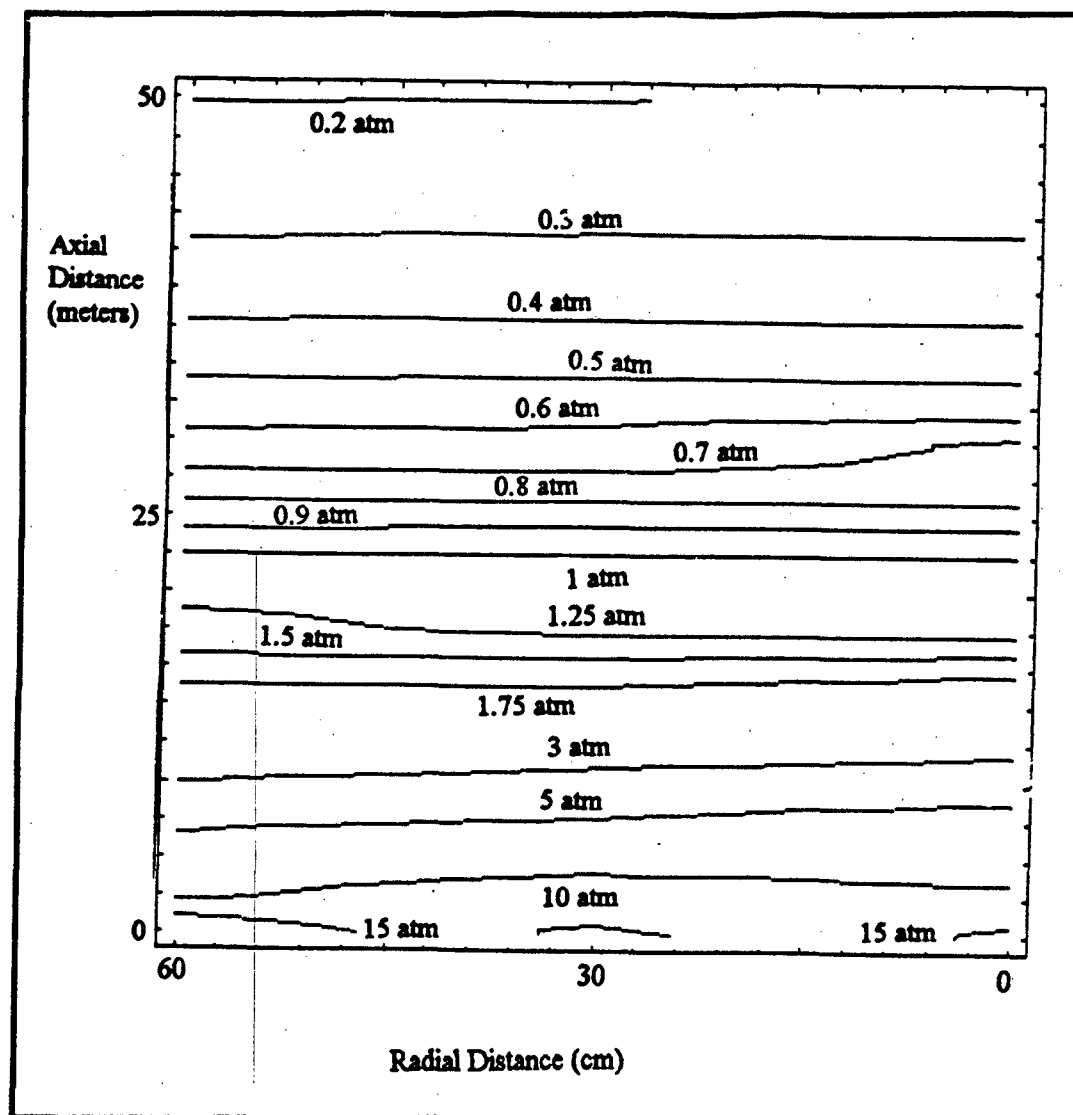


Figure 8. Contour Plot Of Peak Pressures vs. Distance In Tunnel With 30 Cm Foam

The data used to generate the contour plots above are presented in Table 9 on the next page. CTH could not generate the contour plots because the peak pressures occurred at different times for different points. I measured the peak overpressures for each point from the pressure history and then used Mathematica to do the contour plots.

TABLE 9

OVERPRESSURES OBSERVED IN FINAL FOAM TEST CASE (atm)

Axis Dist. Z(m)	No Foam Radius (cm)			10cm Foam Radius (cm)			20cm Foam Radius (cm)			30cm Foam Radius (cm)		
	0	30	60	0	30	60	0	30	60	0	30	60
0.0	20	7.4	3.1	42	8.4	8.4	31	4.1	7.5	16	8.6	20
2.3	15	11	7.4	13	12	5.6	18	13	9.3	12	14	8.8
4.5	6.6	4.1	4.4	6.5	6.2	4.8	8.9	6.2	5	6.5	7.4	5.8
6.8	4.2	4.2	3.7	3.2	3.2	3.1	4.7	4.7	3.9	6.6	5.1	4.5
9.1	3.7	3.4	3.1	2.4	2.6	2.5	2.6	2.5	2.8	3.3	3.2	3.0
11.4	2.8	2.6	2.6	2.3	2.1	2.0	2.0	2	2.2	2.9	2.7	2.4
13.6	2.2	2.2	2.3	1.7	1.7	1.7	1.7	1.8	1.7	2.0	1.9	1.9
15.9	2.3	2.2	2.1	1.4	1.4	1.4	1.6	1.5	1.5	1.7	1.6	1.6
18.2	2.0	2.0	1.9	1.3	1.3	1.3	1.2	1.2	1.2	1.2	1.2	1.3
20.5	1.8	1.7	1.8	1.2	1.2	1.1	1.0	1.0	1.0	1.2	1.2	1.2
22.7	1.7	1.7	1.7	1.1	1.1	1.0	0.88	0.89	0.90	1.0	1.0	1.0
25.0	1.6	1.5	1.5	0.93	0.93	0.93	0.86	0.85	0.85	0.86	0.86	0.85
27.3	1.5	1.5	1.4	0.89	0.89	0.88	0.79	0.79	0.79	0.72	0.72	0.72
29.5	1.5	1.4	1.4	0.89	0.84	0.85	0.79	0.68	0.68	0.72	0.63	0.62
31.8	1.3	1.3	1.3	0.80	0.80	0.79	0.59	0.59	0.59	0.55	0.55	0.55
34.1	1.3	1.3	1.3	0.72	0.72	0.72	0.53	0.53	0.53	0.48	0.48	0.47
36.4	1.2	1.2	1.2	0.67	0.66	0.66	0.47	0.47	0.47	0.41	0.41	0.41
38.6	1.2	1.2	1.2	0.62	0.63	0.63	0.43	0.43	0.43	0.37	0.37	0.36
40.9	1.2	1.2	1.2	0.58	0.58	0.58	0.40	0.40	0.40	0.32	0.32	0.31
43.2	1.1	1.1	1.1	0.55	0.55	0.55	0.37	0.37	0.37	0.28	0.28	0.28
45.5	1.1	1.1	1.1	0.51	0.51	0.51	0.33	0.33	0.33	0.25	0.25	0.25
47.7	1.0	1.0	1.0	0.49	0.49	0.49	0.30	0.30	0.30	0.22	0.22	0.21
50.0	0.96	0.96	0.96	0.46	0.46	0.46	0.28	0.28	0.28	0.21	0.20	0.20

V. Conclusions

The trends show that the best foam is a low density foam. The trends also suggest that a thick layer of foam is best at a greater distance and that a thinner layer of foam is better at smaller distances. Close to the explosion, however, a layer of foam actually increases the overpressure because its mitigating effect is less than the constriction effect. The optimum foam thickness depends on the length of the tunnel and upon how much shock mitigation is desired. As shown in Table 8, a ninety-percent void layer of foam twenty centimeters thick would do best in a twenty-five meter tunnel, provided the explosion occurred at that distance. It would take longer for a thicker layer of the same foam to achieve the same reduction. The next concern is practicality. A thick foam liner is impractical. It would be fine for a tunnel made for experiments, but it is unworkable for an actual tunnel as described on page 10.

The numbers presented are subject to an undetermined amount of error. The paragraphs below attempt to evaluate these numbers and place physical significance on them. Comparing the results in Table 9 at fifty meters, the tunnel with ten centimeters of foam shows over fifty percent reduction in the peak overpressure. The tunnels with twenty and thirty centimeters of foam show even more, a seventy-percent and seventy-eight-percent reduction respectively.

Table 10 presents criteria for direct blast effects on man. Units were converted to atmospheres for comparison. In the plain tunnel, the overpressure exceeds the lung damage threshold values for about the entire length of the tunnel. However, the foam

lined tunnels in Table 7 do much better. With ten centimeters of foam, the overpressure drops below this threshold around thirty meters and with twenty centimeters of foam, it drops below about twenty-five meters. Where the shock drops below this threshold is questionable, because the reverberations are still significant at less than thirty meters from the explosion.

TABLE 9
TENTATIVE CRITERIA FOR DIRECT
BLAST EFFECTS IN MAN (3:552)

<u>Effect</u>	<u>Overpressure (atm)</u>
Lung Damage:	
Threshold	0.82
Severe	1.70
Lethality:	
Threshold	2.72
50 percent	4.22
100 percent	6.26
Eardrum Rupture:	
Threshold	0.34
50 percent *	1.02-1.36
* more than 20 years old	

The error for the figures obtained from CTH is estimated to be less than five percent. This is based on the calculations on page 26. A more exact estimate for the error cannot be calculated for the problem for several reasons: (1) no data with which to compare; (2) insufficient resolution obtained due to problem size and restriction on

number of computational cells; and (3) inability to extract numbers out of program output. The program does have the ability to extract numbers for each cell, but the file storage space required exceeds the available hard drive space. The resolution problem was the most acute. Since the reverberations were significant for over 30 meters, the problem needed to extend 50 meters. The built-in limit of 1000 computational cells restricted the mesh size to 5 centimeters. There are two possible solutions which would have worked around this limit. They are discussed in the next section. Despite these shortcomings, the trends noted and the results are promising.

Overall, the results indicate that foam does significantly reduce the peak overpressure of a shock. The results do not indicate a numerical formula for calculating this reduction. The reason that an analytical relationship is not attainable is because of the limitations of the model. The foam modeled, although determined realistic, was not determined accurate. Also, the boundary conditions used a rigid tunnel wall which did not absorb any of the shocks energy.

VI. *Recommendations*

This project delved into an area that few have studied. Although many have studied the acoustical damping properties of foam, I found no studies of the effectiveness of foam in absorbing large air shocks. This study had many shortcomings, but it also made some promising discoveries. In the next few paragraphs, I will recommend further work in this area and further applications for the CTH code system.

The problem examined in this paper may be expanded in several ways. It is possible, with help from Sandia National Laboratories, to modify the code to allow more computational cells. While this would address the accuracy question, it would introduce extremely long run times. Another option is to do away with symmetry at the tunnel center. Instead of mirroring the left and right sides of the tunnel, move the left boundary back a few cells. Then establish a semi-infinite boundary at the left side. By inserting the same amount of explosive at the same place, in effect the amount of explosive is halved because the explosive is no longer mirrored on the other side. This in turn would decrease the peak pressures that require the small time steps. Non-uniform meshing would have helped to a lesser extent. By applying a smaller mesh close to the explosion, and increasing the mesh size further away, better accuracy would have been obtained. This method would have increased the run time to a lesser extent than other methods discussed here, but it also has practical limits. The cell size must be changed slowly from one cell to the next to avoid numerical instabilities. Rezoning was a possibility ruled out. For example, rezoning is useful when you must build a particular effect, such as an ideal blast

front, and then study its interaction with an object. Rather than build this effect for each problem, you can build it once, and then save it to reuse over and over again. For this research, the foam properties consistently changed and the explosion was occurring a short distance from the foam. There was practically no time between the effect (explosion and blast) and the interaction (foam response) and hence, no time savings. Recognizing these points earlier in my research would have greatly increased the accuracy of the problems.

Much work remains to be done on modeling foam. Future work could include experimental shock tube projects to further numerical work using CTH or a similar code. A particular area that needs work is calculating the speed of sound in foam and building an equation of state for various foams. Most texts on hydrodynamics do not discuss the speed of sound through a multiphase material. They only discuss the flow of the multiphase material. Scientists from DOW Chemical and ARCO were unable to assist in this matter. Any future work using foam should strive to model foam more accurately.

Other shock tube problems of interest include design of a rarefaction wave eliminator, either through shaping the tunnel, using a damping material like foam, or both. Additionally, modeling the effects of a nuclear blast at a tunnel entrance and trying to mitigate the shock inside the tunnel would be a likely project for CTH. These problems would be improved by expanding them to three dimensions, depending on computer resources.

The CTH code system is a very powerful tool. The blast problems presented in this paper only scratch the surface of this program's capabilities. Anyone in the physics

department can find this a useful tool, but CTH does have its limitations. The primary limitation is the computing power and storage space it requires. The initial and intermediate runs took twenty-four hours each to finish on the SUN SPARC 2® workstations. The final runs took two and a half days each. Even with a minimum of file dumps, each problem takes from sixty to one hundred megabytes of disk space to run. Thus, CTH needs a dedicated machine with a storage capacity of at least a gigabyte of hard disk space per user. Also, the machine should be much faster than the Sun workstations used in this project.

Appendix A: Sample Input File For Modeling Tunnel With Foam

The purpose of this appendix is to present and explain a sample input file. From this file and explanation, it is possible to recreate the test cases used in this research.

The first part of the file is the input file for the CTHGEN program. This sets up the model. The second part of the file is the input file for the CTH program. This sets up the run parameters. These are discussed in detail in reference 1.

The first section that is modified for each problem is the title record. This provides a title for the problem that normally appears at the bottom of all plots produced. It is the primary method of keeping the different output plots with their input files. This section appears at the front of both parts of the file and both places should be the same.

The next section is the mesh records. This section establishes the calculation mesh and the active region. (The program does not calculate an inactive region until it becomes active.) By limiting the active region to the area around the explosive, the program does not calculate the cells where nothing is changing. This saves in computation time. X and Y correspond to R and Z in this case.

The material insertion records are modified in two ways. For varying the thickness of the foam liner, the "p1" values for both the air and foam must be adjusted accordingly. Also, for a plain tunnel, the foam is not inserted and the air encompasses the entire region.

The foam section of the equation of state records must be altered in several ways for each problem. The "rp" value represents the foam density and is expressed as a

fraction of the solid density, "r0." The crush strength is represented by two values, "pe" and "ps", the pressure where elastic compression ends and the pressure where the foam is fully compacted respectively. Additionally, the speed of sound may be included by adding a statement "ce= value " where value is the desired speed.

The tracer records establishes tracers throughout the zone of the problem.

Tracers are Lagrangian by default unless specified as fixed. The program numbers the tracers sequentially starting at one in the order that they are introduced in this section.

The tracers are referred to as "Lagrangian Point #", irregardless of whether it is an Eulerian or a Lagrangian tracer.

The problem run time is set in the control records in the CTH input file. This is changed in these problems from 0.5 seconds for the twenty-five meter long calculation mesh to 1.5 seconds for the fifty meter long calculation mesh.


```

        endy
        xact 0 15
        yact 0 15
    endb
endm
*
*****
*
* Material Insertion Records
*
insertion
    block 1
*
        package foam
            material 3
            numsub 50
            pressure 1.0e6
            insert box
                p1 80 0
                p2 100 5000
            endi
        endp
*
        package explosive
            material 2
            numsub 50
            pressure 1.0e6
            insert box
                p1 0 0
                p2 5 5
            endi
        endp
*
        package ambient air
            material 1
            numsub 50
            pressure 1.0e6
            insert box
                p1 0 0
                p2 80 5000
            endi
        endp
*
    endb
endi
*
*****
*
* Edit Records
*
edit
    block 1

```

```

        expanded
    endb
ende
*
*****
*
* Equation of State Records
*
eos
*
* air
*
    mat1  sesame
        eos 5031  feos 'aneos'
*
* explosive - Comp C-4 (similar to SEMTEX)
*
    mat2  jwl
        eos COMPC-4
*
* foam - polyurethane (values from Mie-Gruenisen table)
*
    mat3  mgrun  r0=1.265  cs=2.486e5  s=1.577  g0=1.55
           cv=1.e10  rp=0.1265  pe=1e6  ps=3e6
*
ende
*
*****
*
* HE Burn Records
*
heburn
    mat 2  d 8.8e5
    dp 2 2  r 1  ti 0
endh
*
*****
*
* Tracer Records
*
tracer
    block 1
        add 0 0 to 0 5000 n 23 fixed xy
        add 0 500 to 0 2500 n 5 fixed xy
        add 30 0 to 30 5000 n 23 fixed xy
        add 60 0 to 60 5000 n 23 fixed xy
        add 0 0 to 100 0 n 11
        add 0 1500 to 100 1500 n 11
        add 0 3000 to 100 3000 n 11
        add 0 4500 to 100 4500 n 11
        add 30 1500 to 30 4500 n 101
        add 60 1500 to 60 4500 n 101

```

```

    endb
endt
*
*****
*****
*****
*
*eor* cthin
*
*****
*
* Title Record
*
Shock Waves in 50 m 2DC Tunnel - 90% void 20 cm, tracers
*
*****
*
* Control Records
*
control
    tst 0.15    *stop time in seconds
endc
*
*****
*
* Cell Thermodynamics Records
*
cellthermo
    mmp
endc
*
*****
*
* Convection Records
*
convct
    int high    * high resolution interface tracking
endc
*
*****
*
* Boundary Condition Records
*
boundary
    bhydro
        block 1
            bxtop 0
            bxbot 0
            bytop 1
            bybot 0
        endb
    endh

```

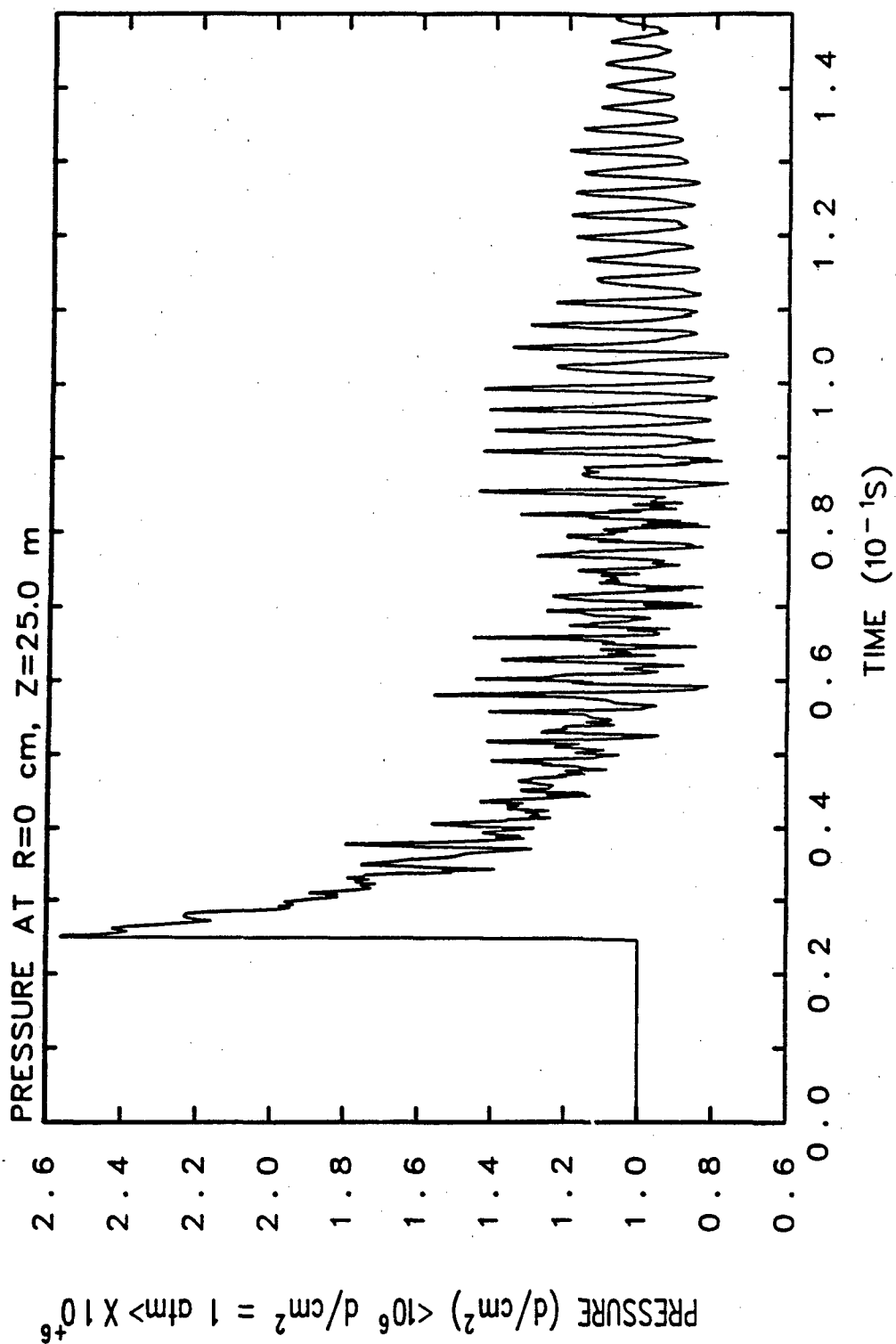
```

endb
*
*****
*
* Edit Records
*
edit
*
    shortt
        time 0.    dt 1e-2
    ends
*
    longt
        time 0.    dt 1e-2
    endl
*
    plott
        time 0.    dt 1e-2
    endp
*
    histt
        time 0.    dt 5e-5
        htr all
    endh
*
ende
*
*****

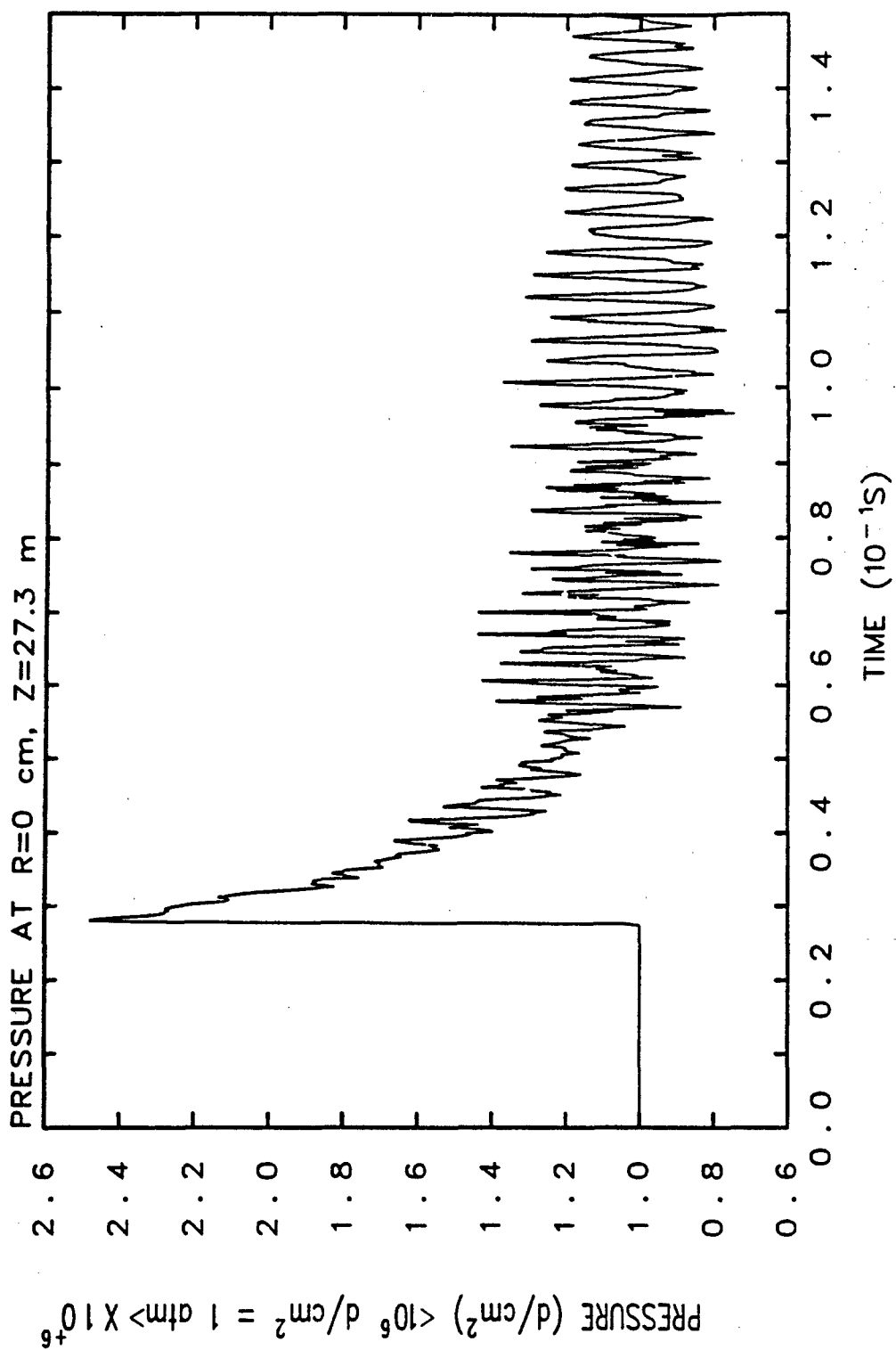
```

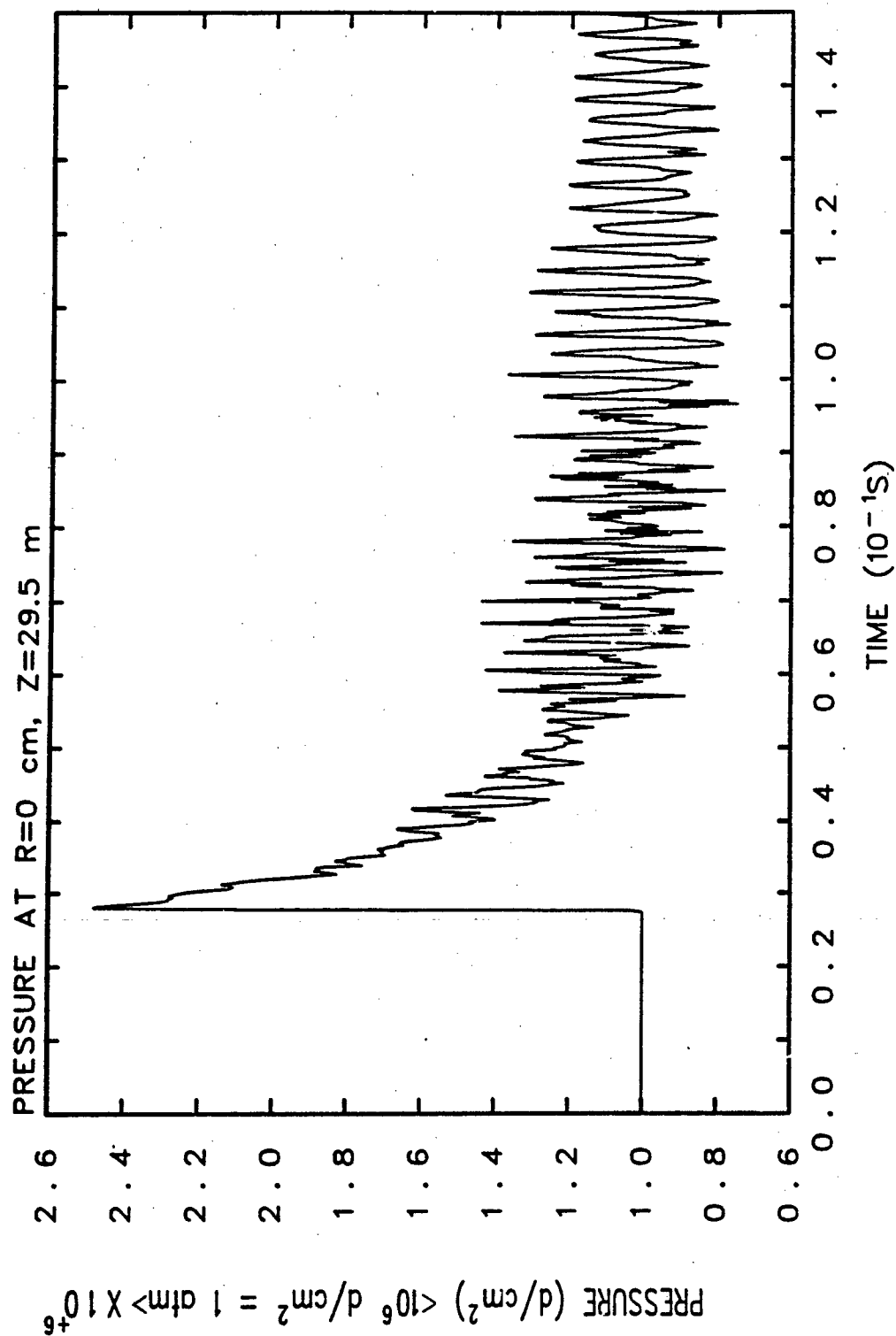
Appendix B: Pressure History Plots of Final Foam Test Case

The following plots are pressure history plots of the four tunnels used in the final test case. The plots are arranged in order of foam thickness, with the plain tunnel first, then the tunnel with ten centimeters of foam, followed by the tunnels with twenty and thirty centimeters of foam respectively. Each tunnel has twelve pressure histories taken at even intervals between twenty-five and fifty meters down the tunnel from the explosion. The location of the pressure history is indicated at the top of the plot while the tunnel is listed at the bottom.

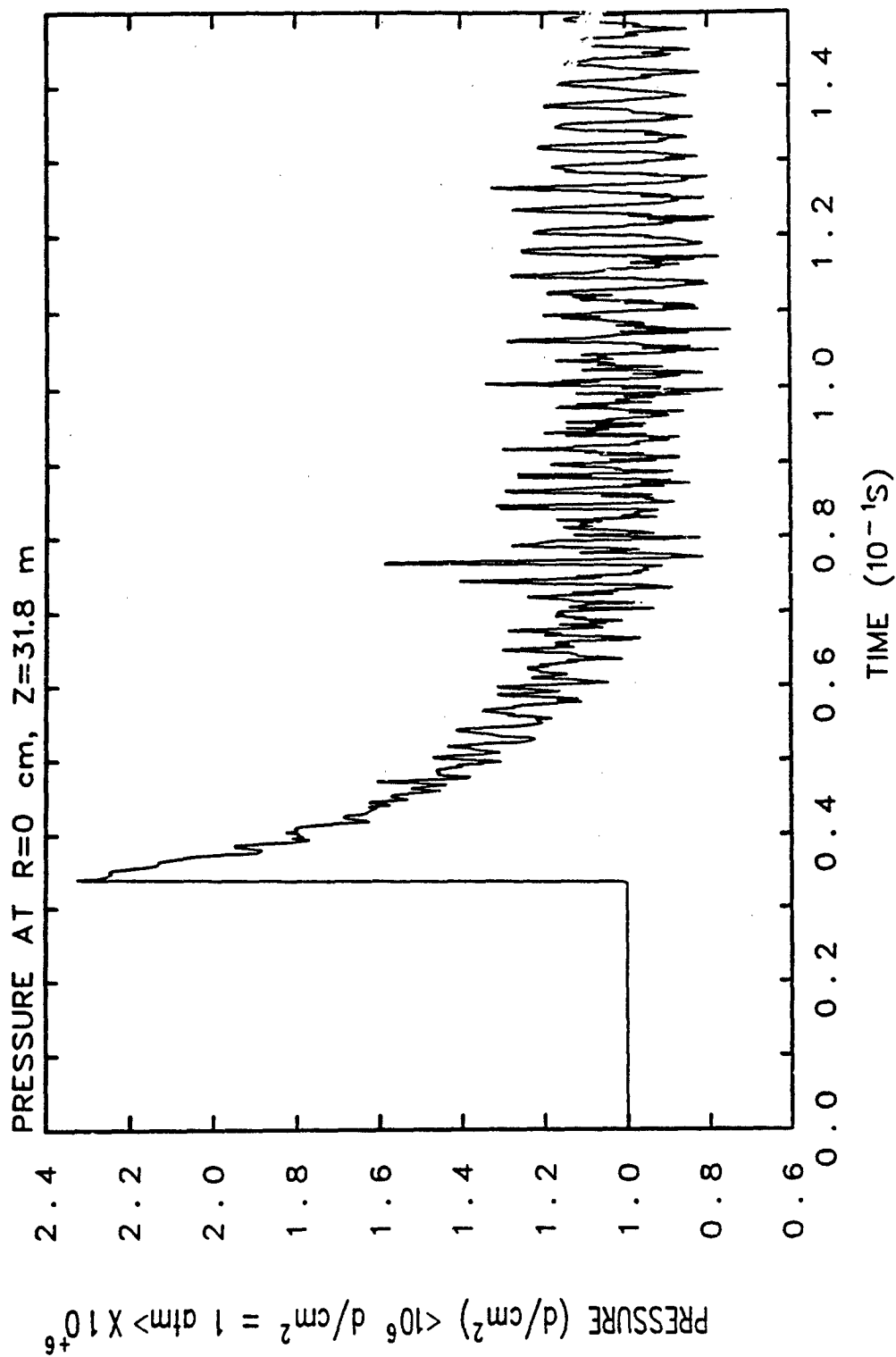


TUNNEL WITH NO FOAM

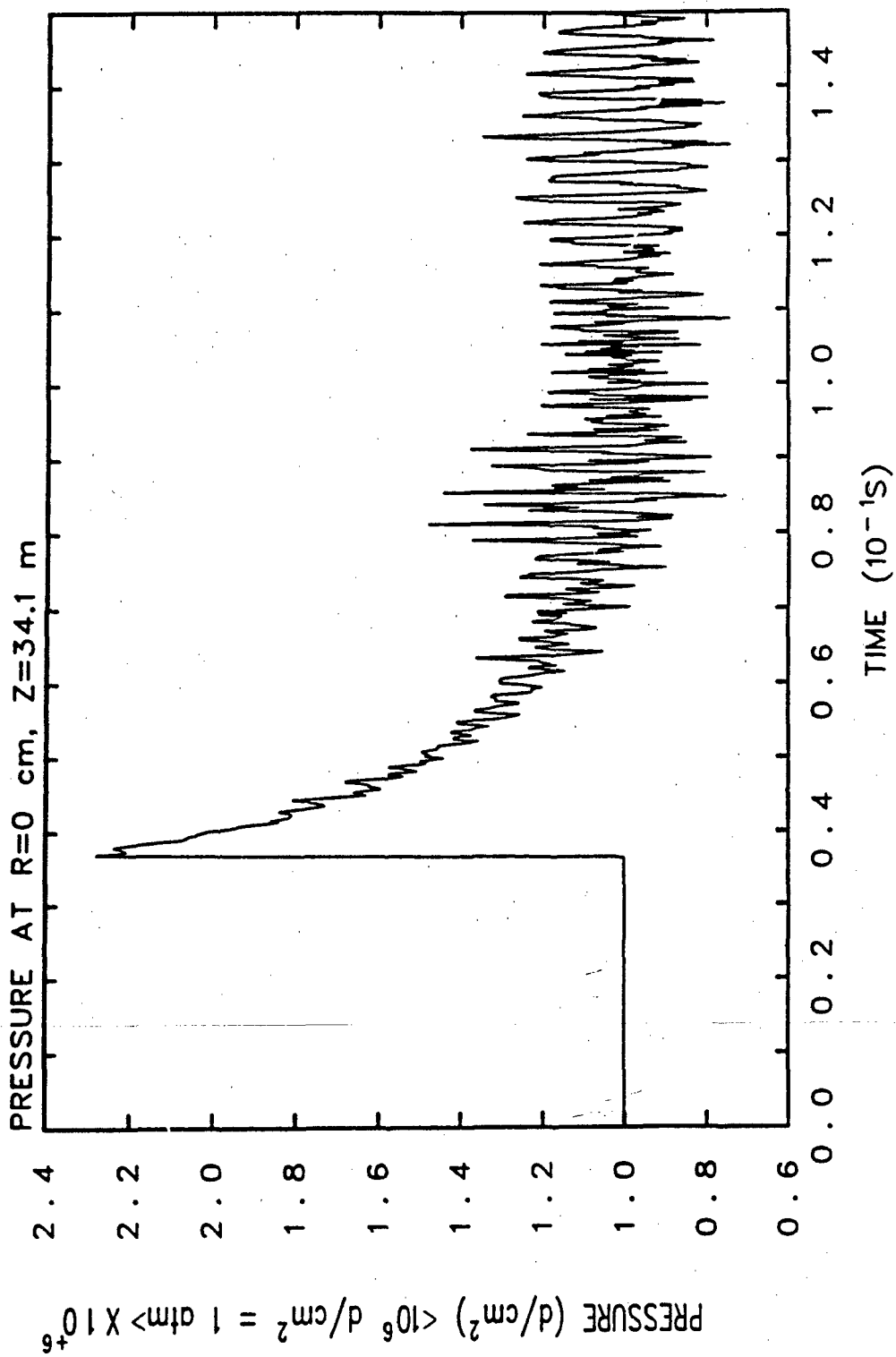




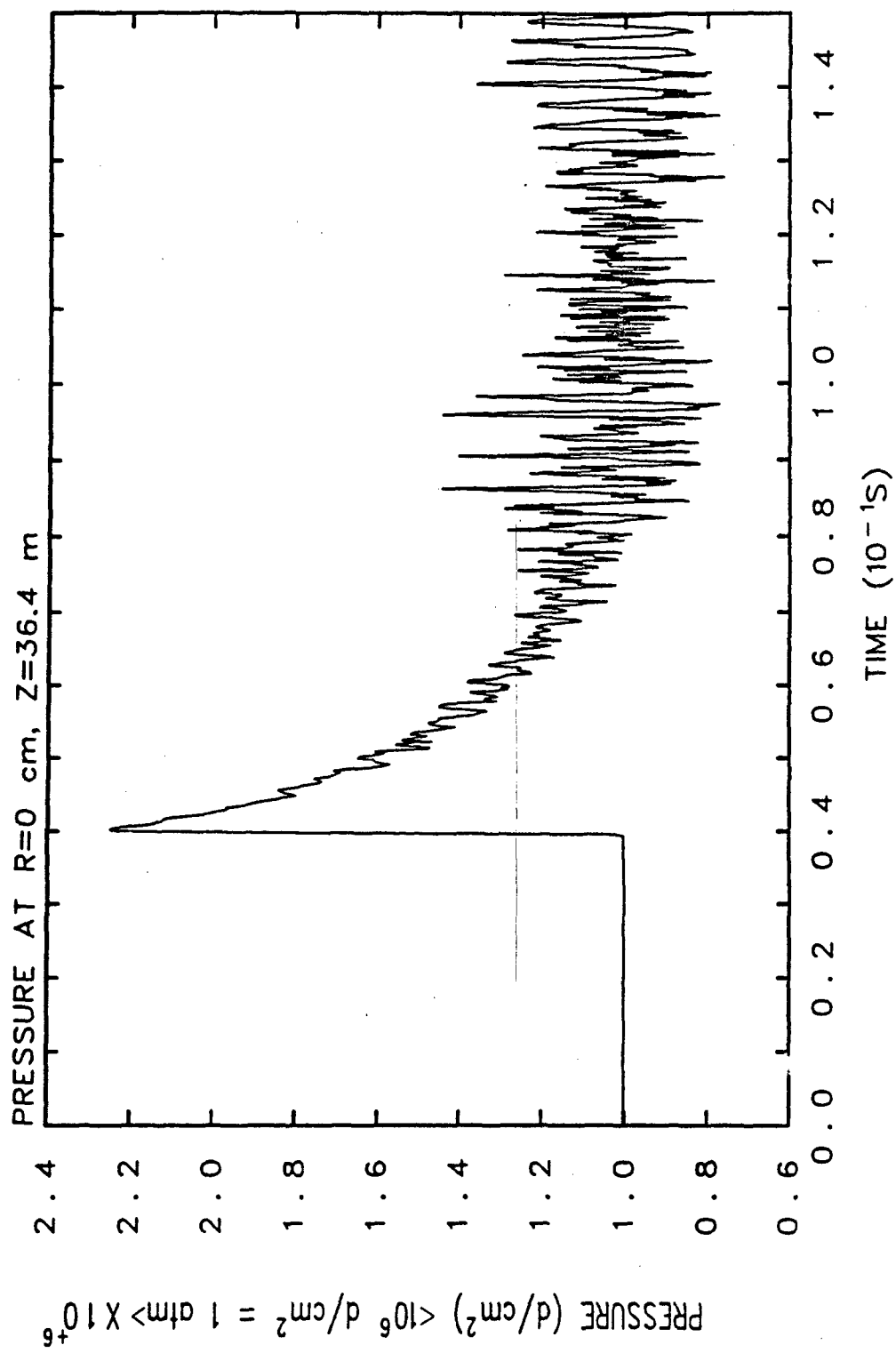
TUNNEL WITH NO FOAM



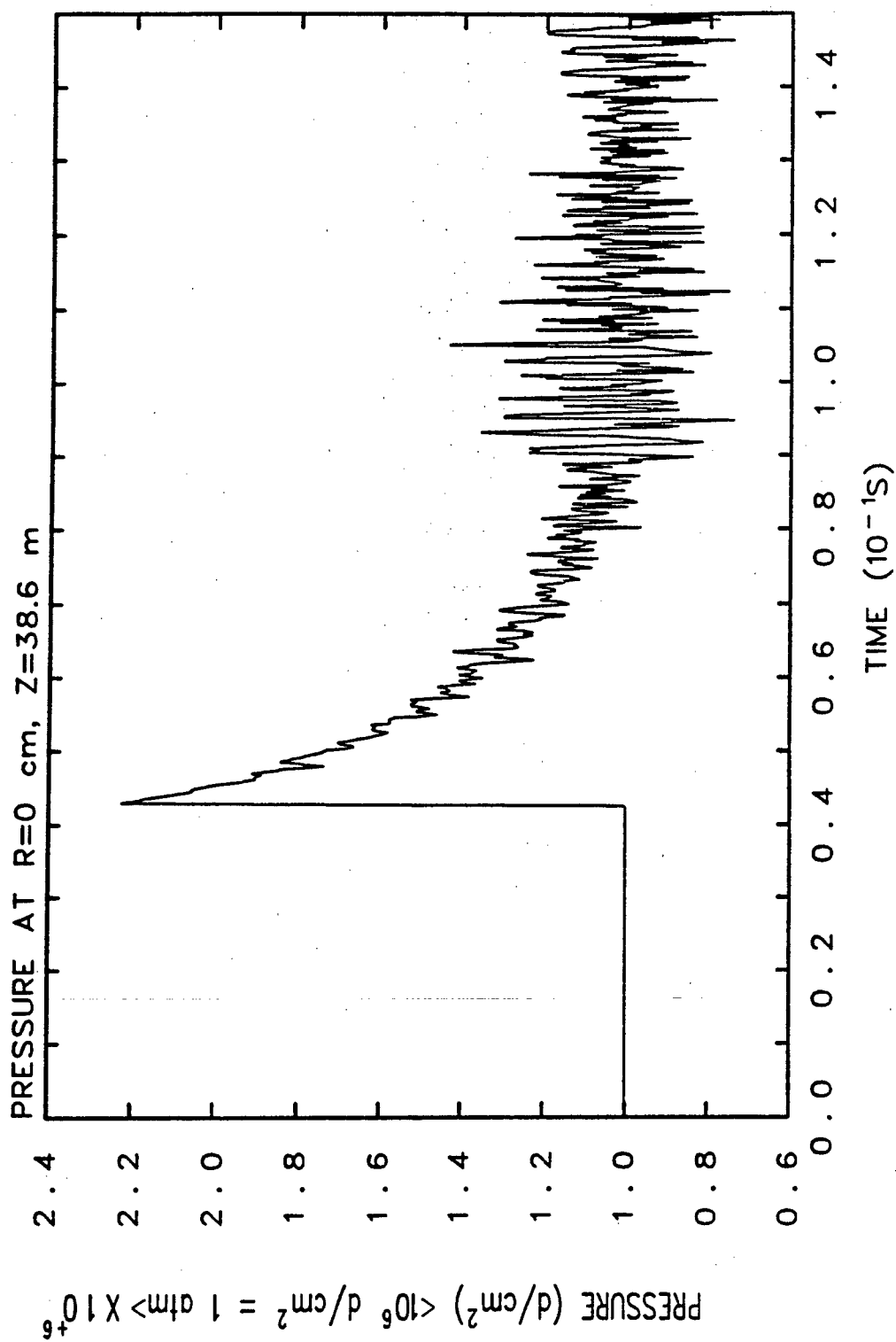
TUNNEL WITH NO FOAM



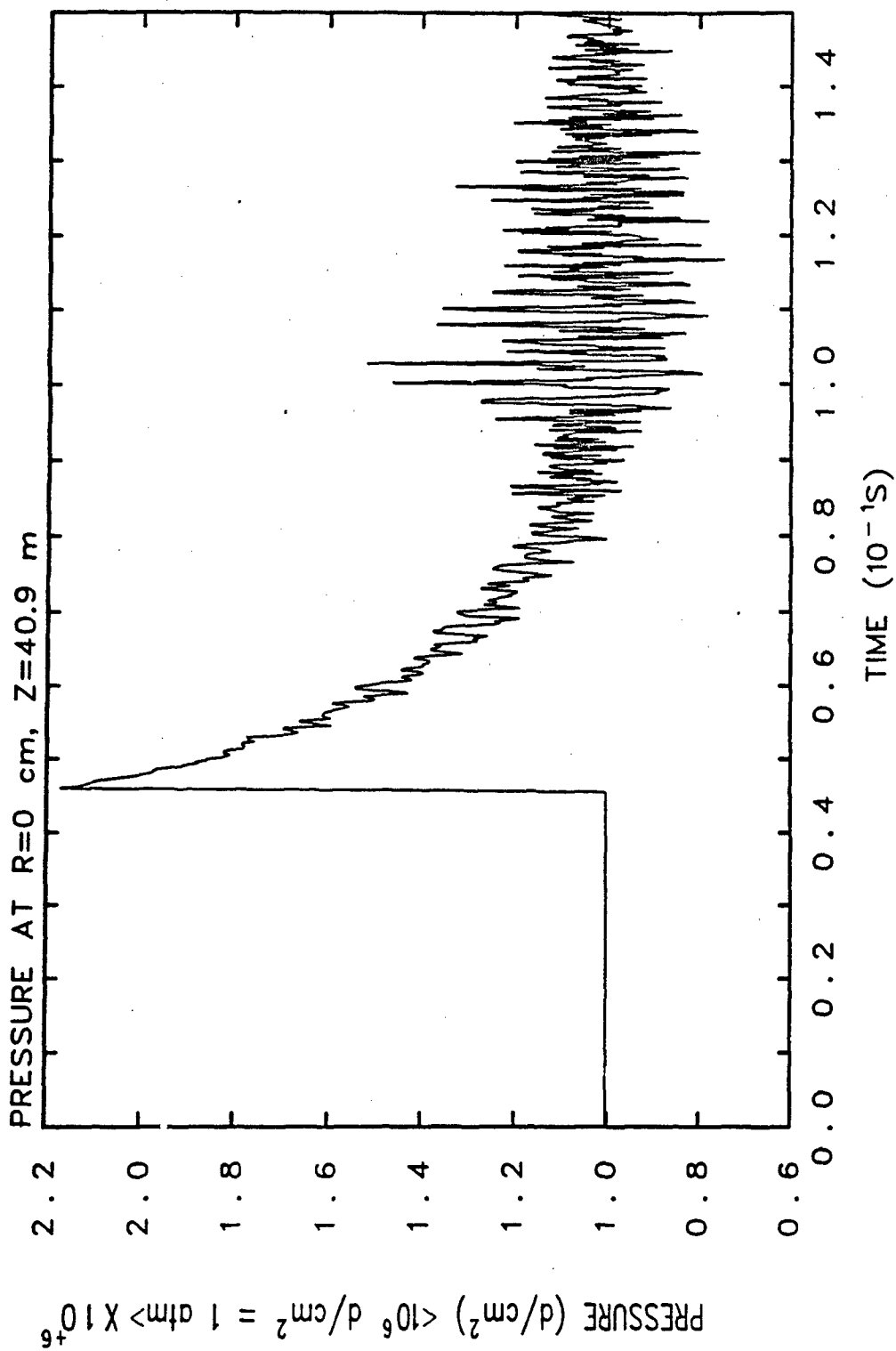
TUNNEL WITH NO FOAM



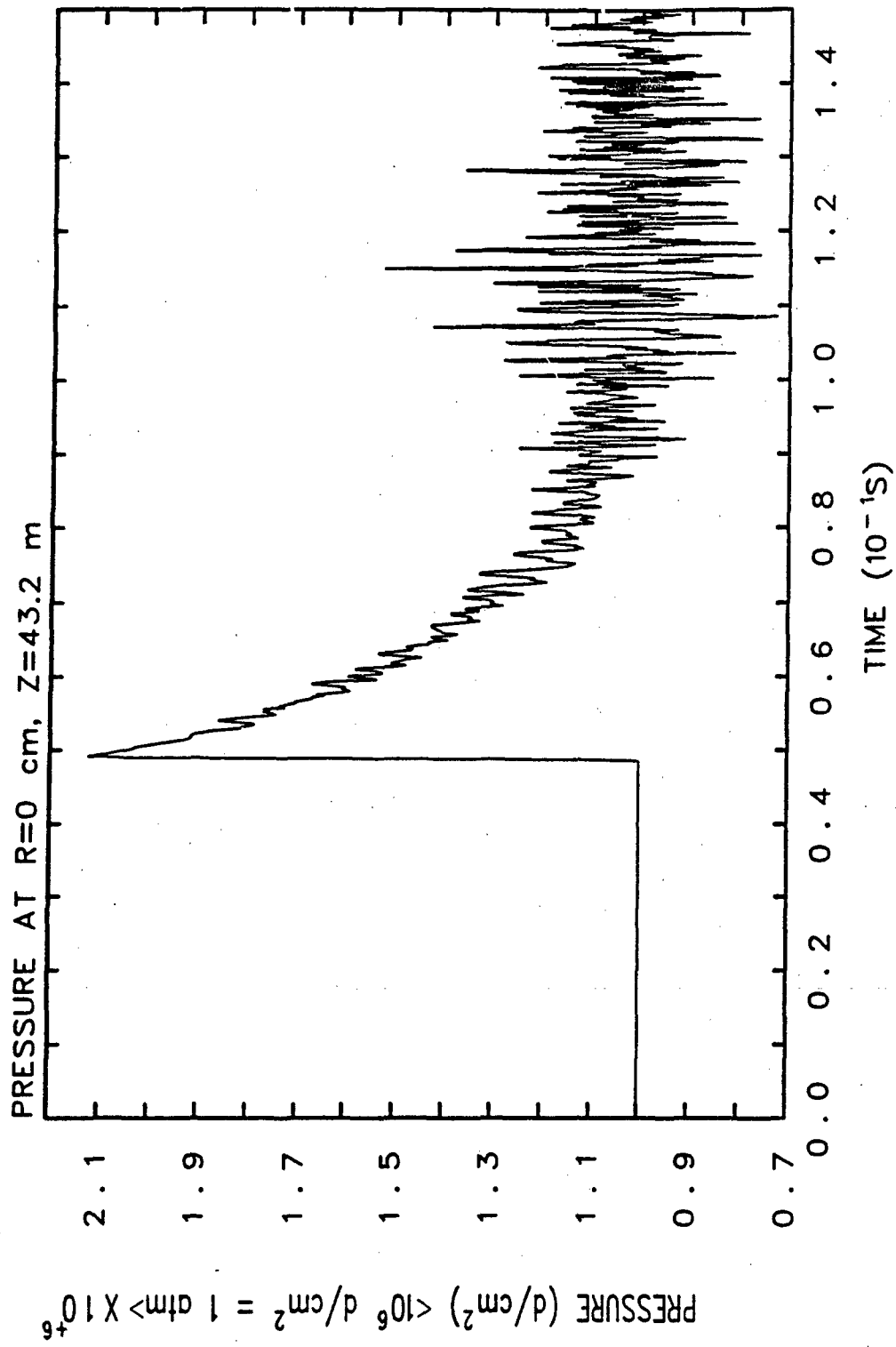
TUNNEL WITH NO FOAM



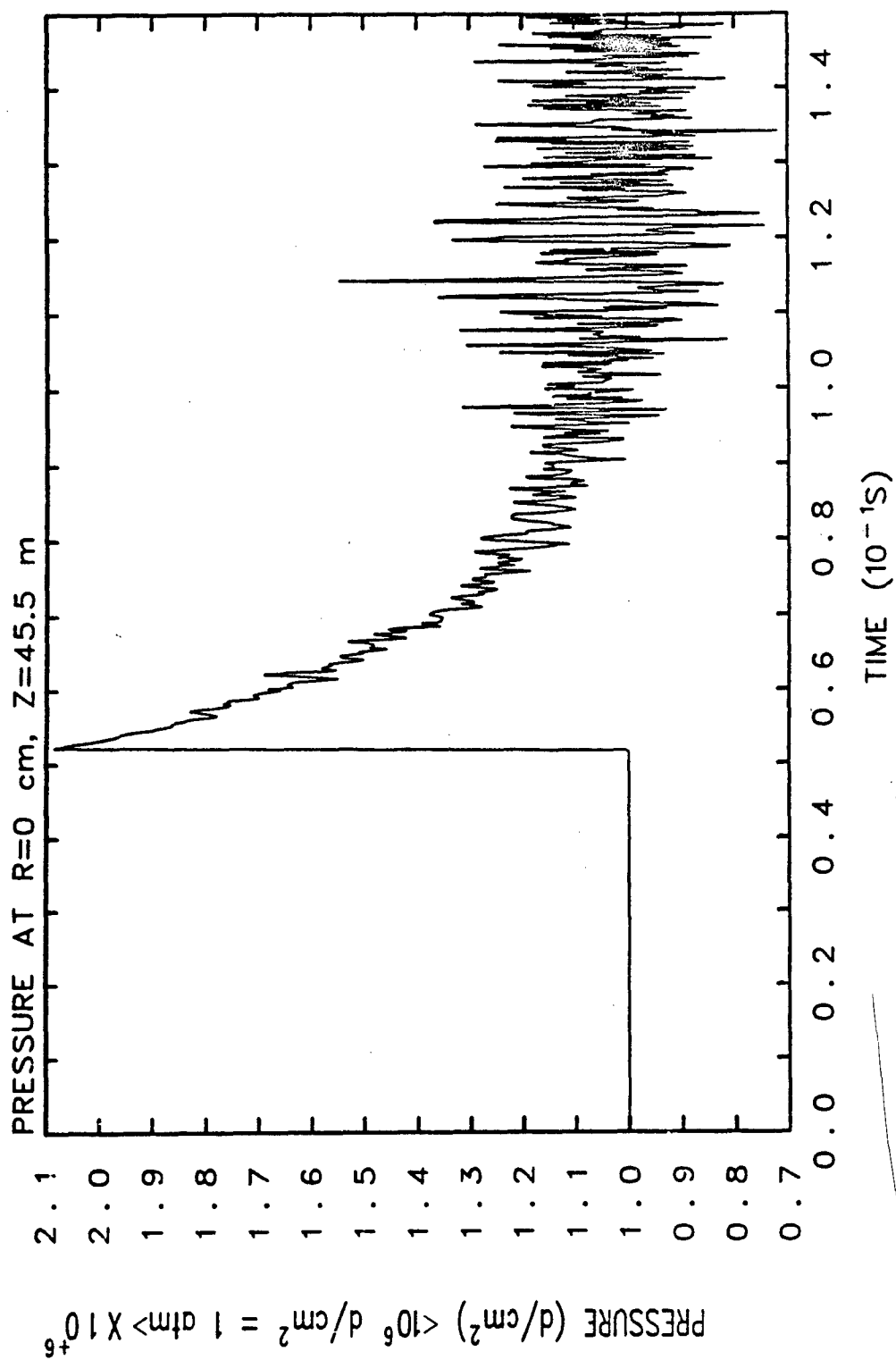
TUNNEL WITH NO FOAM



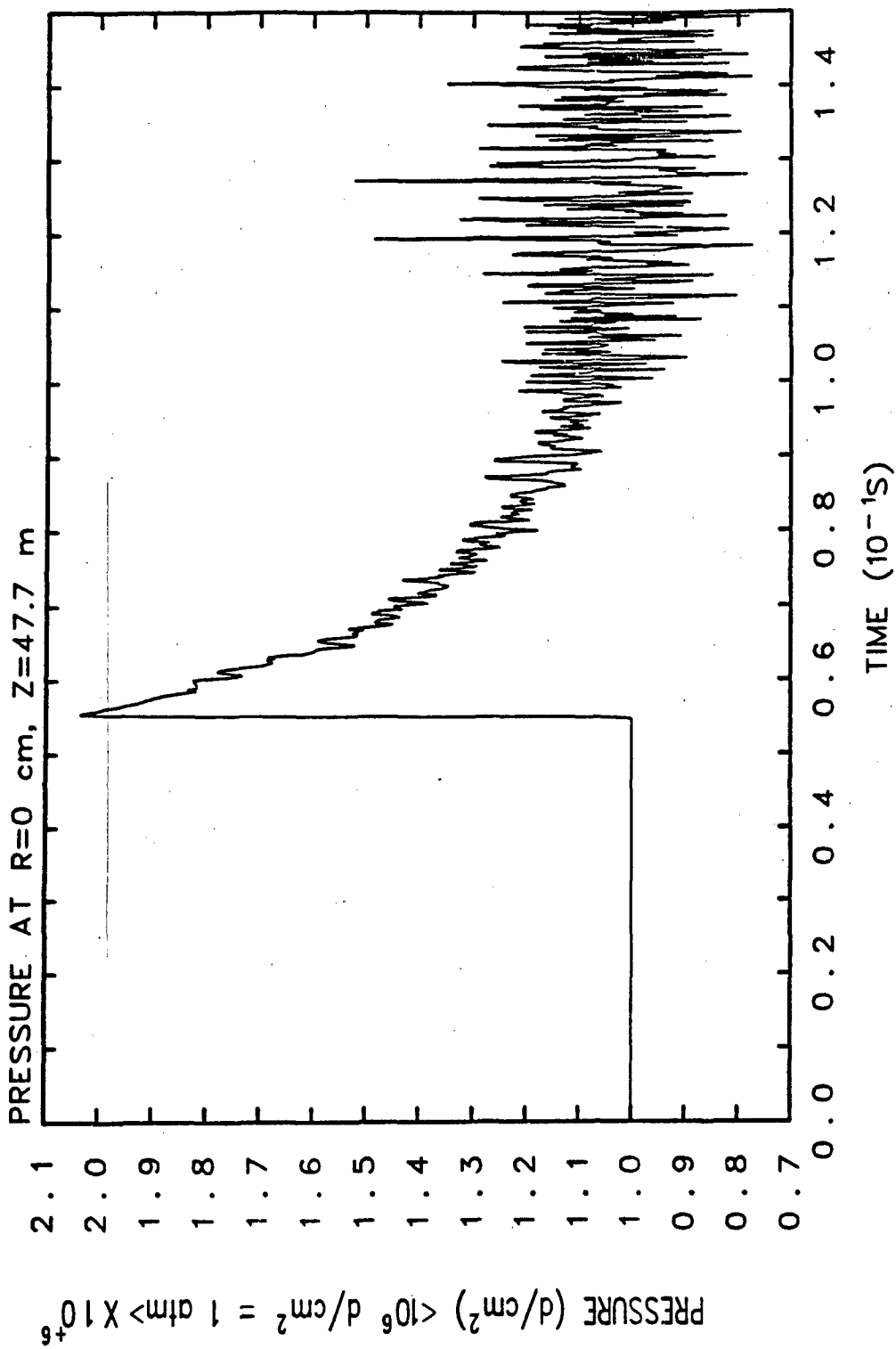
TUNNEL WITH NO FOAM



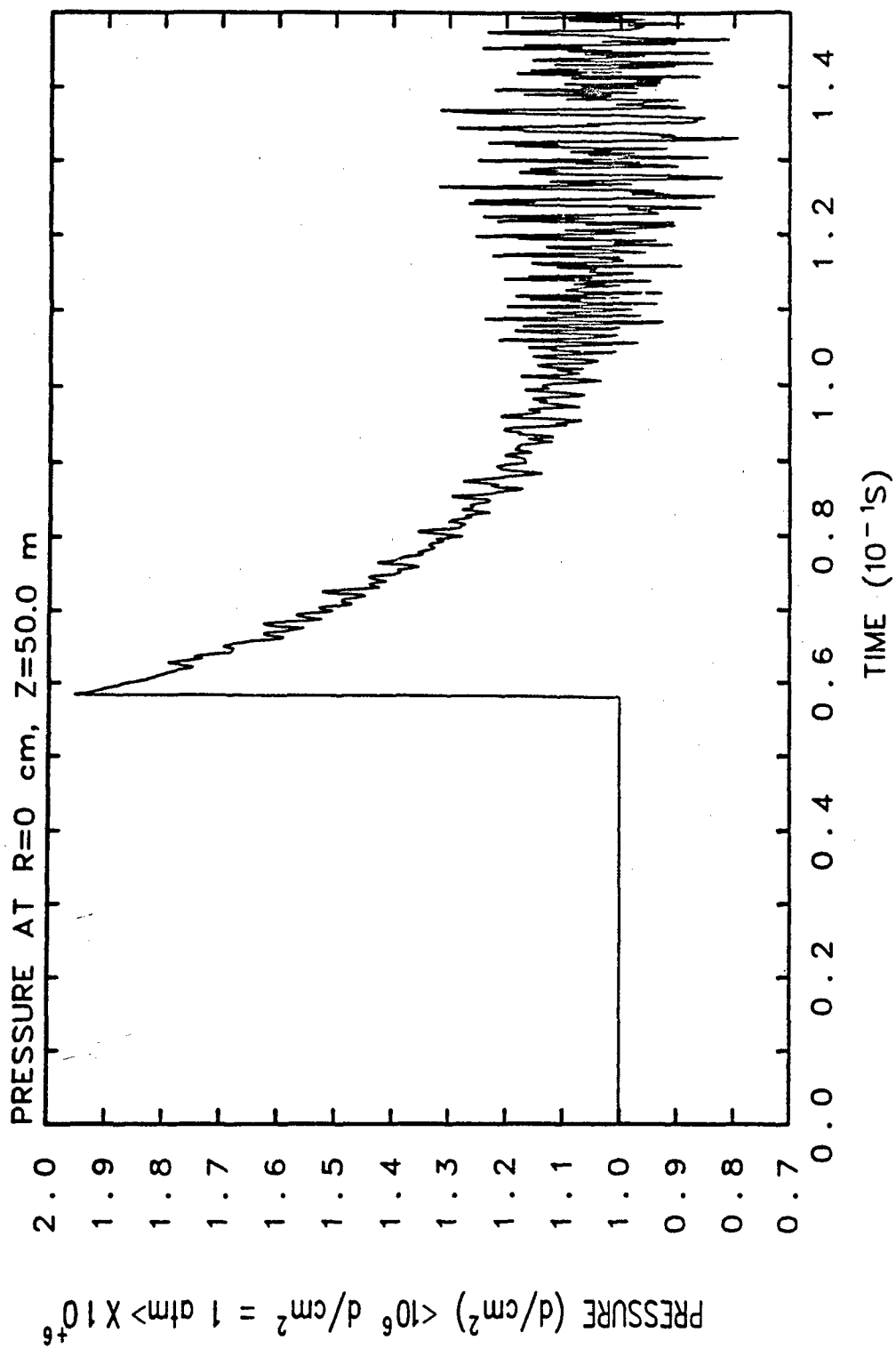
TUNNEL WITH NO FOAM



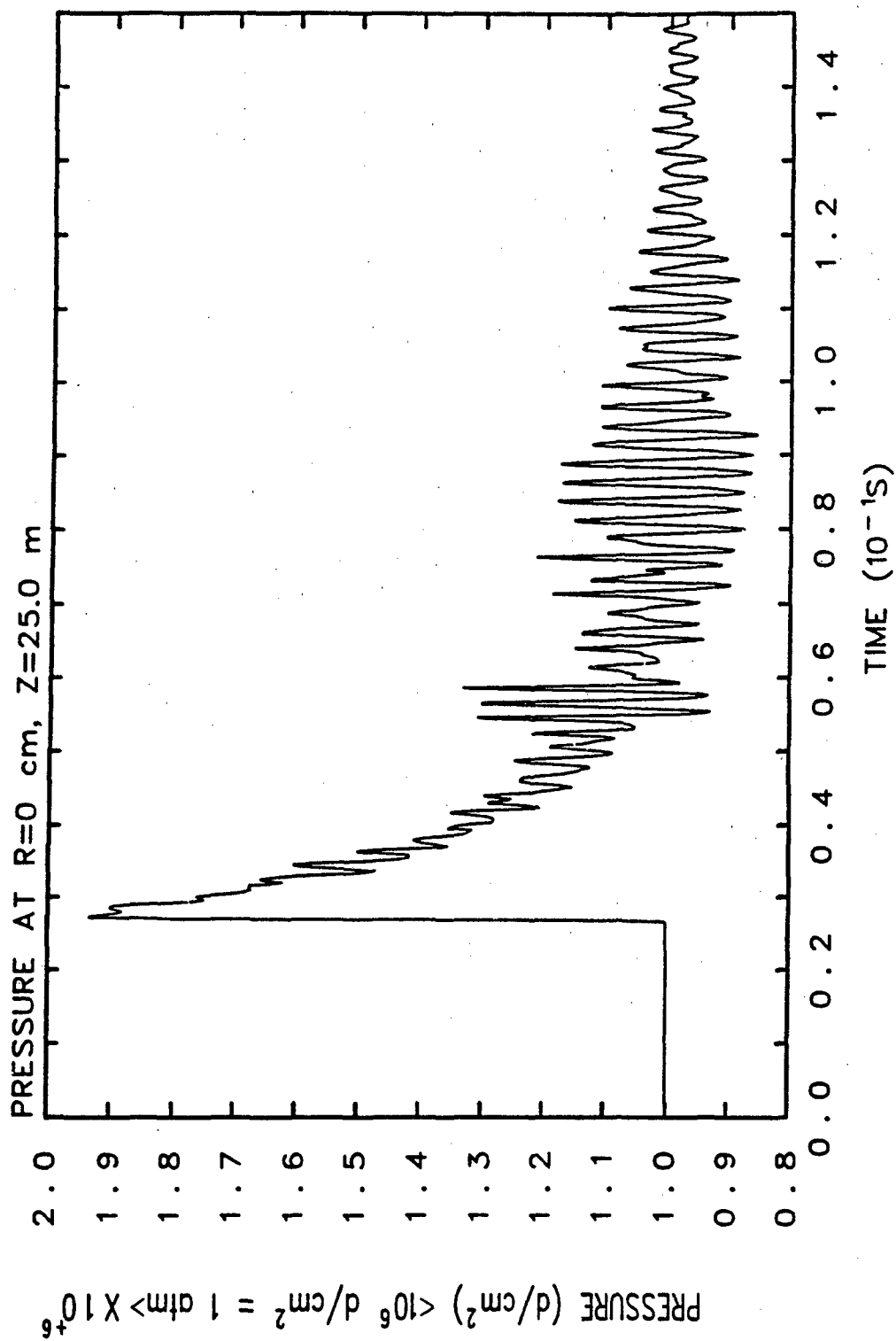
TUNNEL WITH NO FOAM



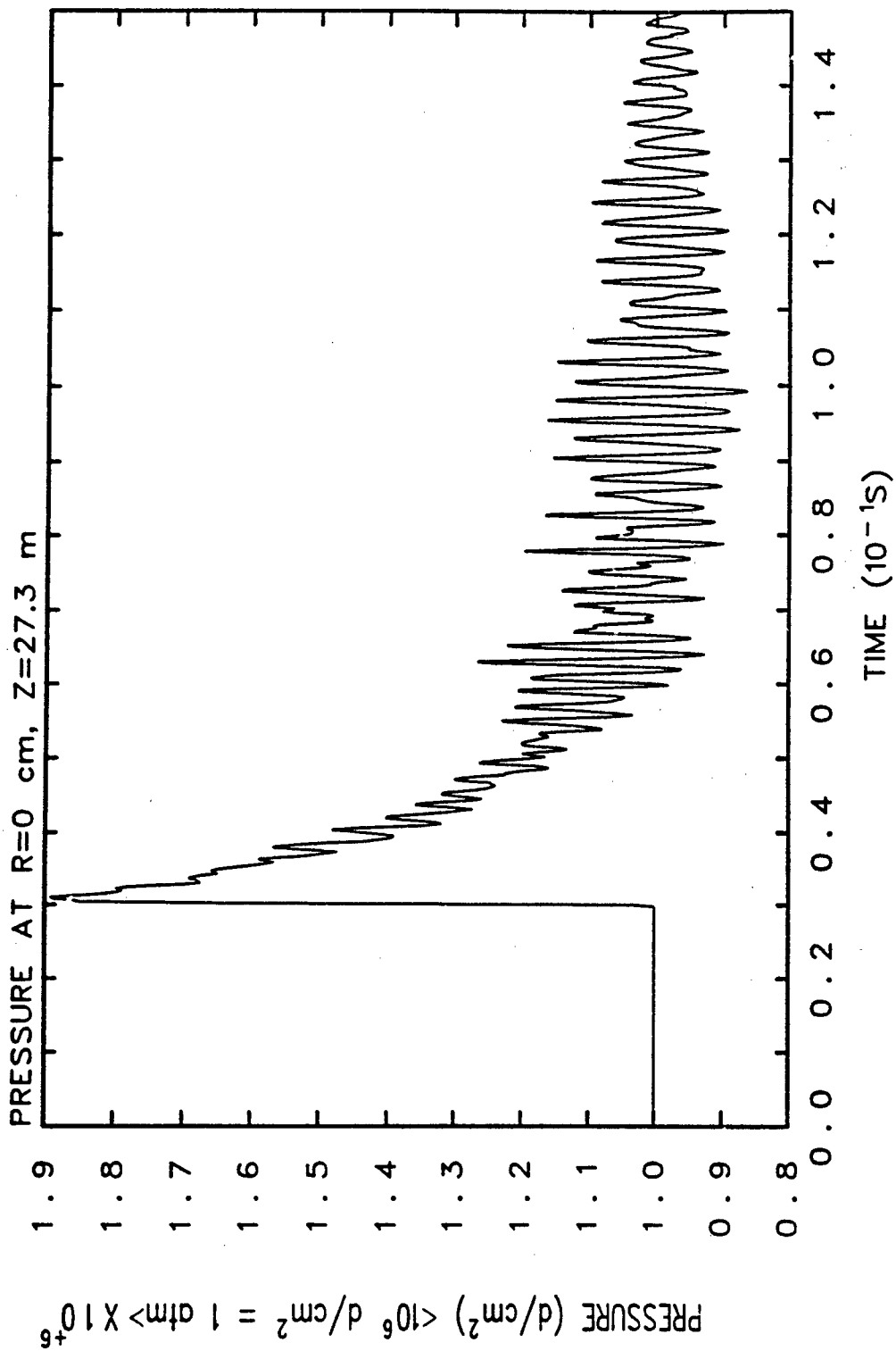
TUNNEL WITH NO FOAM



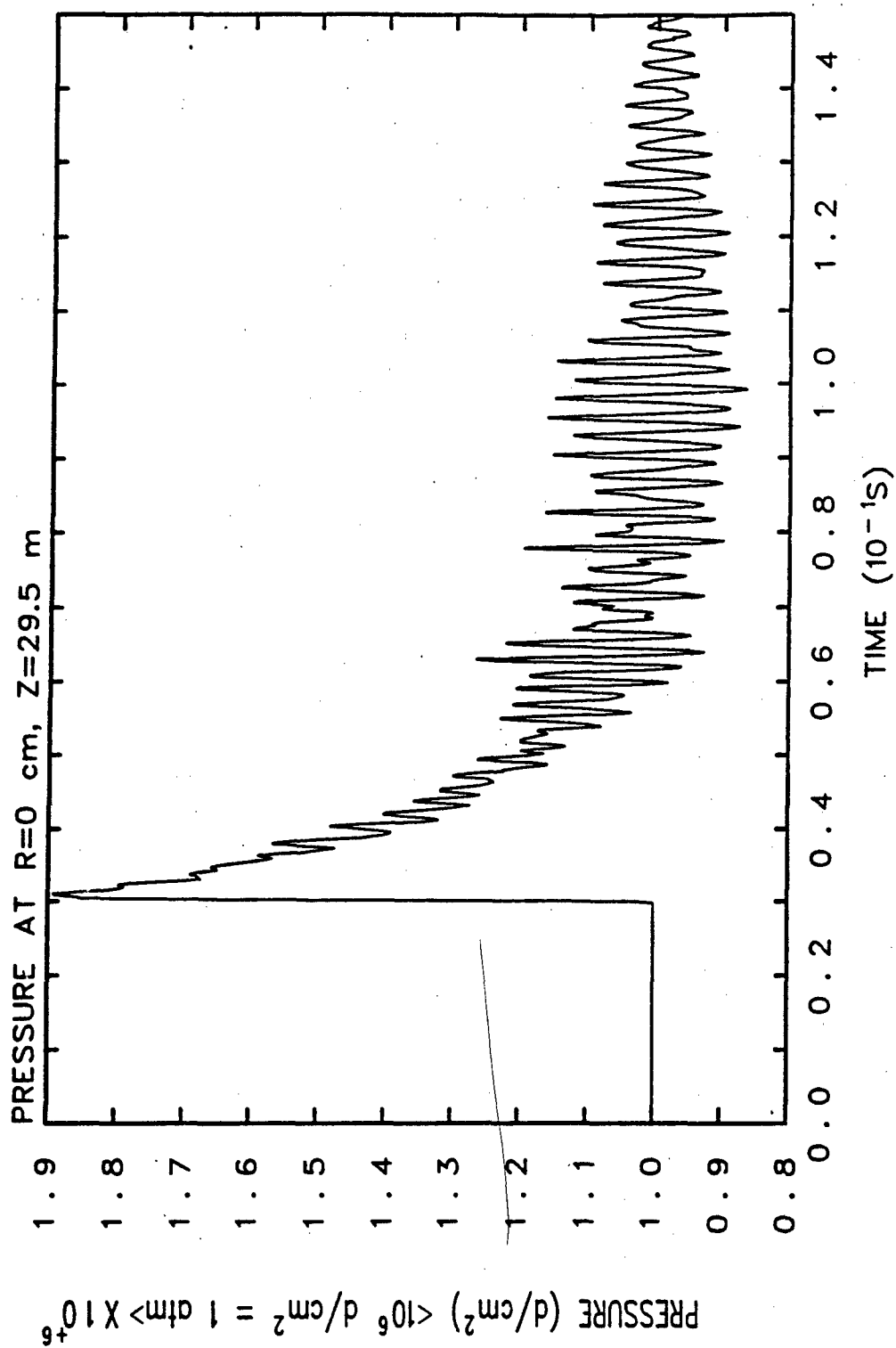
TUNNEL WITH NO FOAM



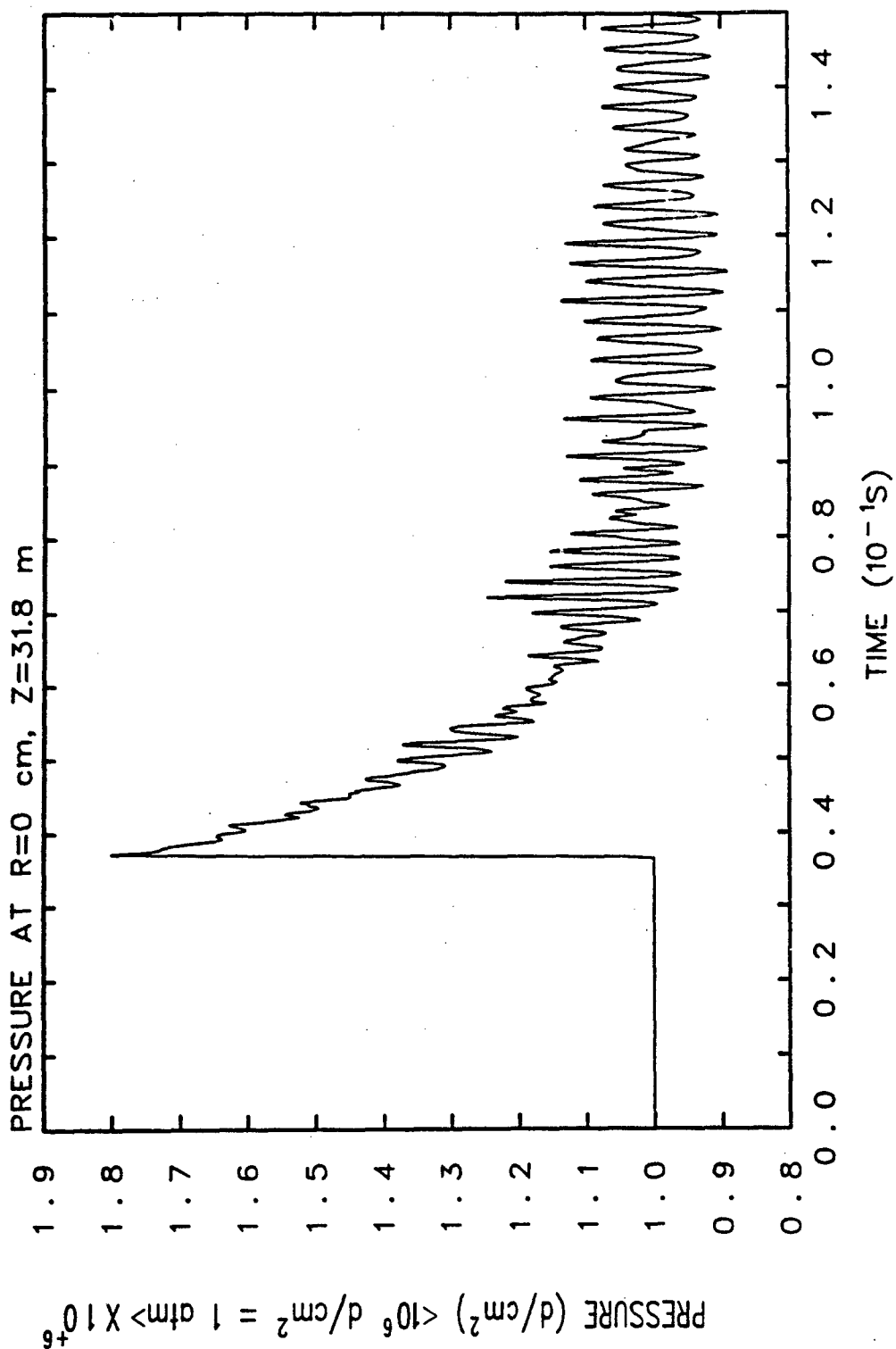
TUNNEL WITH 10 cm FOAM



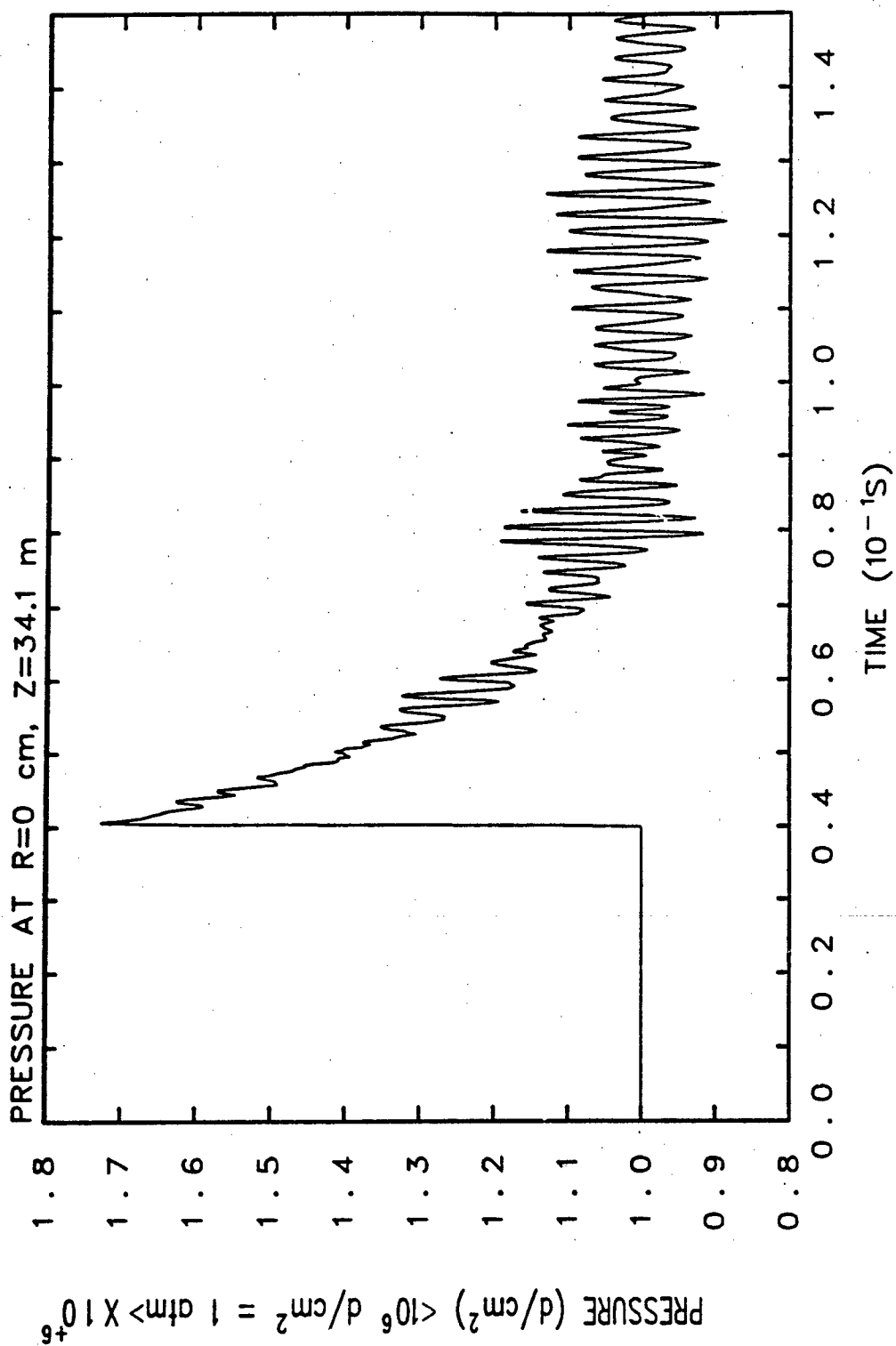
TUNNEL WITH 10 cm FOAM



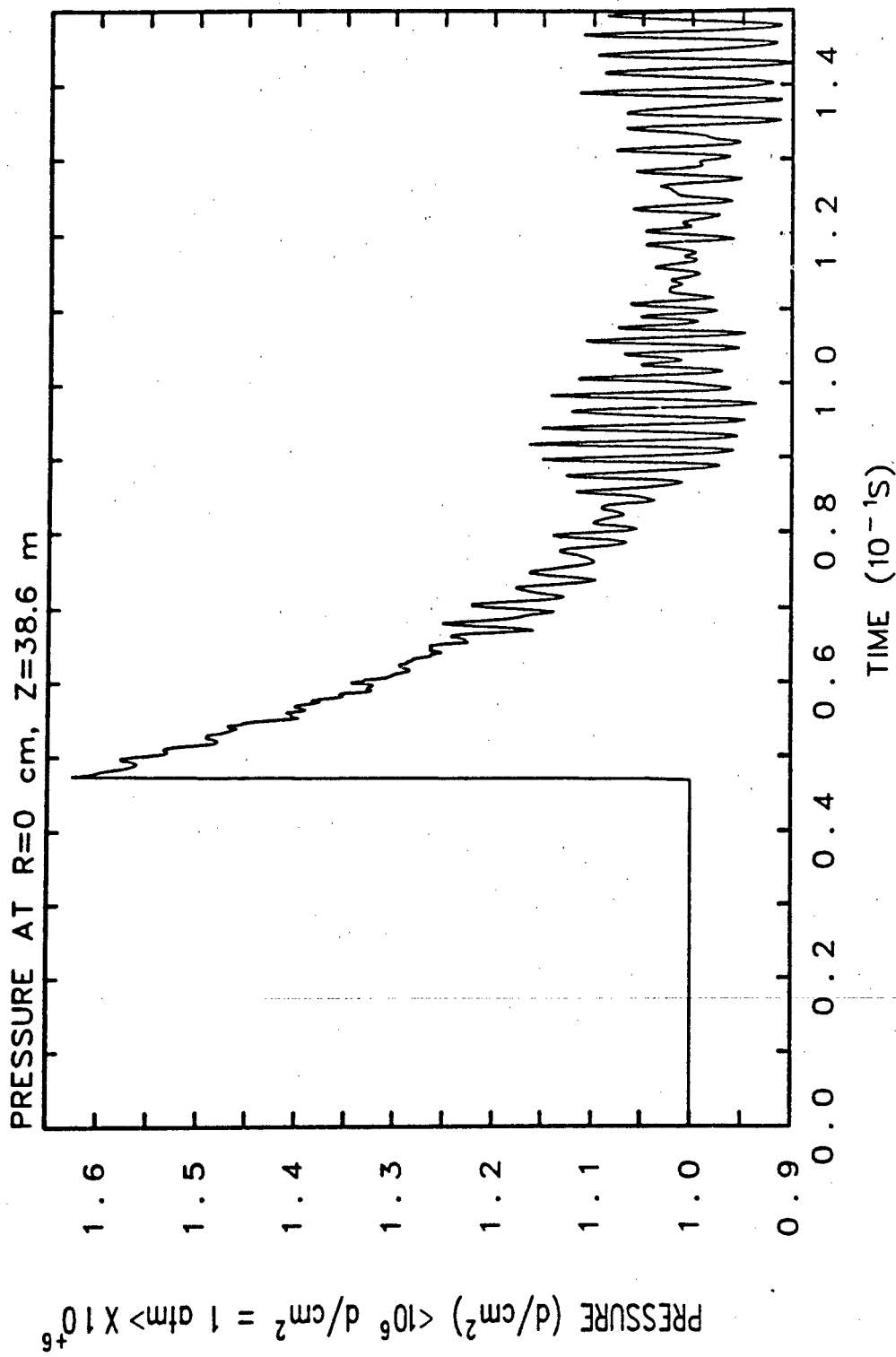
TUNNEL WITH 10 cm FOAM

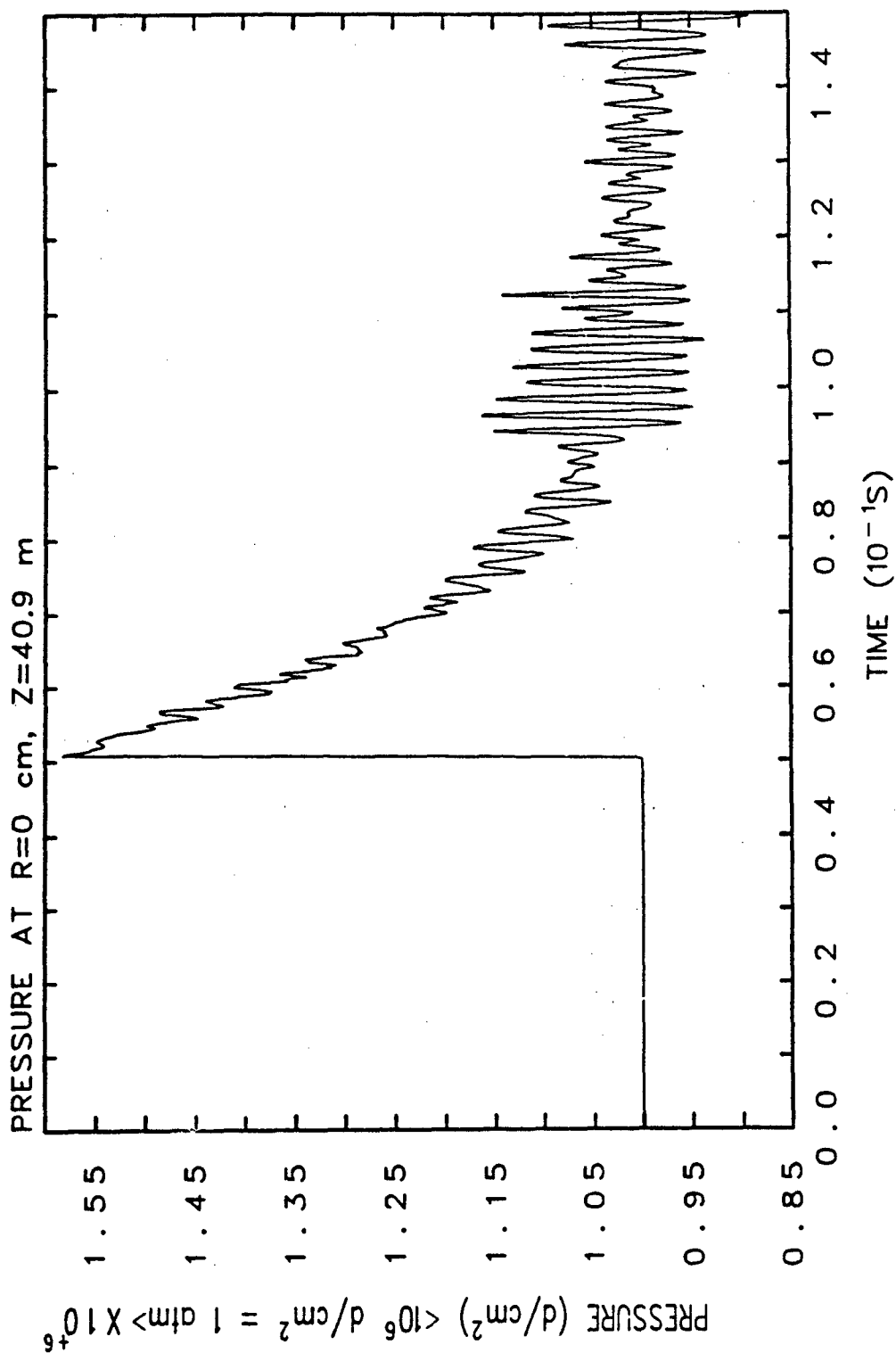


TUNNEL WITH 10 cm FOAM

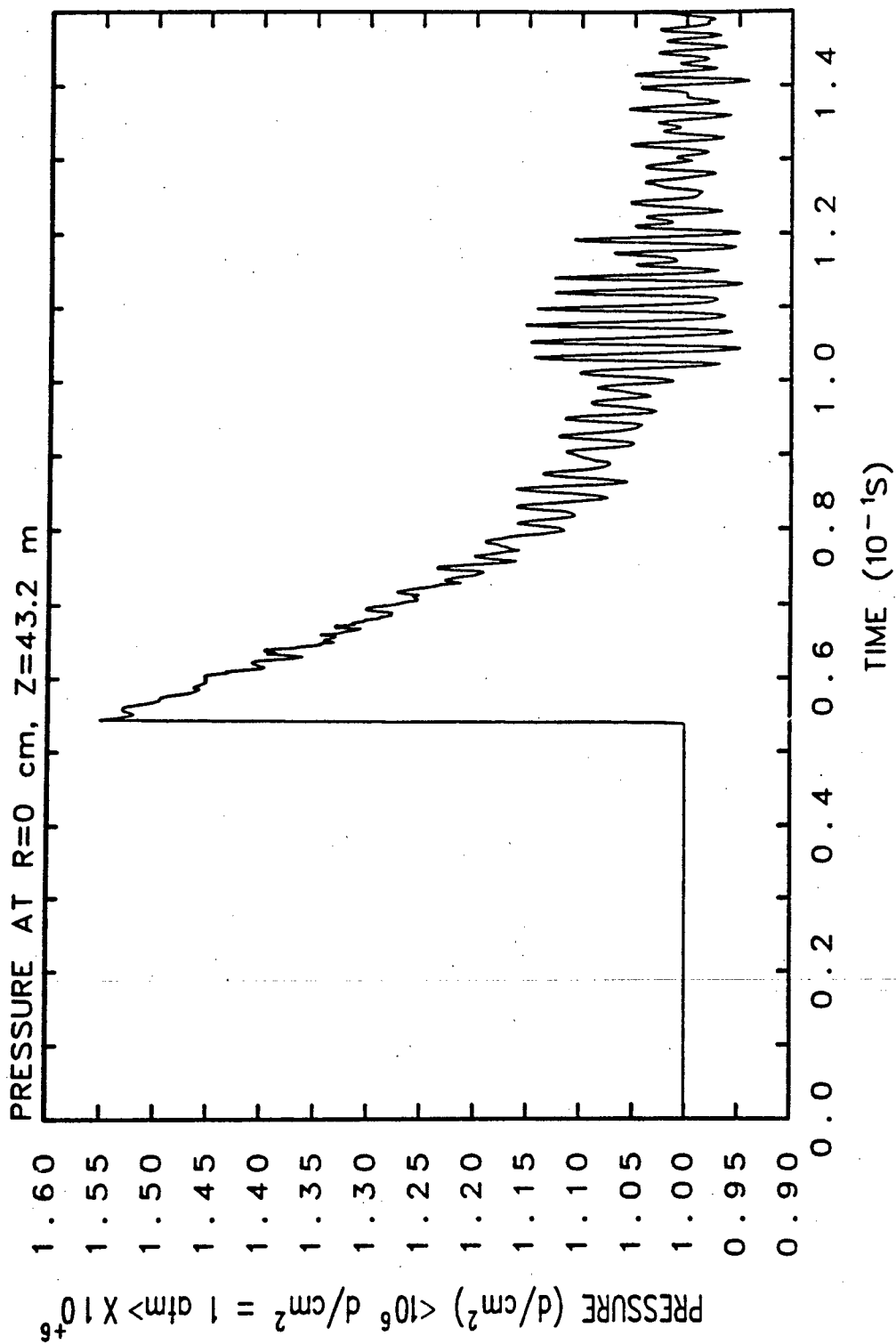


TUNNEL WITH 10 cm FOAM

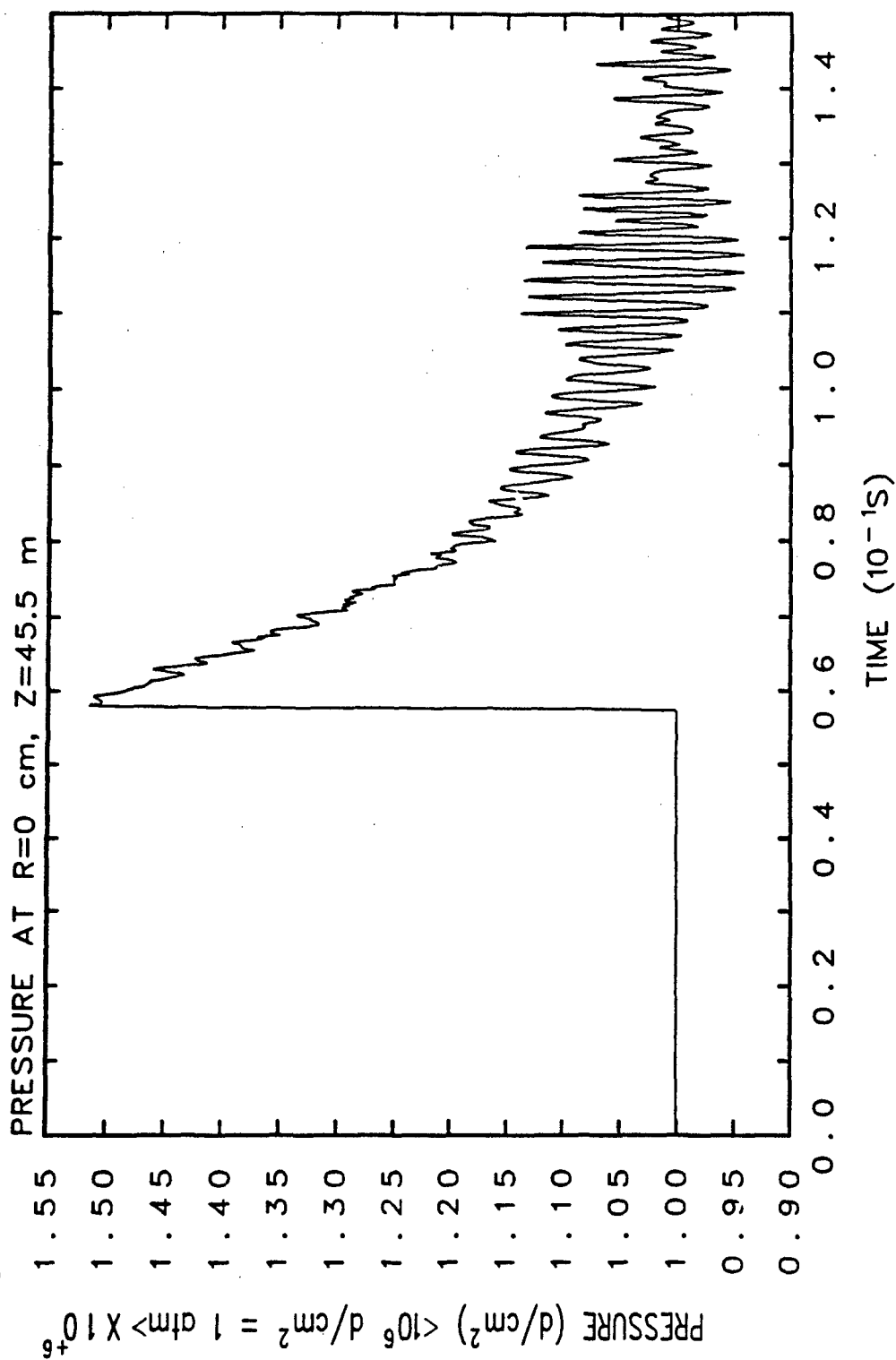




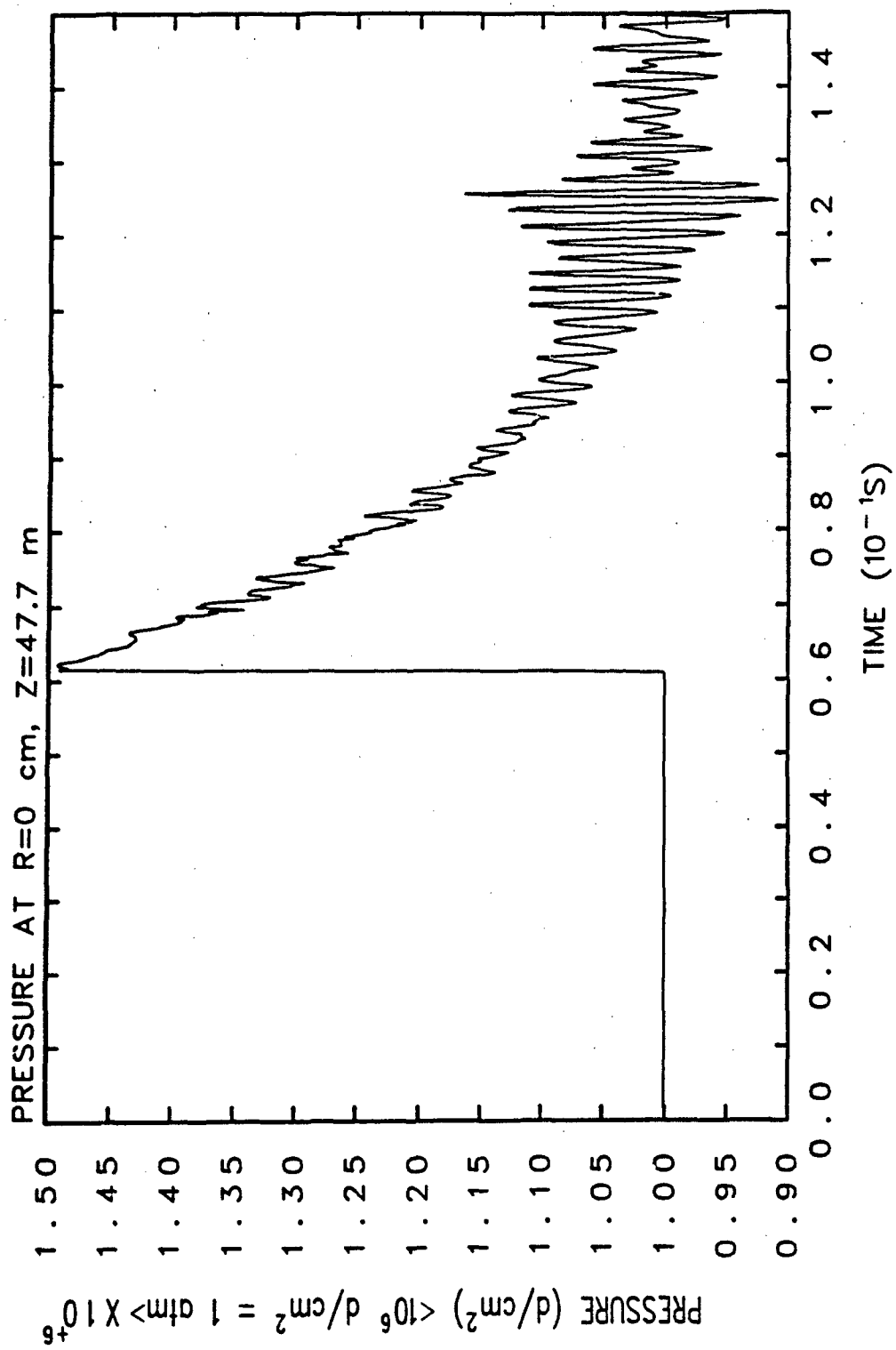
TUNNEL WITH 10 cm FOAM



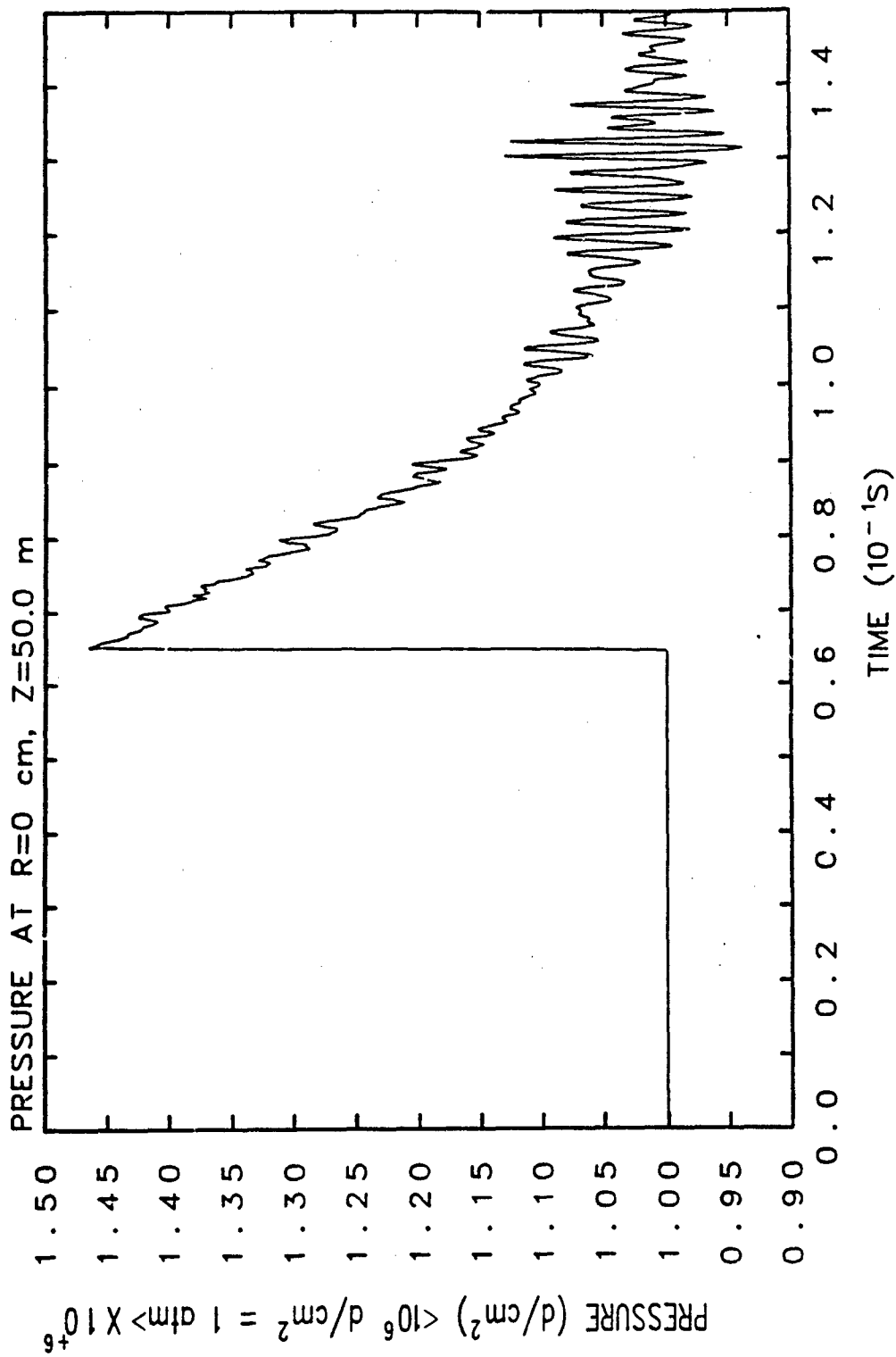
TUNNEL WITH 10 cm FOAM



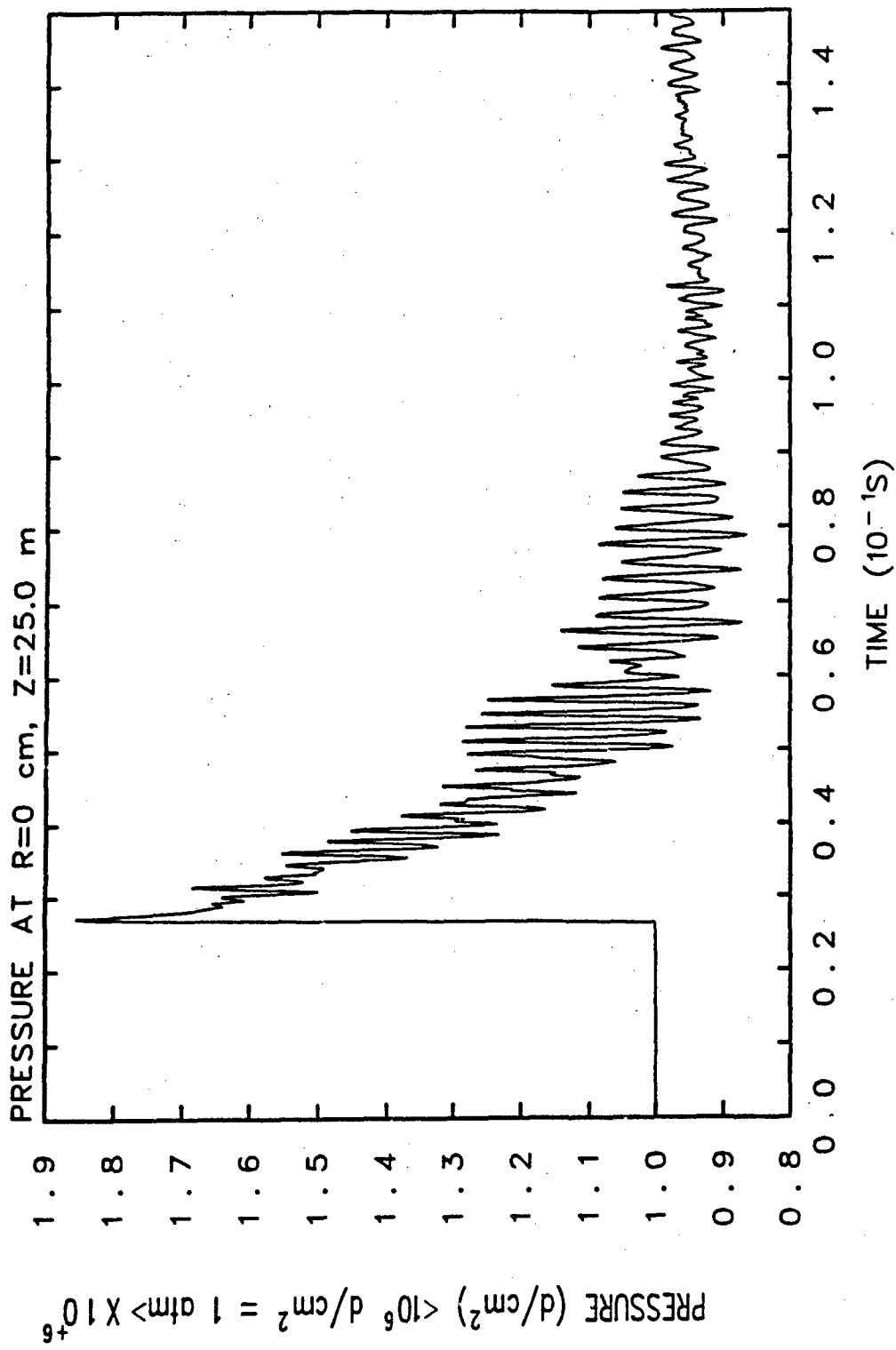
TUNNEL WITH 10 cm FOAM



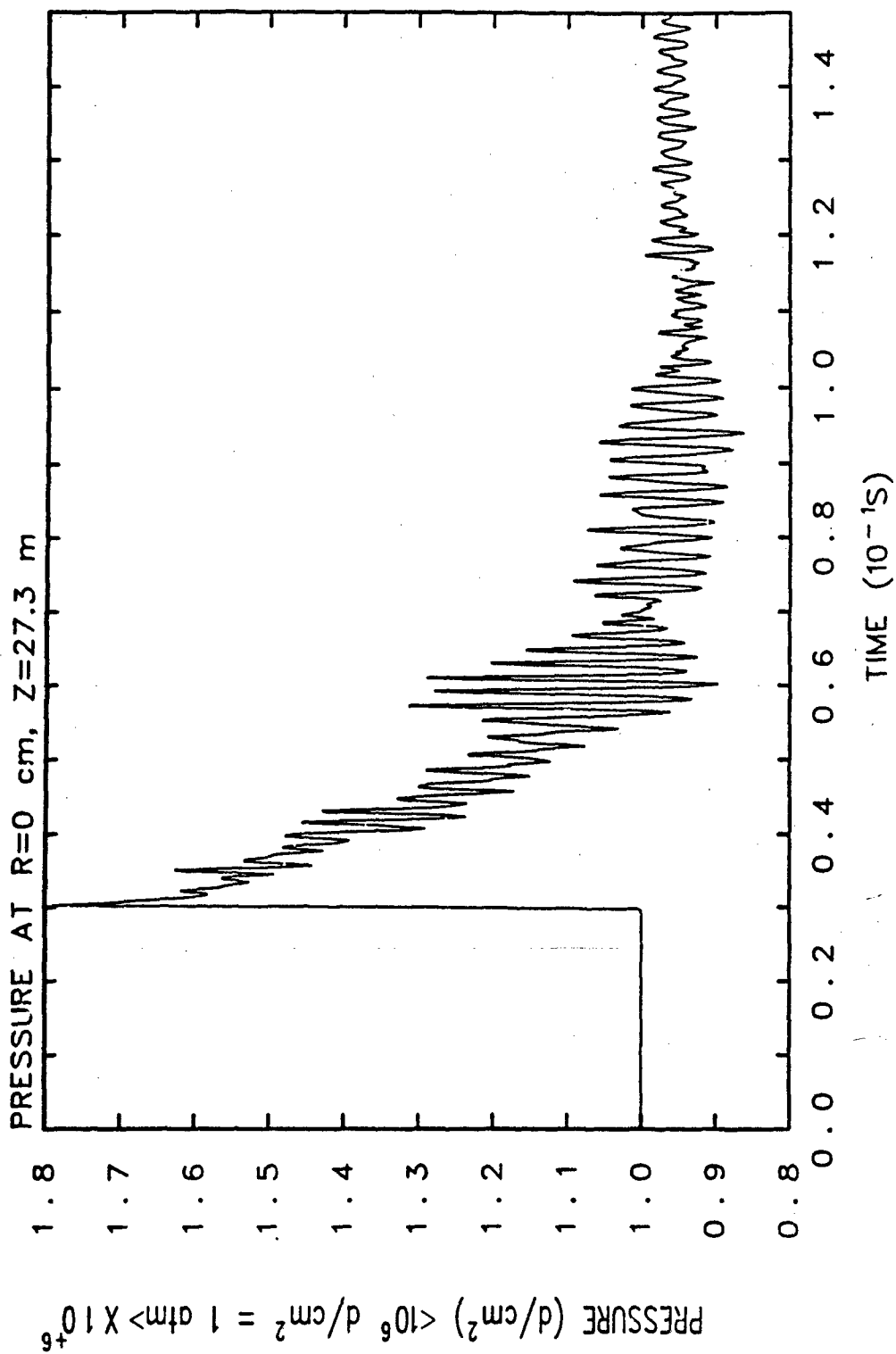
TUNNEL WITH 10 cm FOAM



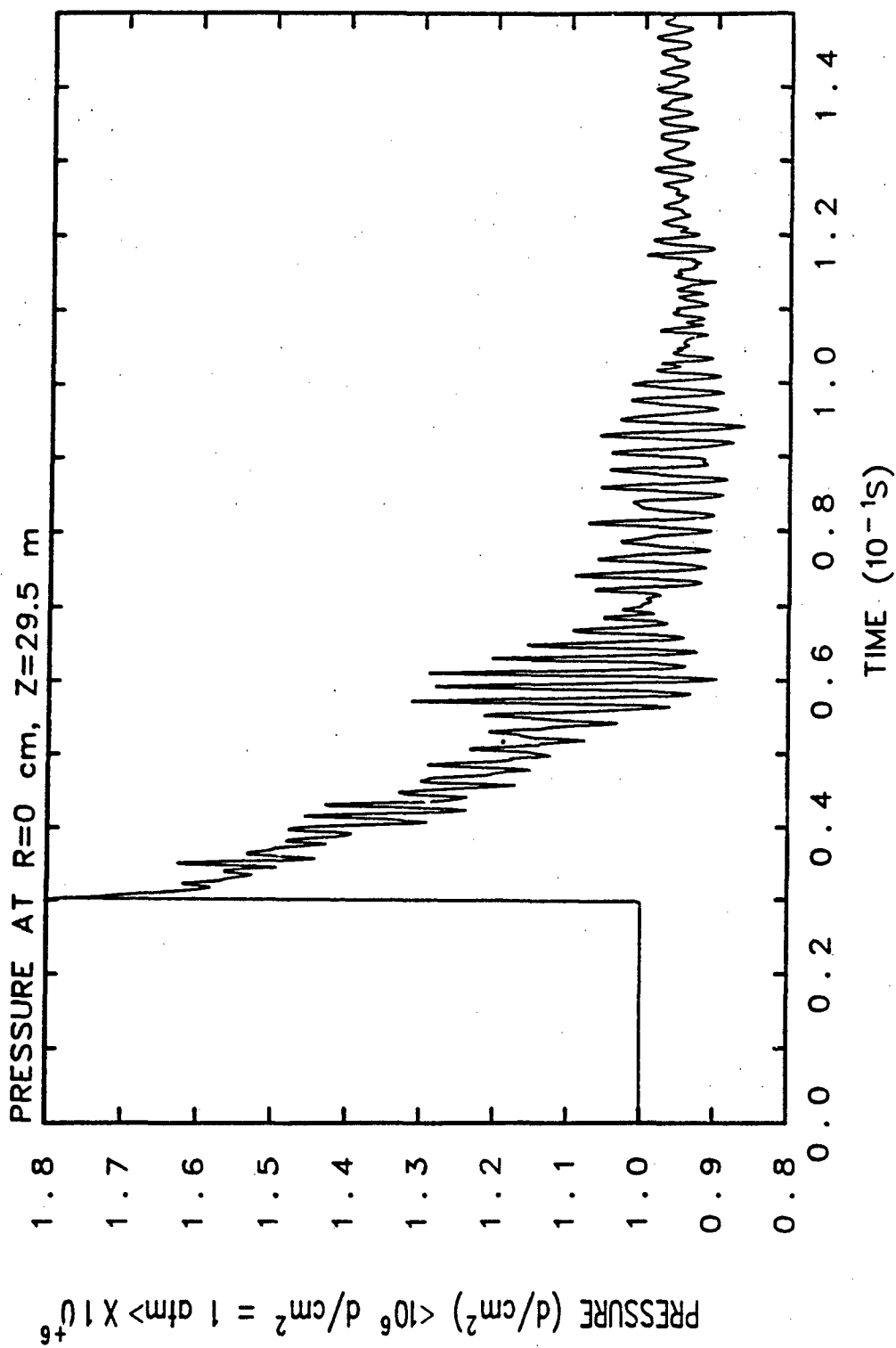
TUNNEL WITH 10 cm FOAM



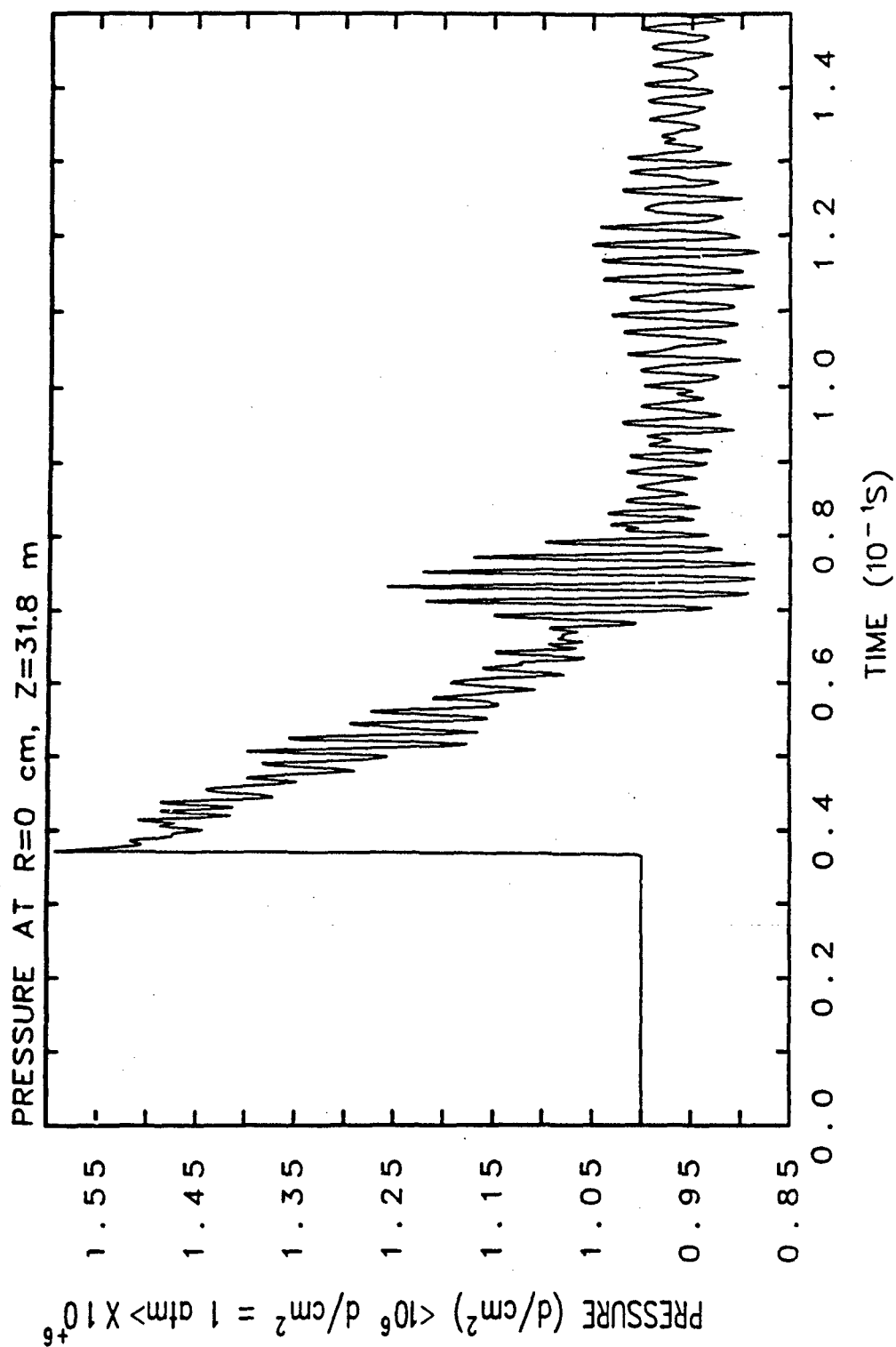
TUNNEL WITH 20 cm FOAM



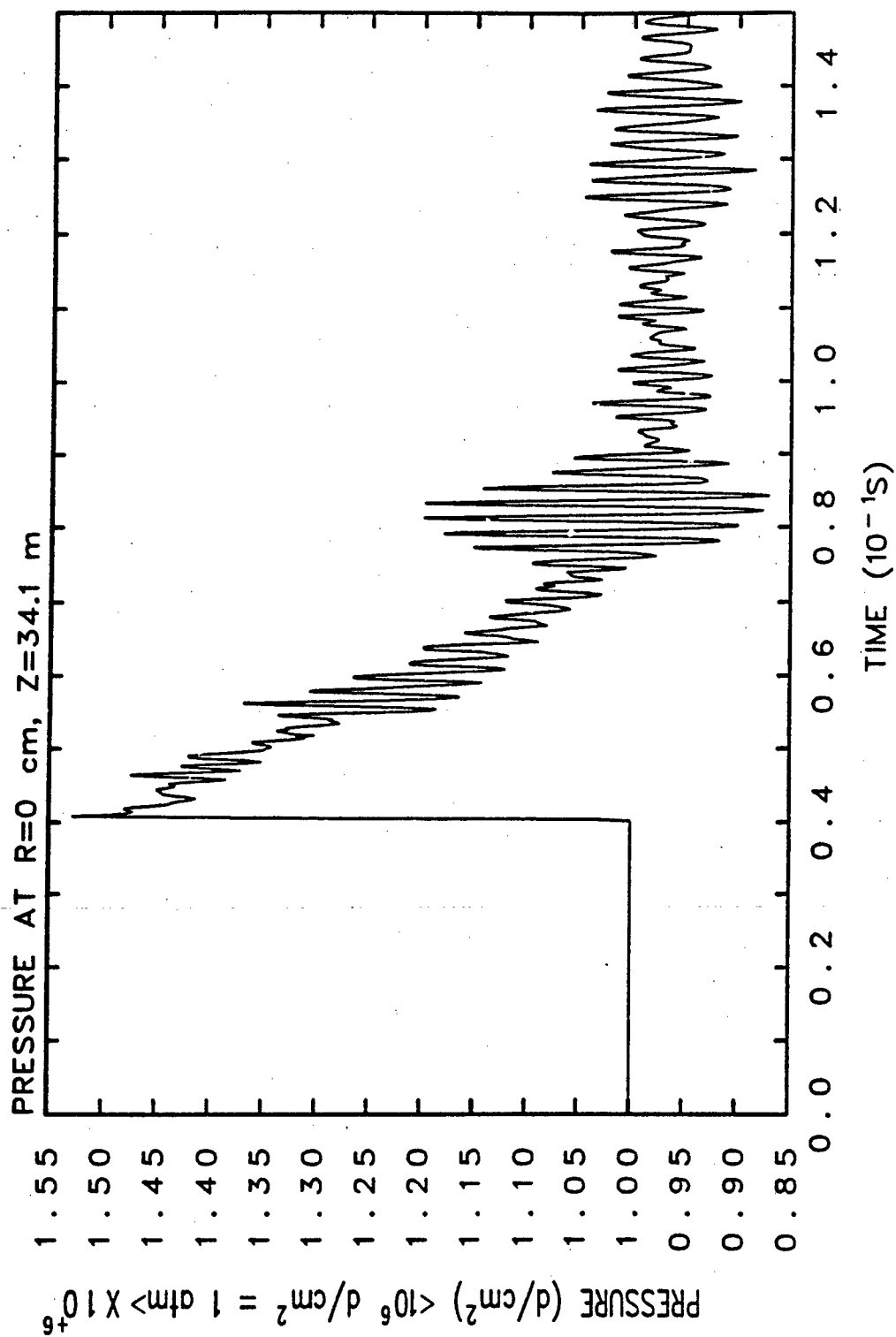
TUNNEL WITH 20 cm FOAM



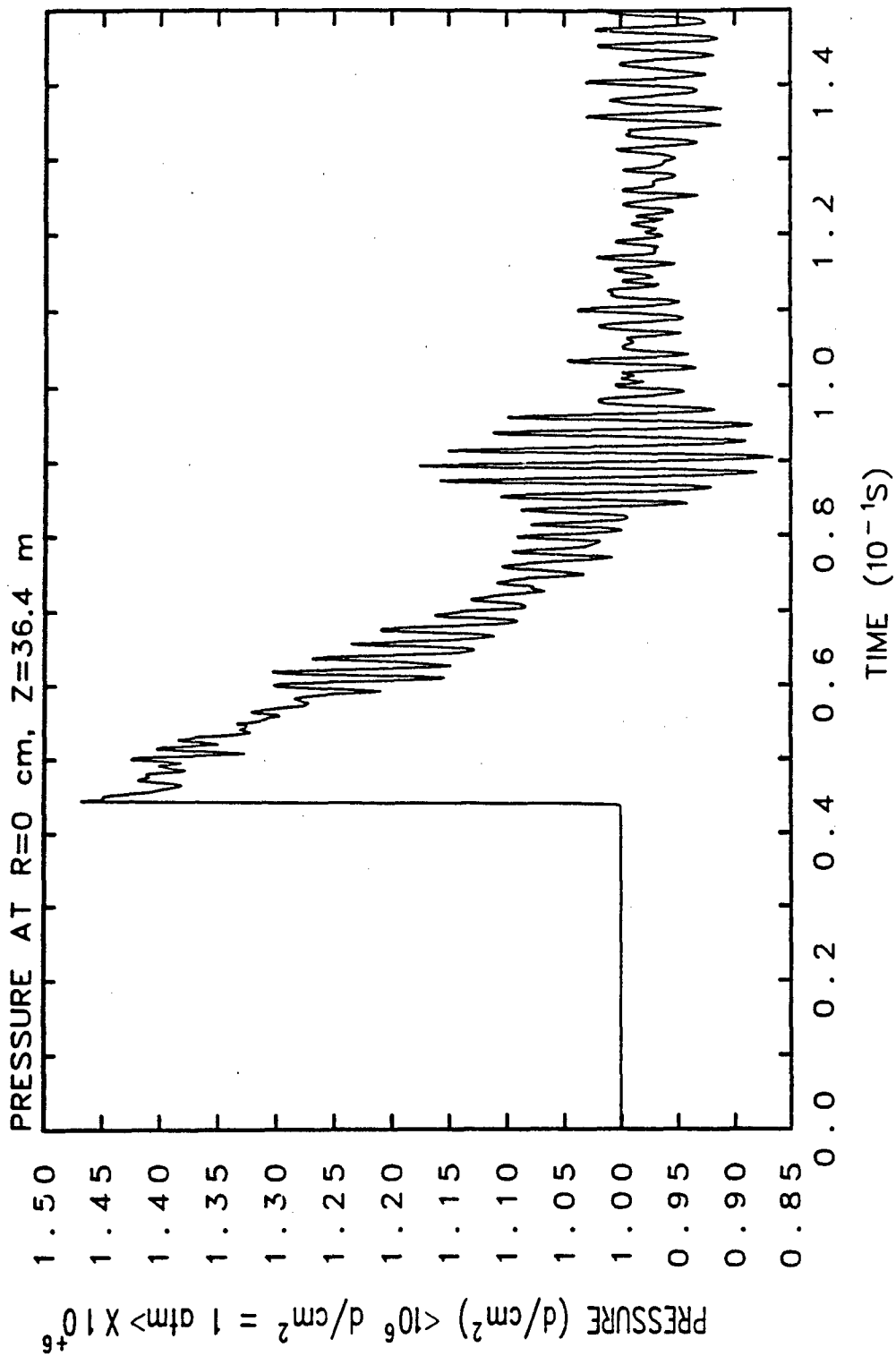
TUNNEL WITH 20 cm FOAM



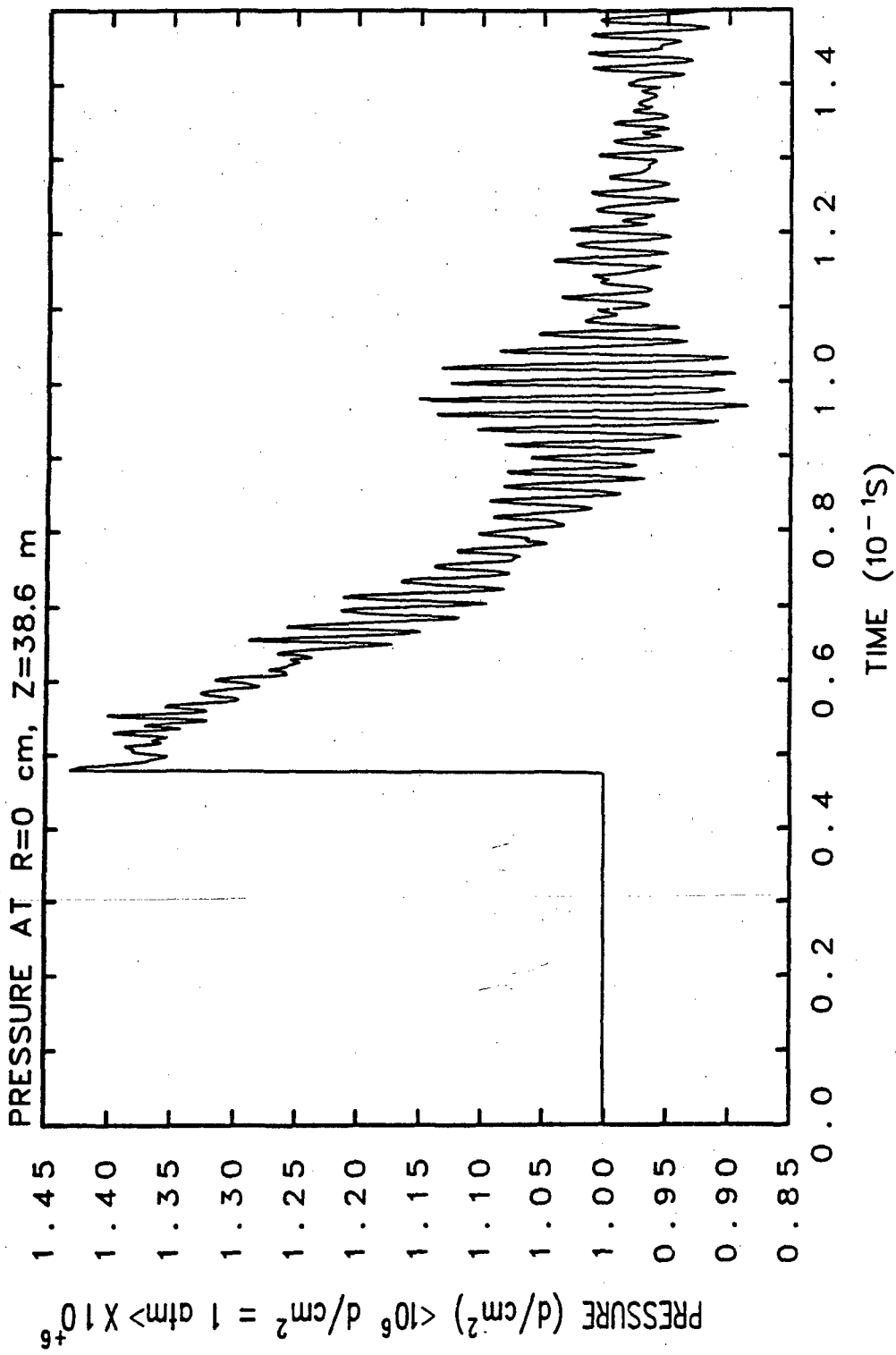
TUNNEL WITH 20 cm FOAM



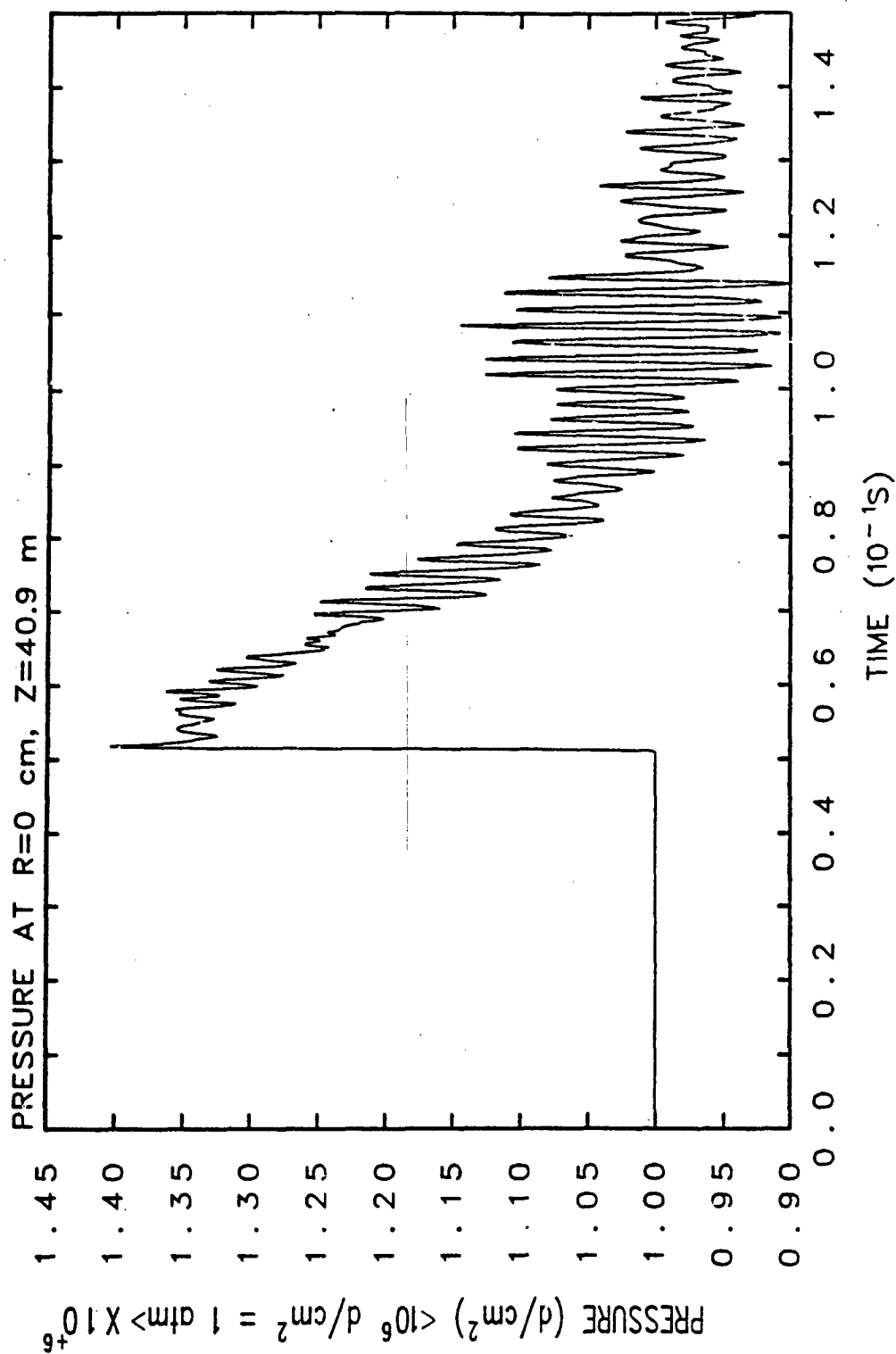
TUNNEL WITH 20 cm FOAM



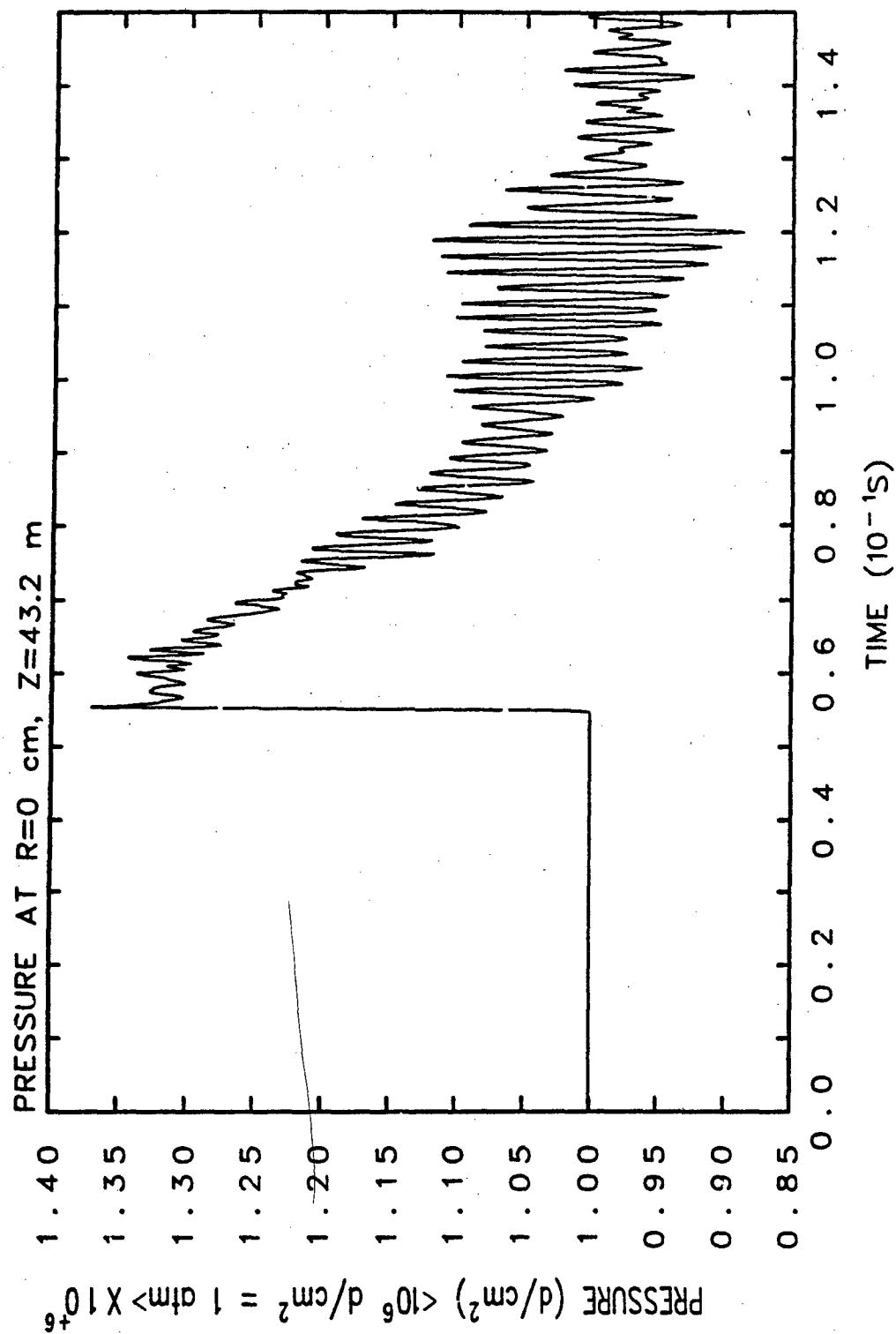
TUNNEL WITH 20 cm FOAM



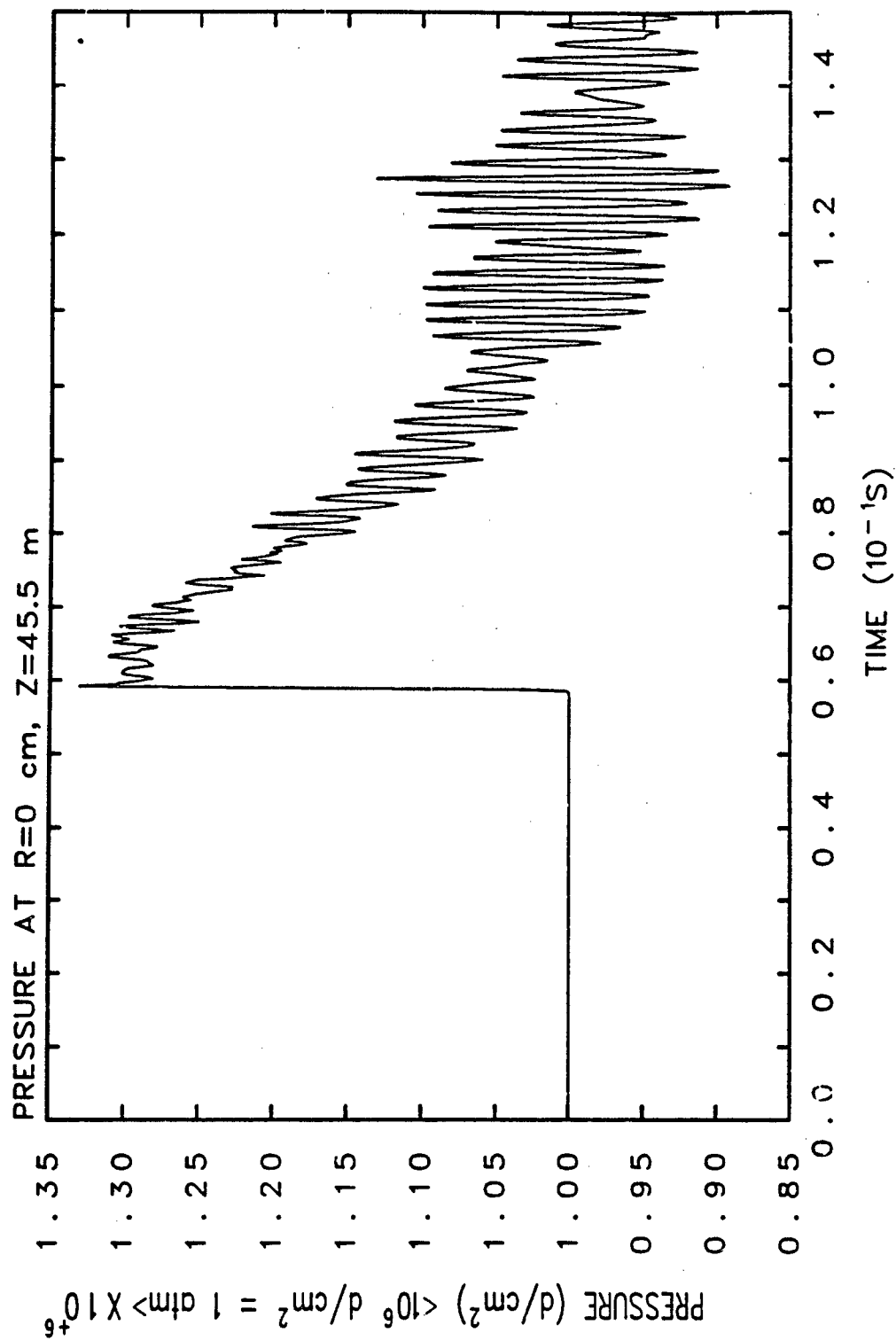
TUNNEL WITH 20 cm FOAM



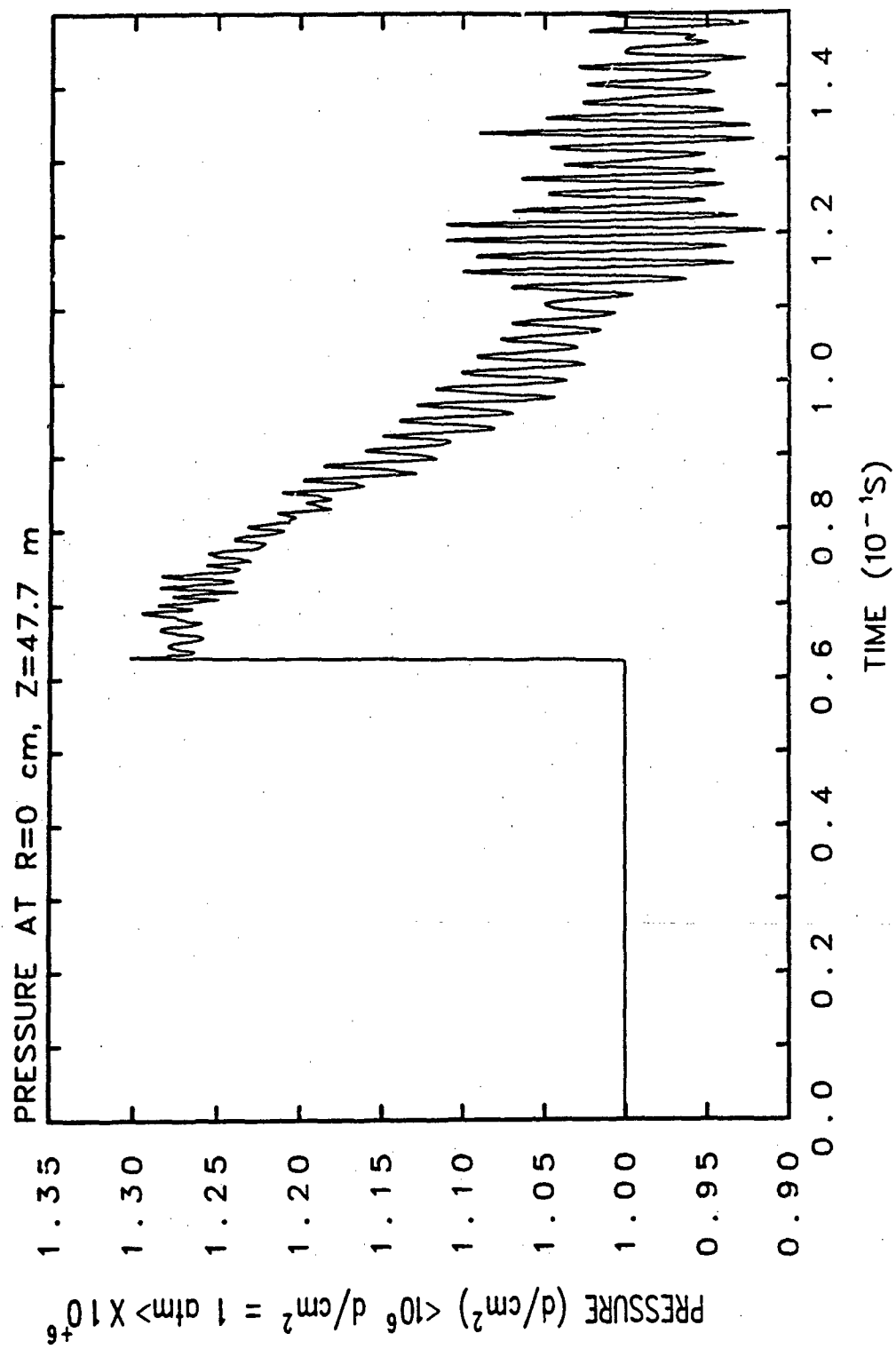
TUNNEL WITH 20 cm FOAM



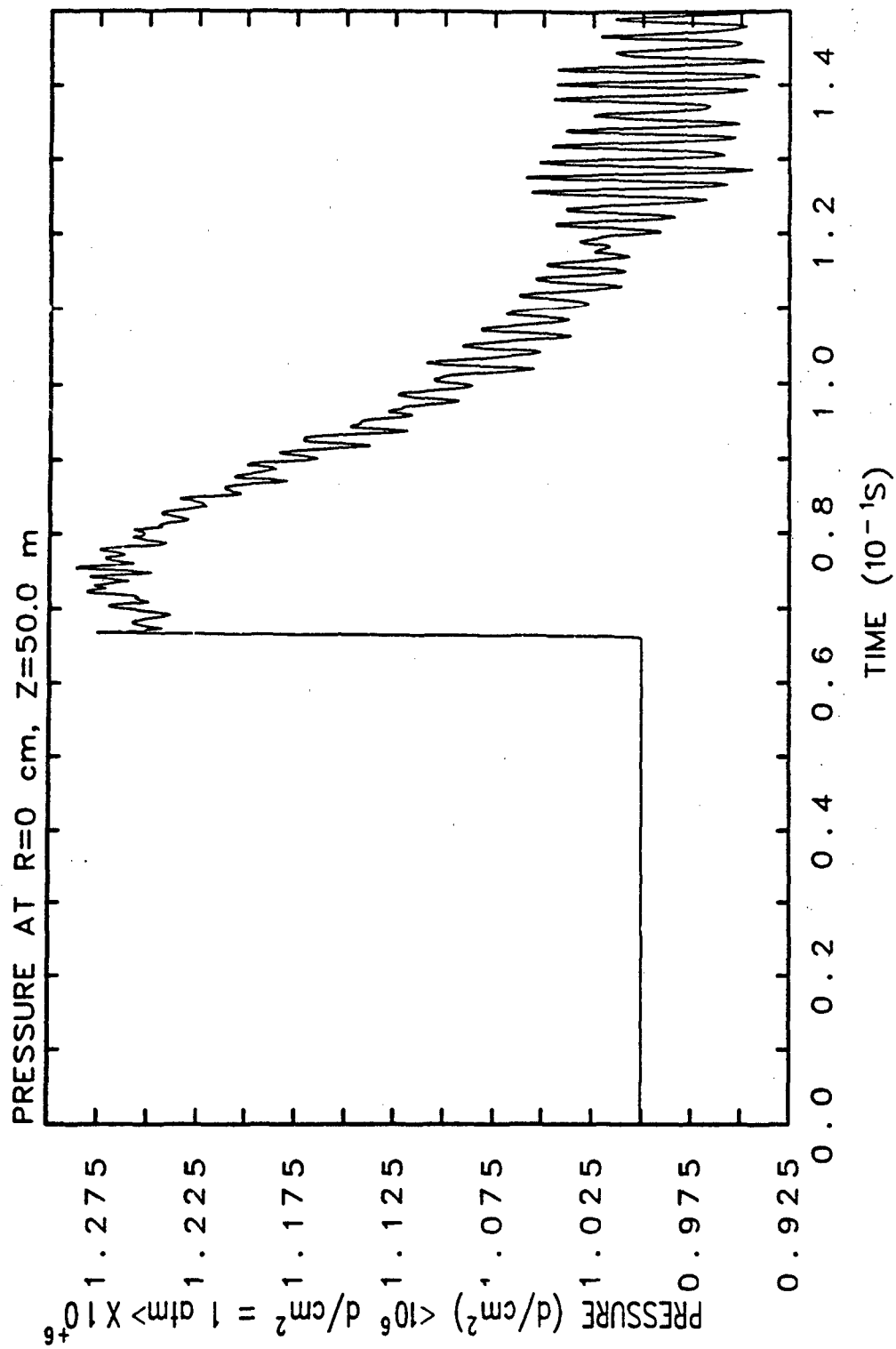
TUNNEL WITH 20 cm FOAM



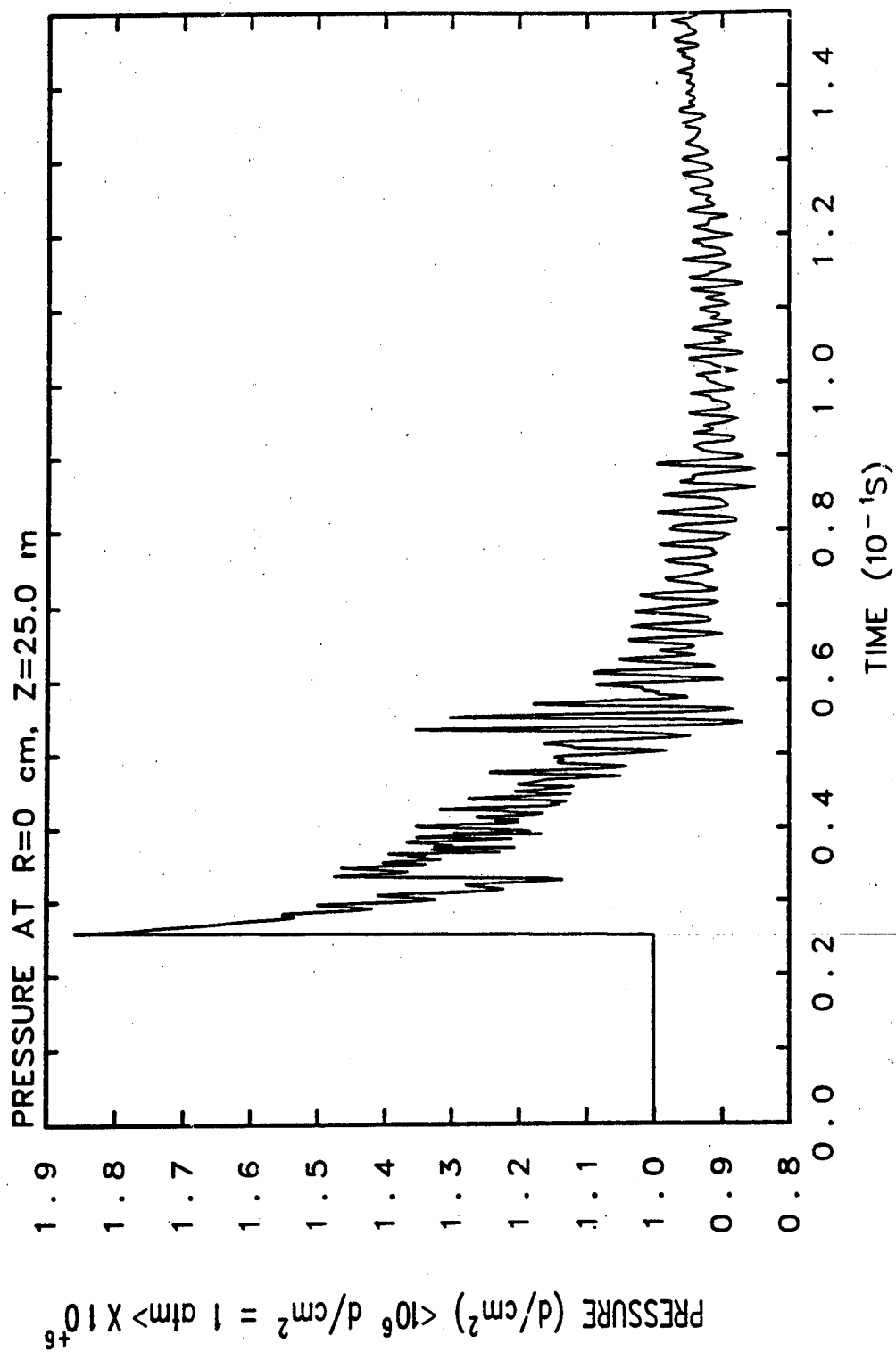
TUNNEL WITH 20 cm FOAM



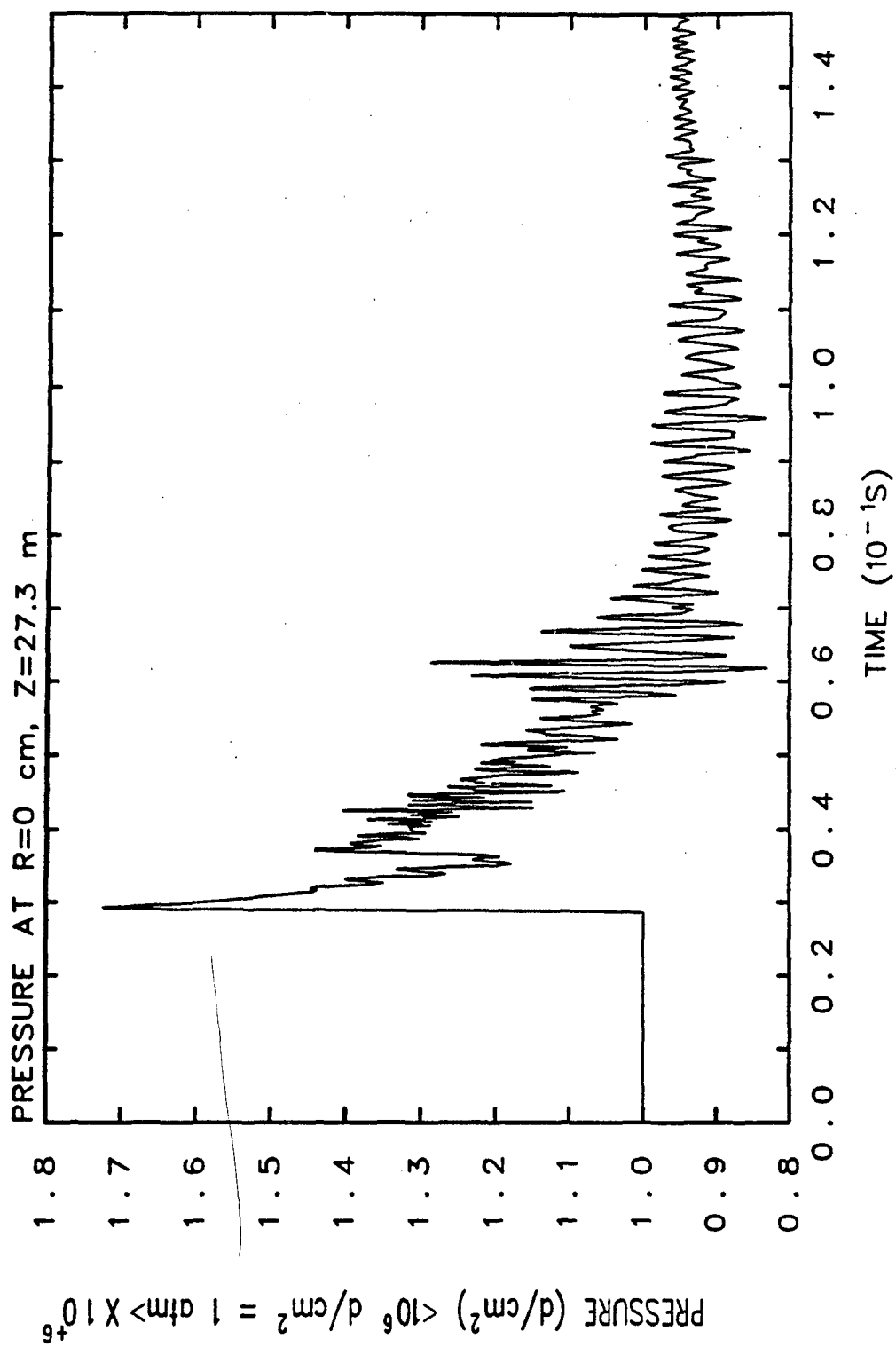
TUNNEL WITH 20 cm FOAM



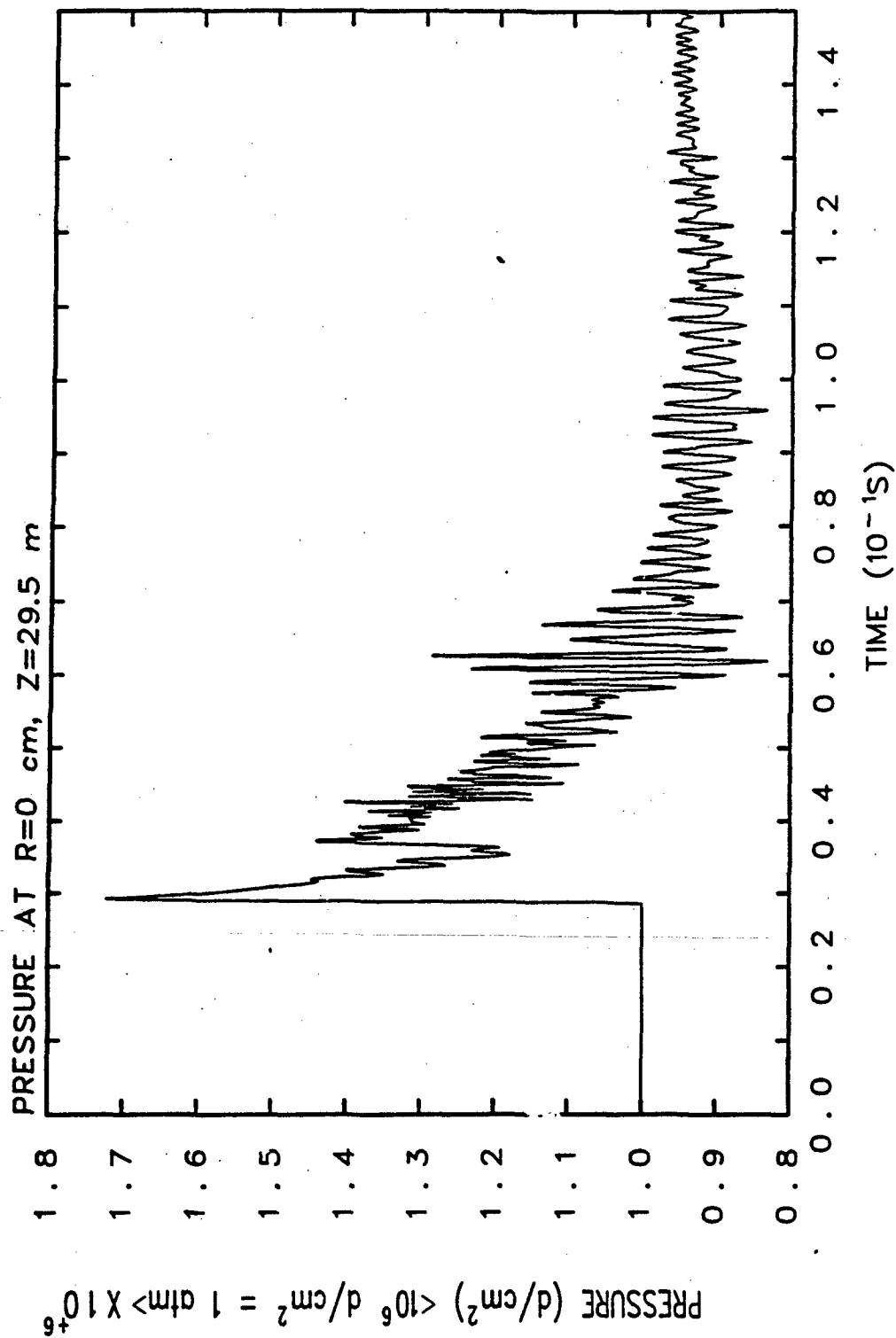
TUNNEL WITH 20 cm FOAM



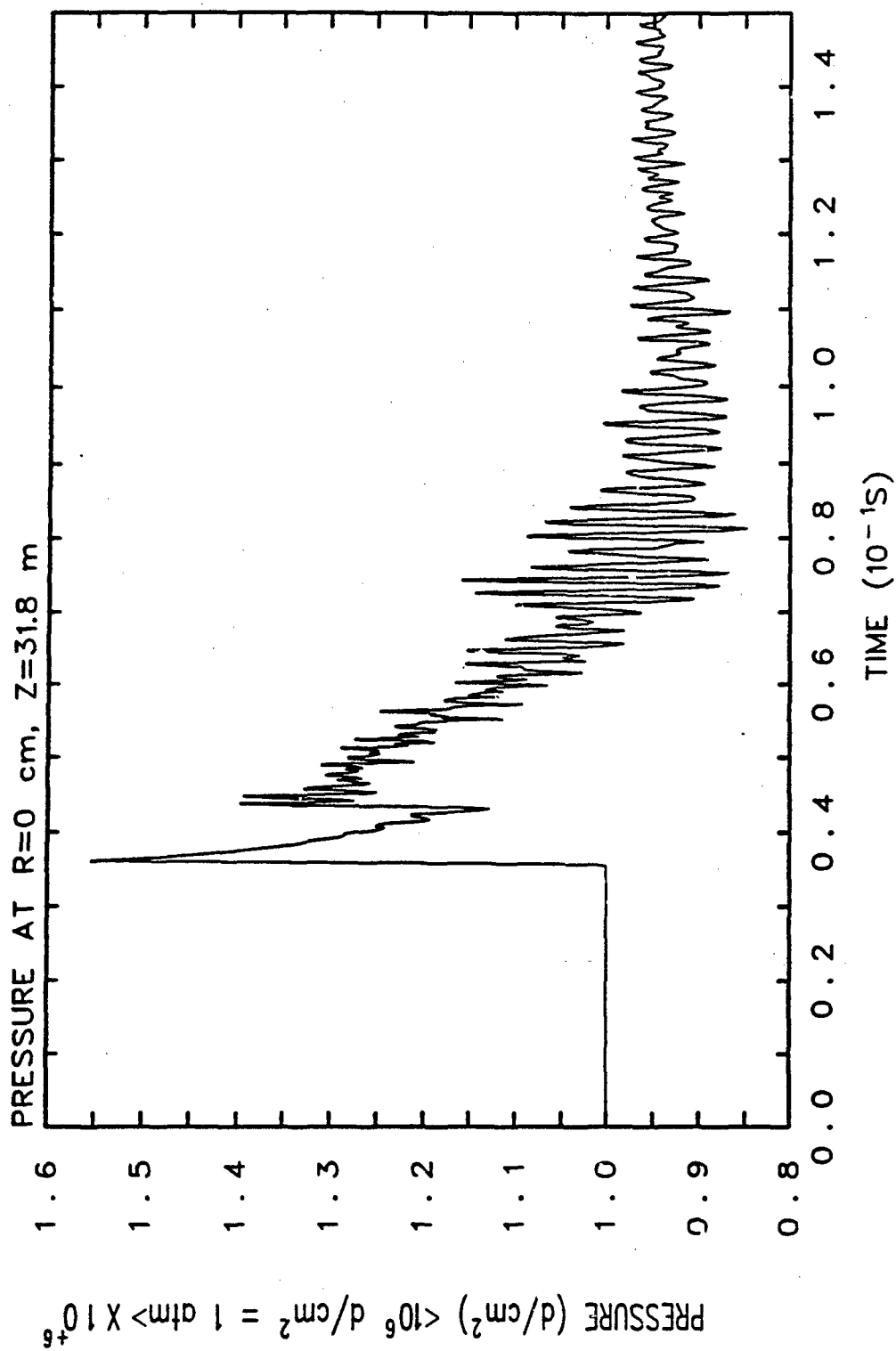
TUNNEL WITH 30 cm FOAM



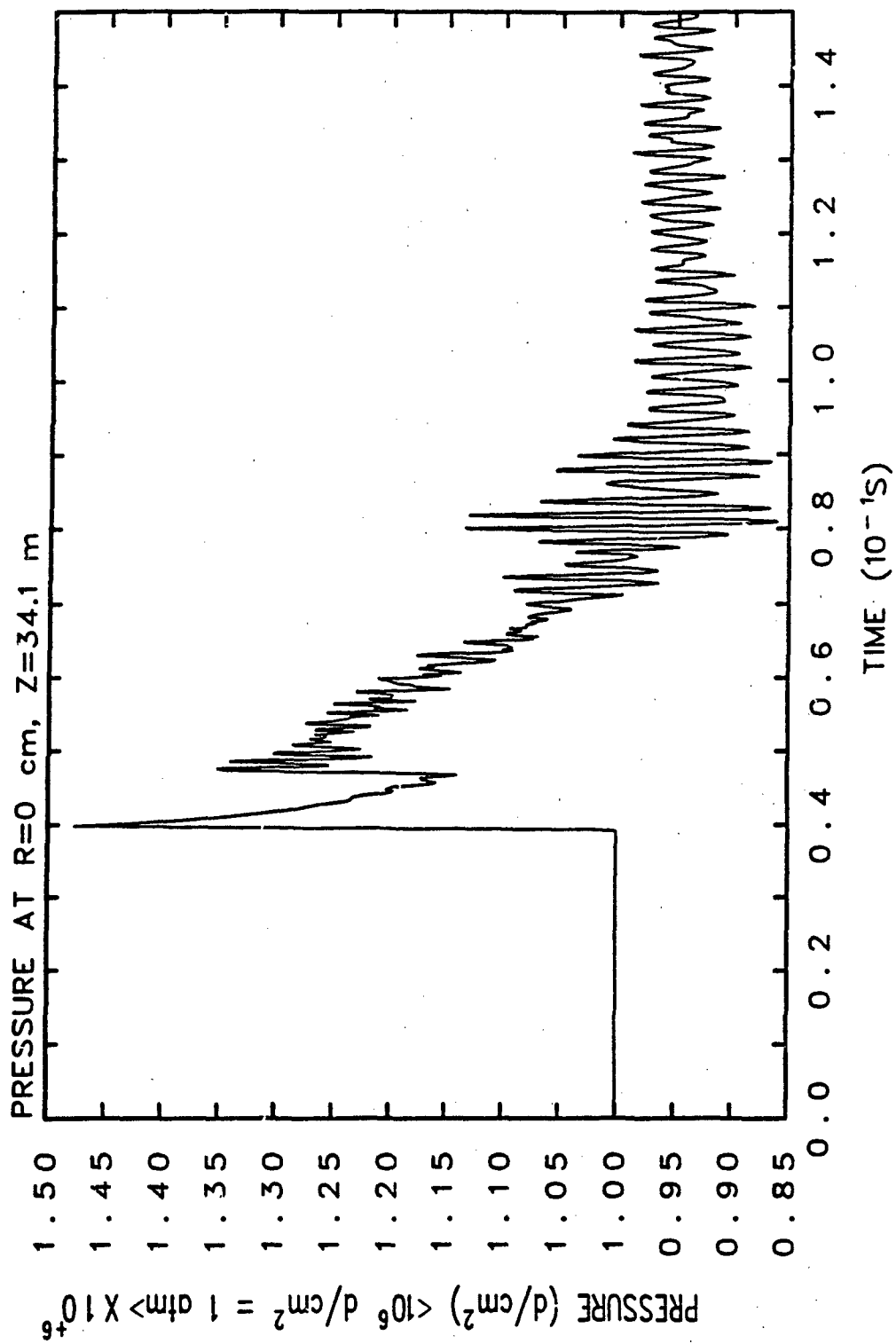
TUNNEL WITH 30 cm FOAM

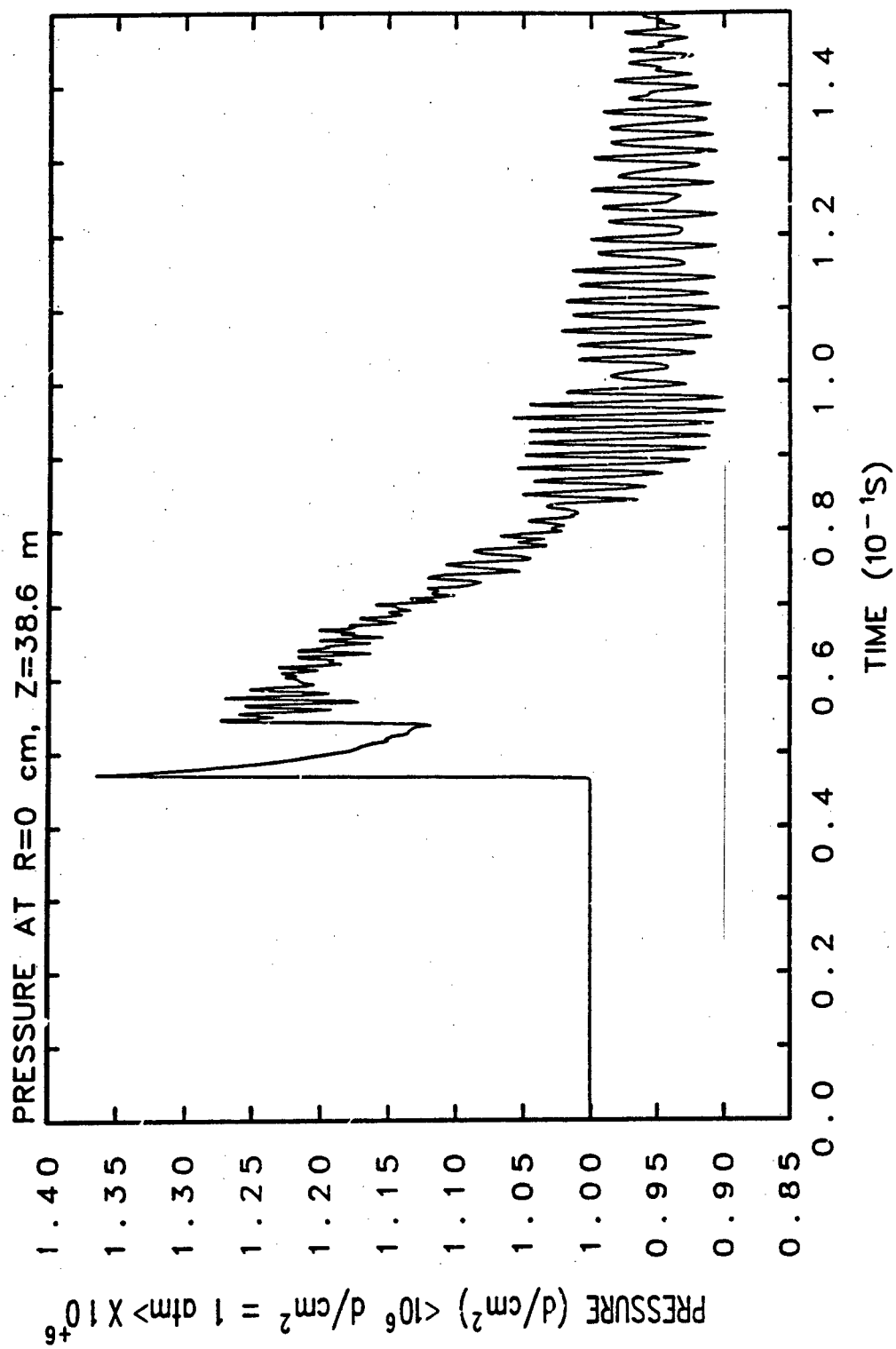


TUNNEL WITH 30 cm FOAM

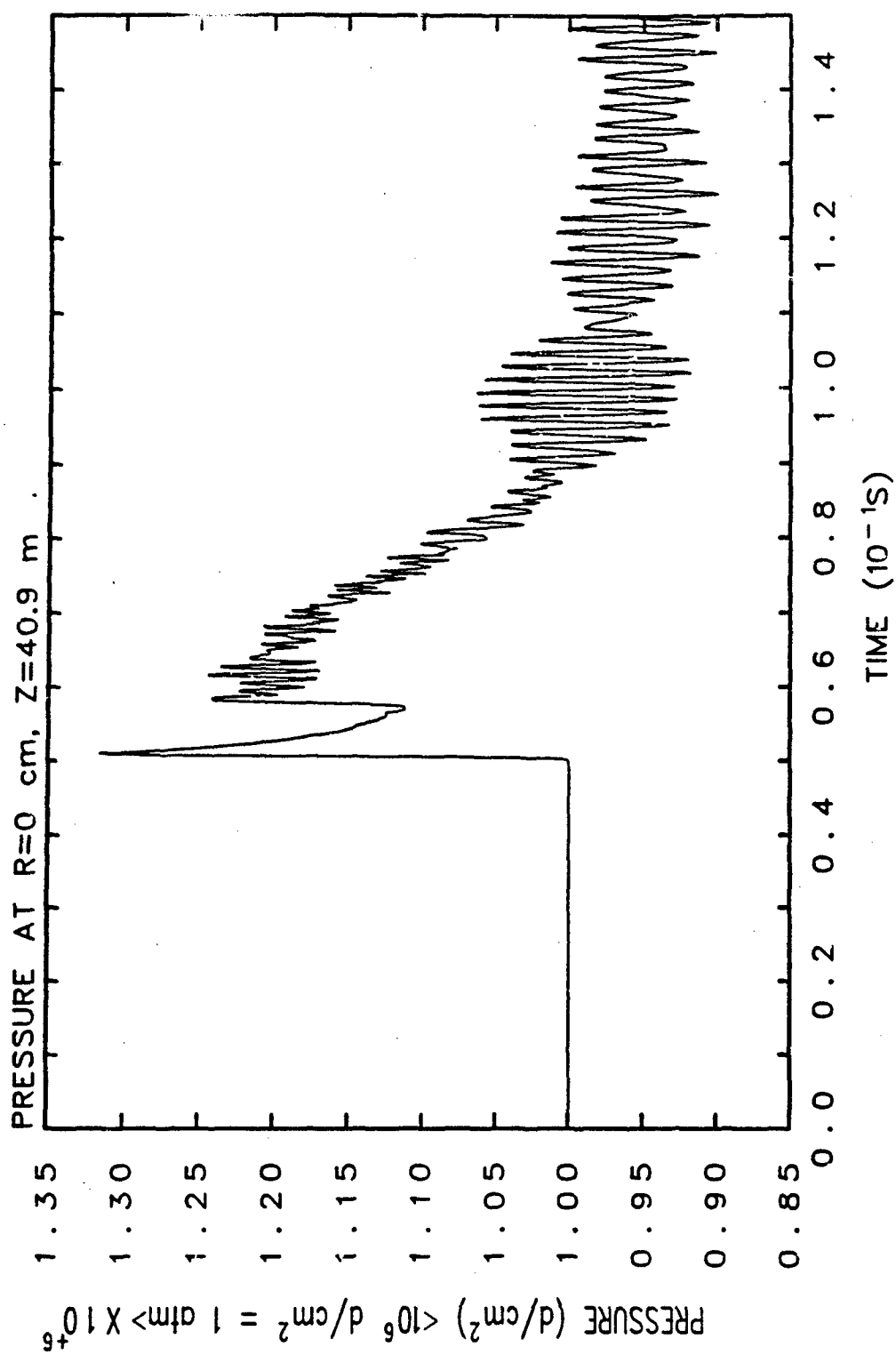


TUNNEL WITH 30 cm FOAM

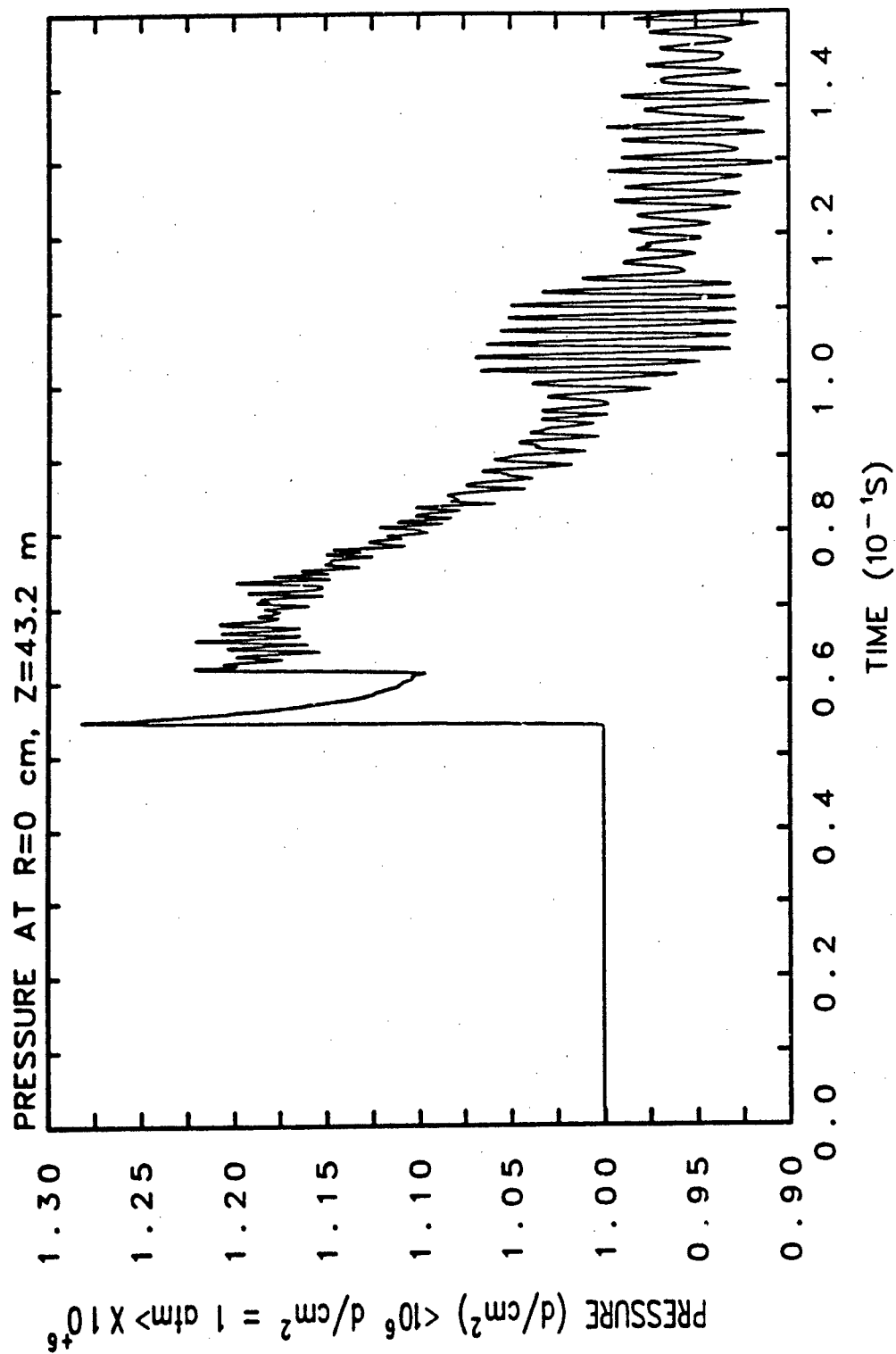




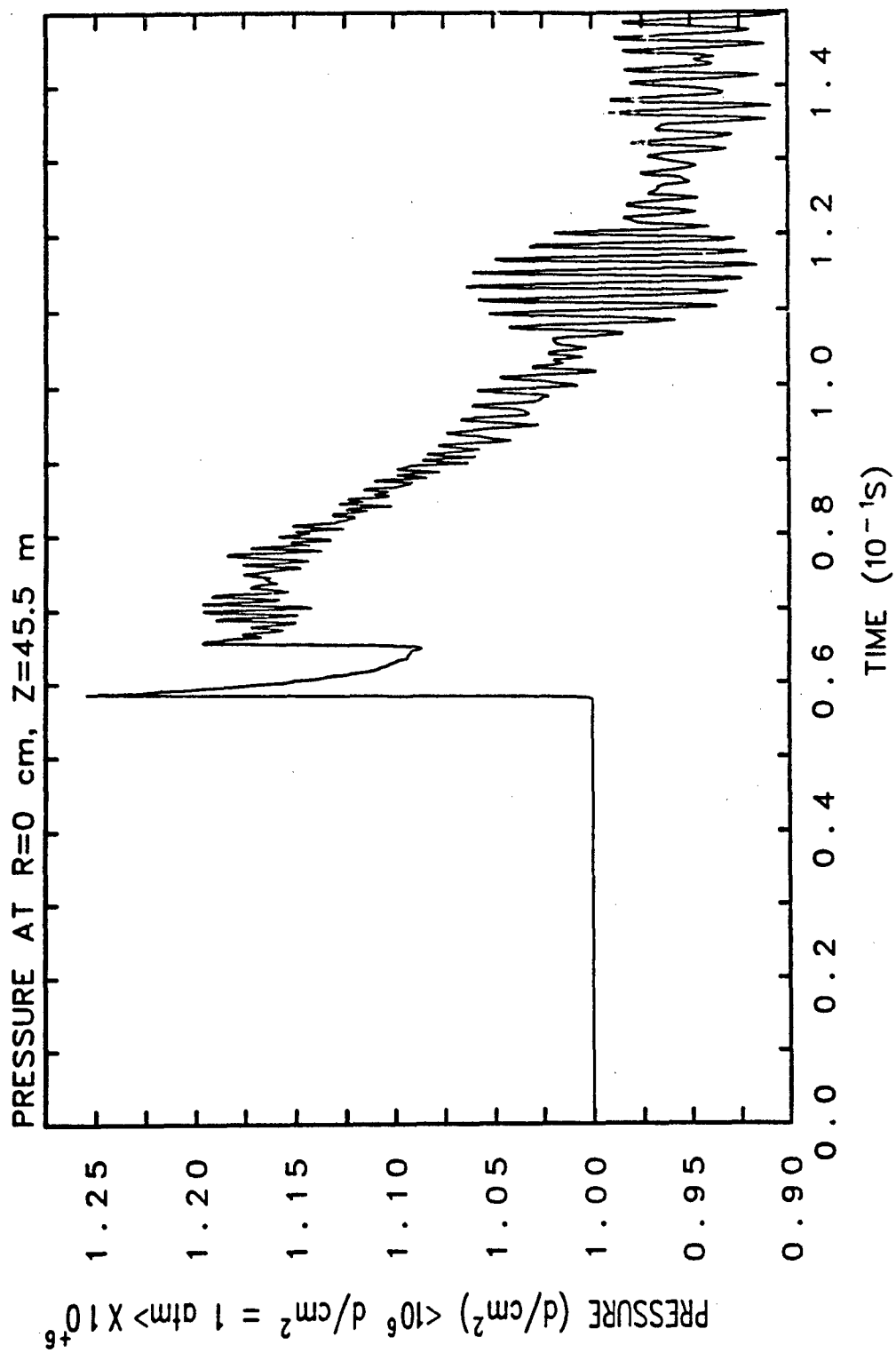
TUNNEL WITH 30 cm FOAM



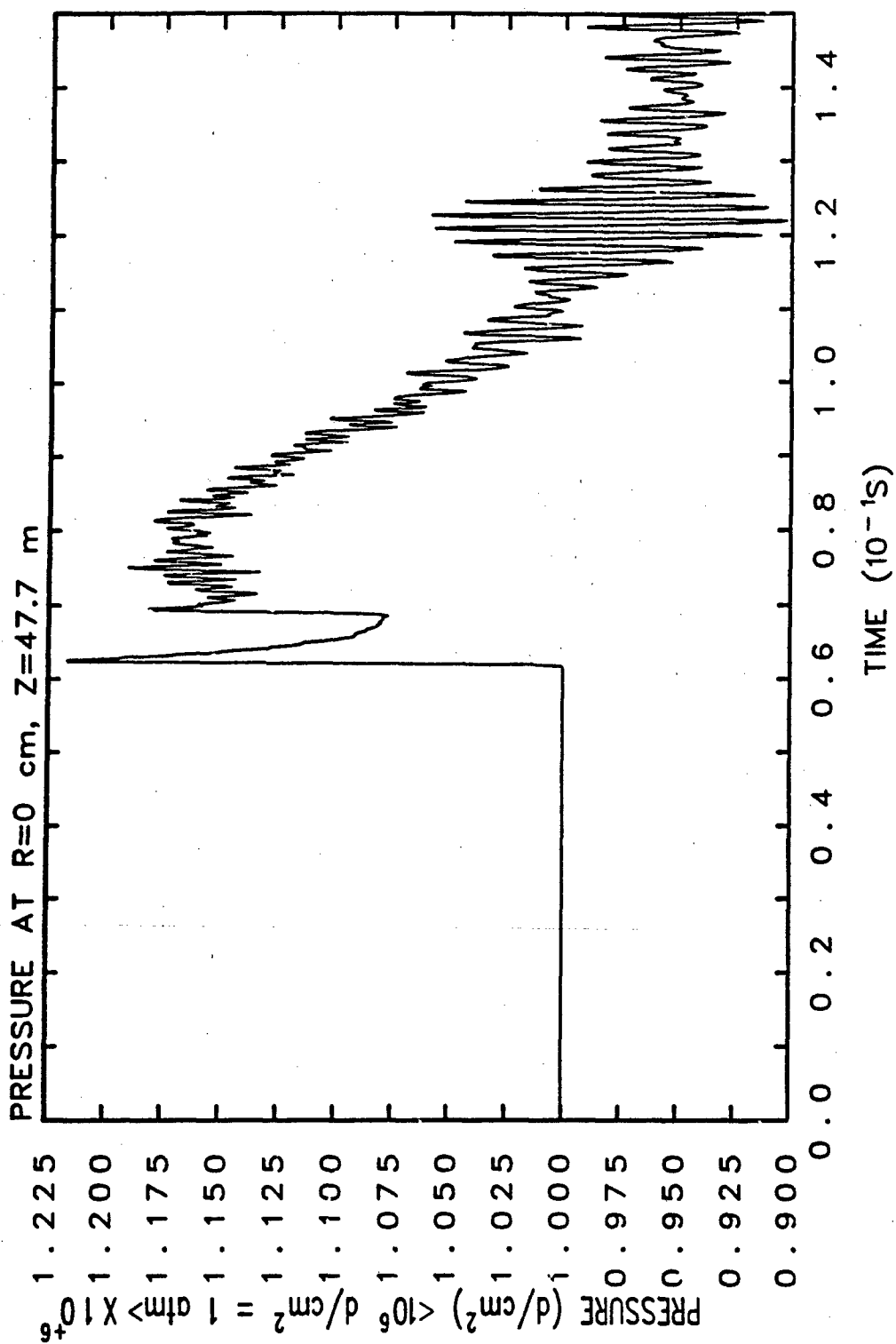
TUNNEL WITH 30 cm FOAM



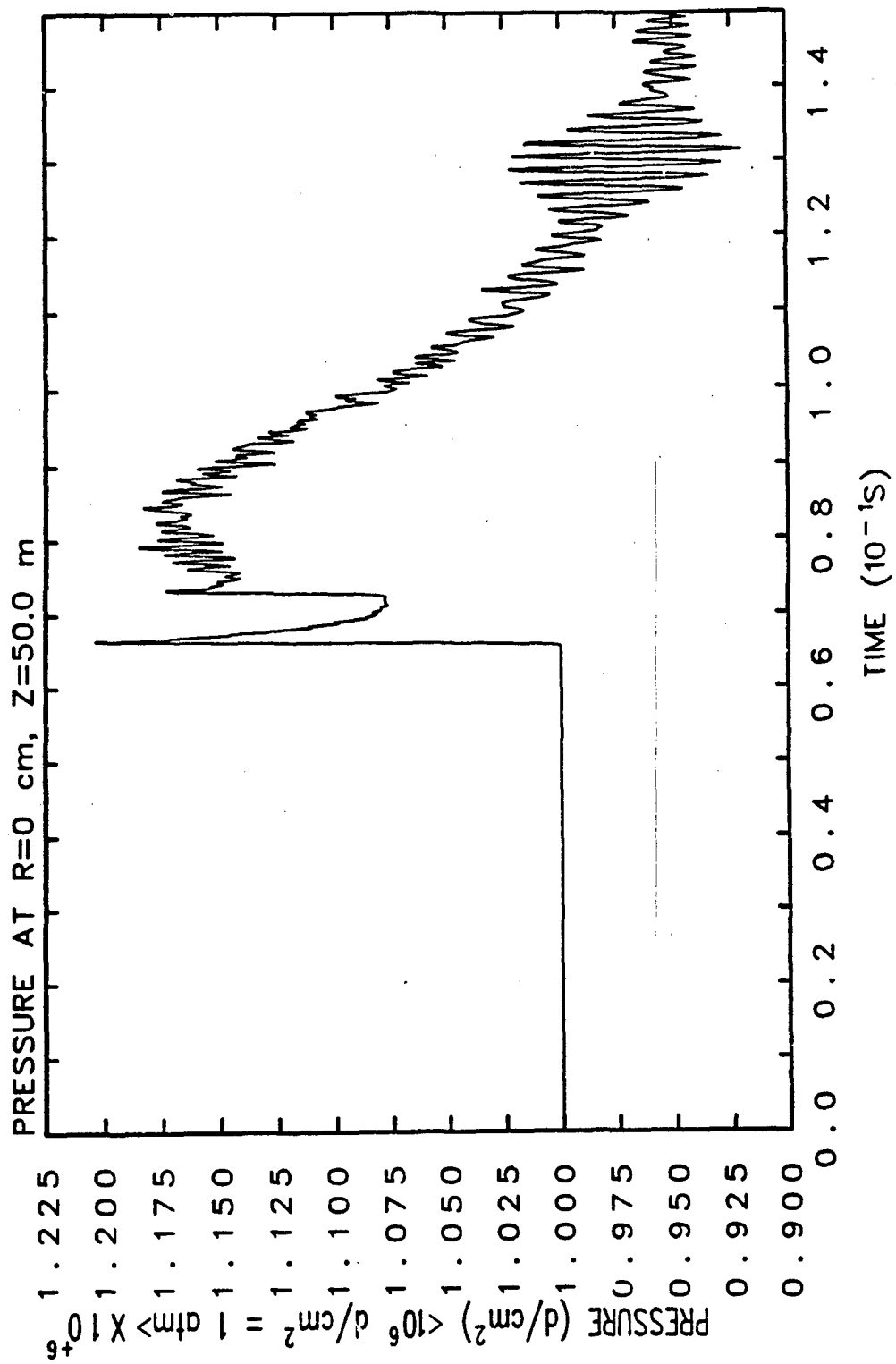
TUNNEL WITH 30 cm FOAM



TUNNEL WITH 30 cm FOAM



TUNNEL WITH 30 cm FOAM



TUNNEL WITH 30 cm FOAM

Bibliography

1. Bell, R. L., et al. *CTH User's Manual and Input Instructions* (Version 1.026). Albuquerque, NM: Sandia National Laboratories, 1992.
2. Bridgman, Charles J. *The Physics of Nuclear Explosives*. Class notes distributed in NENG 6.05, Physics of Nuclear Explosives and NENG 6.31, Prompt Effects of Nuclear Weapons. School of Engineering, Air Force Institute of Technology (AU), Wright- Patterson AFB, OH, 1992.
3. Glasstone, Samuel and Philip J. Dolan. *The Effects of Nuclear Weapons* (Third Edition). Washington: Government Printing Office, 1977.
4. Harlow, Francis H. and Anthony A. Amsden. *Fluid Dynamics*. Springfield, VA: National Technical Information Service, 1971.
5. Kerley, Gerald I. *CTH Reference Manual: The Equation of State Package*. Albuquerque, NM: Sandia National Laboratories, 1991.
6. Kerley, Gerald I. *CTH Equation of State Package: Porosity and Reactive Burn Models*. Albuquerque, NM: Sandia National Laboratories, 1992.
7. LeVeque, Randall J. *Numerical Methods for Conservation Laws* (Second Edition). Basel, Germany: Birkhauser Verlag, 1992.
8. McGlaun, Mike. *CTH Reference Manual: Lagrangian Step for Hydrodynamic Materials*. Albuquerque, NM: Sandia National Laboratories, 1990.
9. Morse, Philip M. "The Transmission of Sound Inside Pipes," *The Journal of the Acoustical Society of America*, 11, #2: 205-210 (October 1939).
10. Scott, R. A. "The Propagation of Sound Between Walls of Porous Material," *The Proceedings of the Physical Society*, 58, part 4: 358-368 (1 July 1946).

Vita

Grant Warner Fondaw was born on 1 March 1961 in Paducah, Kentucky. He graduated from Ballard Memorial High School, LaCenter, Kentucky in 1979 and then entered Rose Hulman Institute of Technology. In 1983, he received a Bachelor of Science degree in Electrical Engineering as well as his commission as a second lieutenant in the United States Army. After completing the Officer's Basic Course in Munitions Materiel Management at Redstone Arsenal, Alabama, he was assigned to the 25th Infantry Division, Schofield Barracks, Hawaii. In 1987, he completed the Officer's Advanced Course in Munitions Materiel Management with honors and was promoted to Captain. He graduated from the Explosive Ordnance Disposal course at Indian Head Naval Ordnance Station in 1988. From August of 1988 through July of 1991, he was the commander of the 56th Ordnance Detachment (Explosive Ordnance Disposal) at Fort Indiantown Gap, Pennsylvania. During this time, he attended the Advanced Access and Disablement Course at Indian Head Naval Ordnance Station. He is currently assigned to the U.S. Army Student Detachment, Fort Benjamin Harrison, Indiana with duty at Wright Patterson Air Force Base, Ohio. He is a member of the Order of the Engineer and the American Nuclear Society.

Permanent Address: Route 1 Box 90
LaCenter, KY 42056

REPORT DOCUMENTATION PAGEForm Approved
OMB No. 0704-0188

Public reporting burden for this collection of information is estimated to average 1 hour per response, including the time for reviewing instructions, searching existing data sources, gathering and maintaining the data needed, and completing and reviewing the collection of information. Send comments regarding this burden estimate or any other aspect of this collection of information, including suggestions for reducing this burden, to Washington Headquarters Services, Directorate for Information Operations and Reports, 1215 Jefferson Davis Highway, Suite 1204, Arlington, VA 22202-4302, and to the Office of Management and Budget, Paperwork Reduction Project (0704-0188), Washington, DC 20503.

1. AGENCY USE ONLY (Leave blank)		2. REPORT DATE March 1993	3. REPORT TYPE AND DATES COVERED Master's Thesis	
4. TITLE AND SUBTITLE Mitigation of Shock Waves in a Cylindrical Tunnel by Foam			5. FUNDING NUMBERS	
6. AUTHOR(S) Grant W. Fondaw, CPT, USA			8. PERFORMING ORGANIZATION REPORT NUMBER AFIT/GNE/ENP/93M-2	
7. PERFORMING ORGANIZATION NAME(S) AND ADDRESS(ES) Air Force Institute of Technology, WPAFB OH 45433-6583			10. SPONSORING / MONITORING AGENCY REPORT NUMBER	
9. SPONSORING / MONITORING AGENCY NAME(S) AND ADDRESS(ES) Lt Col Mark Byers DNA/SPWE... 6801 Telegraph Road Alexandria, VA 22310-3398				
11. SUPPLEMENTARY NOTES				
12a. DISTRIBUTION / AVAILABILITY STATEMENT Approved for public release; distribution unlimited			12b. DISTRIBUTION CODE	
13. ABSTRACT (Maximum 200 words) This study investigated the effectiveness of foam linings in mitigating shock waves in tunnels. A polyurethane foam liner of varying density, crush strength and thickness was modeled inside a 1 meter radius tunnel and an explosion of 1.25 kg of plastic explosive was simulated. Using CTH, an Eulerian-Lagrangian hydrodynamics code from Sandia National Laboratories, the overpressures were computed and compared graphically to determine the effect of varying each foam parameter. The wall of the tunnel consisted of a perfectly reflecting boundary, and in some cases, a foam liner. Low density foam provided the most shock attenuation, with a 20 cm thick layer of 90% void (0.1265 g/cm ³) foam reducing the shock overpressure by 70% at 50 meters. The effects of foam thickness on the shock pressure varied with the distance from the explosion. The thicker foams raised the initial pressure near the explosion due to constriction of the tunnel area. However, the thicker layers reduced the shock faster. Varying the crush strength of the foam from 1 atm to 3 atm overpressure did not affect its ability to mitigate shock propagation in the tunnel. The results of this study strongly suggest that foam can mitigate shock waves significantly.				
14. SUBJECT TERMS Air Shock, Shock Mitigation, Foam, Explosions			15. NUMBER OF PAGES 124	
			16. PRICE CODE	
17. SECURITY CLASSIFICATION OF REPORT Unclassified	18. SECURITY CLASSIFICATION OF THIS PAGE Unclassified	19. SECURITY CLASSIFICATION OF ABSTRACT Unclassified	20. LIMITATION OF ABSTRACT UL	

**END
FILMED**

DATE:

4-93

DTIC